

Utilizing Volatile Organic Compound Detection for Whipworm Diagnosis

LOUISE TURNER

This thesis is submitted for the degree of Master's by Research

Department of Biomedical and Life Sciences
Lancaster University
United Kingdom

Abstract

Soil-transmitted helminth (STH) infections afflict approximately 1/4 of the world's population. *Trichuris trichiura* 'whipworm' accounts for about 40% of this statistic, reducing quality of life and causing significant morbidity in mainly children through stunting nutrition, cognition, and growth. Currently available diagnostic methods are often limited by specificity and sensitivity, with cost, time, and training often inaccessible to the low income/resource areas where STH infections are most prevalent. Appropriate, accurate, and obtainable diagnostic tools would aid successful intervention and parasite control. Infection status alters volatile organic compound (VOC) emissions and immune responses with distinct, complex interactions between multiple different cells and cytokines may cause such modifications. Currently research is sparse concerning trichuriasis-induced odour changes, and the identification, recognition, and understanding of disease-specific VOCs could progress investigation into the pathophysiological mechanisms of trichuriasis and provide alternative diagnostic routes. Mouse urine is an intraspecific olfactory communication method, abundant with notable VOC contributors, such as major urinary proteins (MUPs), that relay health/social status and so may exhibit detectable odour changes specific to *Trichuris muris* infection. To scrutinize the influence *T. muris*-induced immune response has on urine odour, we used a well-studied C57BL/6 mouse model to determine if infected odour profiles were distinct, utilising qPCR analysis of MUP expression, flow cytometry, and portable VOC analysis. As biological detectors of immune response, sandfly attraction choice experiments were conducted, aligning with unpublished research suggesting sandflies can distinguish *T. muris*-induced odour changes

from mouse hair. We found infection-induced changes in MUP expression, with VOC analysis confirming the presence of detectable *T. muris*-induced differences, with discriminable differences between acute and chronic infections. Whilst acute *T. muris* infection induced changes in bladder monocytes, other immune cell subsets had no clear involvement within the liver and bladder, and sandflies did not exhibit significant attraction to infected urine groups nor towards isolated specific Th1 and Th2-related cytokines. Interestingly, preliminary VOC analysis could distinguish between infected and uninfected faecal samples with 100% accuracy, with moderate distinguishment between acute and chronic infections. These data suggest further examination into *T. muris*-induced faecal odour changes could reveal a potential diagnostic source and clarify the potential mechanistic involvement of the microbiome in infection-induced odour changes.

Contents

Abstract.....	i
Acknowledgements	vii
Author's Declaration.....	viii
Chapter 1: Literature Review	1
1.1 The Impact of Whipworm.....	1
1.1.1 Diagnosis and Importance	4
1.2 Volatile Organic Compounds.....	7
1.2.1 VOCs and the Microbiome	10
1.2.2 Major Urinary Proteins as a Source of Disease Detection.....	11
1.2.3 Disease Detection Utilising VOC Detection.....	13
1.3 VOC Utilisation by Vectors	15
1.4 Linking Odour Changes to Immunity Post-Parasitic Infection.....	16
1.4.1 Parasite Manipulation.....	17
1.4.2 Contradictions	23
1.5 Mechanisms of Immune Response.....	30
1.5.1 Whipworm as an Immunological Tool	31
1.5.2 Immune Responses to <i>T. muris</i> Infection.....	33
1.5.3 Components of Immunity	38
1.5.4 Adaptive Immune Cell involvement.....	47
1.5.5 Expulsion	51
1.5.6 Microbiome and Immune Response.....	56
1.6 Aims	60
Chapter 2: Methods.....	63
2.1 Sample Collection	63
2.1.1 Animals.....	63

2.1.2 <i>T. muris</i> Infection	63
2.2 Y-Tube Olfactometer Bioassays	64
2.2.1 Experimental Set Up	65
2.2.2 Conducting Bioassays	66
2.2.3 Bioassay Blind Control.....	67
2.3 VOC Analysis.....	67
2.3.1 VOC Sample Preparation.....	67
2.3.2 VOC Sampling	68
2.4 qPCR	69
2.4.1 RNA Extraction.....	69
2.4.2 Reverse Transcription of T cell cDNA.....	70
2.4.3 RT-qPCR Analysis	71
2.5 Flow Cytometry	73
2.5.1 Single Colour Compensation Controls	73
2.5.2 Enzymatic Digestion of the Liver and Bladder	74
2.5.3 Preparation for Flow Cytometry Staining	74
2.5.4 Staining for Flow Cytometry.....	75
2.5.5 Gating Strategy	77
2.6 Data Analysis and Statistics	79
Chapter 3: Results.....	81
3.1 Expression of MUP-related genes are altered during chronic <i>T. muris</i> infection.....	81
3.2 <i>T. muris</i> Infection Does Not Influence the Innate or Adaptive Profile of Liver Immune Cells in Both the Chronic and Acute State	83
3.2.1 Analysis of Myeloid Cells in the Liver	84
3.2.2 Analysis of Myeloid Cells in the Bladder	89

3.2.3 Analysis of T Cells in the Liver.....	96
3.2.4 Analysis of T Cells in the Bladder.....	102
3.3 Preliminary Testing of Mouse Urine Suggested That Low Dose <i>T. muris</i> Infection was Not Detectable by VOC Analysis	110
3.4 More extensive testing over the course of infection suggests that the VOC profiles present in mouse urine do change with infection	113
3.4.1 Day-Dose Classification.....	116
3.4.2 3-Class Dose Classification	117
3.4.3 Binary Classification	120
3.5 Infected Urine Exhibited No Significant Signs of Differential Sandfly Attraction.....	122
3.5.1 Sandfly Response to the Urine of Mice Infected with Low Doses of <i>T.</i> <i>muris</i> Showed No Significant Attraction	123
3.5.2 Sandfly Response to the Urine of Mice Infected with High Doses of <i>T.</i> <i>muris</i> Showed No Significant Attraction	125
3.5.3 Sandfly Response Showed No Significant Preference for Either Low Dose or High Dose <i>T. muris</i> Infection That Could be Separated from Chance.....	127
3.6 Th1/Th2 Cytokines Do Not Induce Any Differential Vector Attraction in Isolation That Could be Separated from Chance.....	129
3.7 VOC Profile of Mouse Faeces Exhibits Detectable <i>T. Muris</i> -Induced Changes.....	132
3.7.1 Day-Dose Classification.....	135
3.7.2 3-Class Dose Classification	137
3.7.3 Binary Dose Classification.....	139
Chapter 4: Discussion.....	141
4.1 Infection Induced Differences in Hepatic MUP Expression	142
4.2 Monocyte Changes Present in the Bladder of Mice with Acute <i>T. muris</i>	

Infection.....	149
4.3 Clear Differences Between the VOC Profiles of Infected Urine and Naïve Urine	158
4.4 Infected Urine Odour Does Not Induce Differential Sandfly Attraction	163
4.5 Th1/Th2 Cytokines Alone Do Not Induce Differential Sandfly Attraction	170
4.6 VOC Profile Differences Present in Faeces	172
4.7 Conclusions.....	177
References	180

Chapter 1: Literature Review

1.1 The Impact of Whipworm

Soil-transmitted helminth (STH) infections are estimated to impact 24% of the world's population (WHO, 2023), inflicting substantial morbidity and prompting further health issues. These infections are major burdens on global health, greatly stunting quality of life and infected/affected communities' economic growth (Colombo and Grecis, 2020, Hotez *et al.*, 2014). This is further aggravated by the current limitations acting on whipworm diagnosis and detection.

The most effective and feasible treatment option for helminth infections was presumptive treatment involving albendazole and ivermectin, as in comparison screening and treatment was approximately 7.5 times more expensive, and no treatment incurred costs due to more hospitalizations, deaths, and lower quality of life (Maskery *et al.*, 2016). For an annual cohort of 27,700 Asian refugees, overseas presumptive treatment cost the USA \$418,824 as of 2016.

Of the 1.5 billion people infected worldwide with STHs (WHO, 2023), human whipworm (*Trichuris trichiura*) infects an estimated 289-465 million (Rosa *et al.*, 2021, Yousefi *et al.*, 2021, see Fig.1).

Whipworm has been categorized as a neglected tropical disease and is linked with nutritional deficiency and impaired physical, cognitive, and learning development, in addition to other ailments like adverse neonatal and maternal outcomes (Blackwell, 2016, Nokes *et al.*, 1992, Nokes and Bundy, 1994, Loukas *et al.*, 2022). Although rarely fatal, when the burden and relative impact

of infection is quantified, it is estimated that trichuriasis causes 0.64 million disability-adjusted life years (DALYs) to be lost annually (Pullan *et al.*, 2014). These effects are exacerbated by the infection's distribution: prevalence is greater in Sub-Saharan Africa, China, South America and Asia, namely in lower income areas with reduced or limited access to clean water and sufficient sanitation (WHO, 2023), causing these economic impacts to be felt more significantly. DALYs only implicate direct health loss, and do not consider economic, agricultural and social impacts, nor do they cover the cost of prevention, surveillance and treatment (Hotez *et al.*, 2014), most of which disproportionately impacting lower income countries. These effects particularly impact children, who are more vulnerable and more commonly infected.

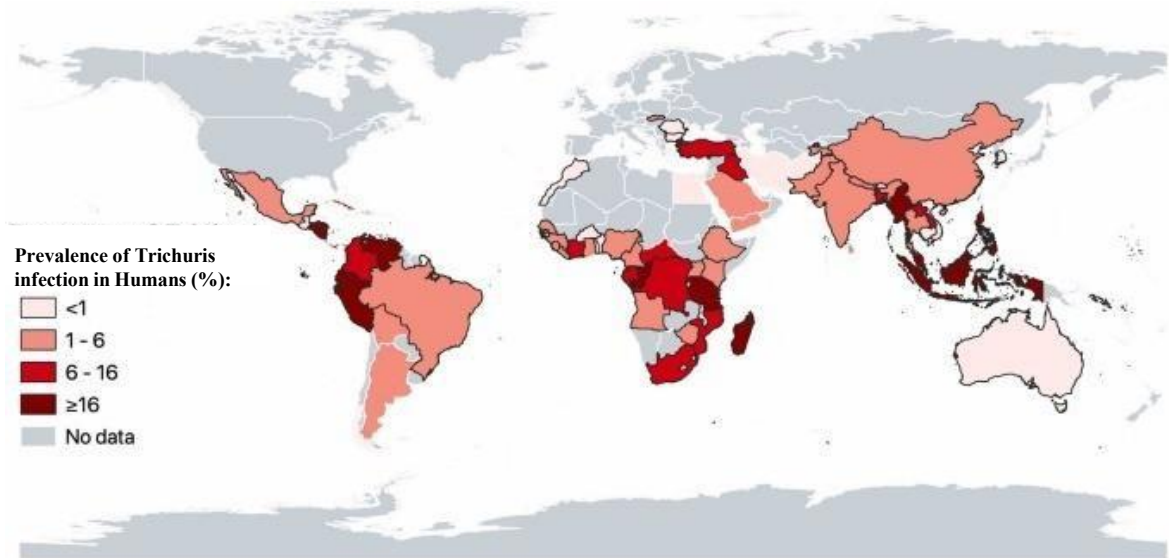


Fig.1. The geographical distribution of *Trichuris trichiura* prevalence (Behniafar *et al.*, 2024).

This figure was taken from a systematic review and meta-analysis of global whipworm prevalence undertaken by Behniafar *et al.*, (2024), based on the data of eligible, peer-reviewed studies from January 1st 2010 to July 30th 2023.

Prevalence is expressed as the percentage of infected people per country. Highest prevalence was found in the regions of Central America at 21.72% (8.90-38.18%) and South-Eastern Asia at 20.95% (2.11-21.46%). countries with the highest prevalence include Honduras, Congo, and Malaysia, at 52.35%, 47.65%, and 47.31% respectively.

Prevalence (%) is colour-coded, denoted by the key on the left side of the figure.

The life cycle of trichuriasis is preceded by ingestion of embryonated eggs, which are released from infected hosts via faeces. In humans this can be through contaminated water sources, soil, or unwashed vegetables, leading to the establishment of worms in the cecum and colon (WHO, 2023, see Fig. 2).

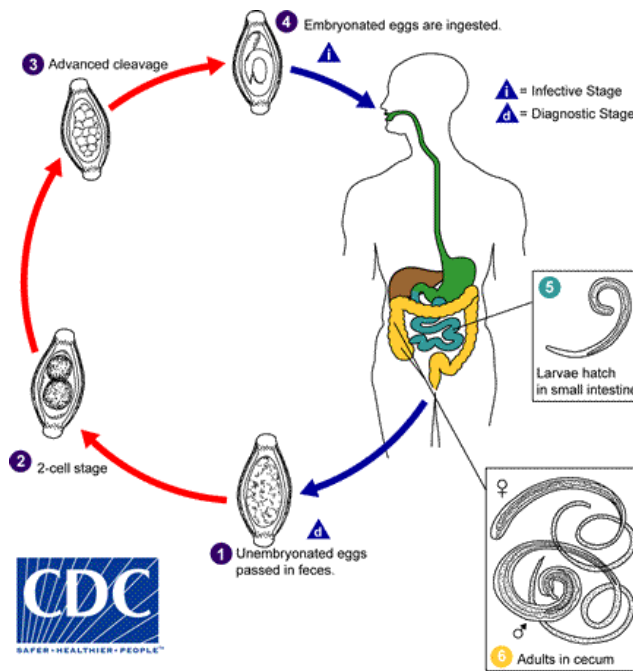


Fig.2. The life cycle of *Trichuris trichiura* (Figure from CDC, 2024)

Denoted by key 1, embryonated eggs are expelled within the stool, and in the soil can progress into a two-cell stage, an advanced cleavage stage, and eventually embryonate (keys 2,3, and 4 respectively). It takes 15-30 days for eggs to become infective, marked by 'i'. Upon ingestion, eggs hatch and release larvae in the small intestine (5), which mature into approximately 4cm long adults that establish in the host's colon (6). Adult worms reside with the anterior of the worm threaded into the mucosa in a fixed location within the cecum and ascending colon. Female oviposition can occur 60-70 days post-infection, with female worms shedding 3,000-20,000 eggs per day in the cecum. Adult worms can live for roughly a year. Diagnostic stage is indicated by 'd'.

1.1.1 Diagnosis and Importance

Prevention and treatment strategies for trichuriasis currently involve improving sanitation, water quality and hygiene, and periodic mass drug administration for populations most at risk. Despite interventions, successful cure rates remain low (Else *et al.*, 2020), as these programs are rarely able to cover whole populations. Cure rates calculated by Moser *et al.*, (2017) using a 38 clinical trail meta-analysis at being ~42% for mebendazole and ~30% for albendazole. Other notable considerations concern both the low efficacy of current

trichuriasis drugs and the worrying potential of drug resistance involving notable mass-administered benzimidazole drugs (Mendes de Oliveira *et al.*, 2022, Grau-Pujol *et al.*, 2022). Mendes de Oliveria *et al.*, noted in 2022 single nucleotide polymorphisms (SNPs) present in 4.8% of 420 individual egg samples from Brazil.

Appropriate and accurate diagnostic techniques are the keystone for successful intervention and would allow for said interventions to become more targeted. Targeted treatments and accurate detection would stunt the development of drug resistance and make treatment more efficient. Useable, precise, and readily available tools for point of care diagnosis would therefore greatly aid treatment provision and parasite control.

Current available diagnostic techniques for STHs are difficult to conduct in the developing communities that are the most impacted and are additionally often limited by specificity and sensitivity (Mbong Ngwese *et al.*, 2020). Laboratory diagnosis for trichuriasis involves microscopic stool sample examination, to determine parasite load and presence (Viswanath *et al.*, 2023). In heavy infestations, eggs may appear in stool saline smears, which are widely used despite low sensitivity. The Kato-Katz method (Fig.3) is recommended by the WHO for egg counting per unit of faeces (Else *et al.*, 2020). Furthermore, stool samples may also display both red and white blood cells, and anemia could also be detected during a complete blood count, although this is not strictly diagnostic criteria for whipworm. A drawback of the studying stool samples is that from ingestion to the maturation of the whipworms, there may be no visible signs of infection, shedding, or eggs. Microscopic diagnosis techniques for light intensity infections are restrained by low sensitivity, whilst in areas with sufficient

resources, more invasive options like colonoscopies, sigmoidoscopies or proctoscopies could provide a diagnosis. However, these diagnostic methods require expensive equipment, are very time consuming and needs training that is not easily available in the low income and resource areas where STH infection is most prevalent.

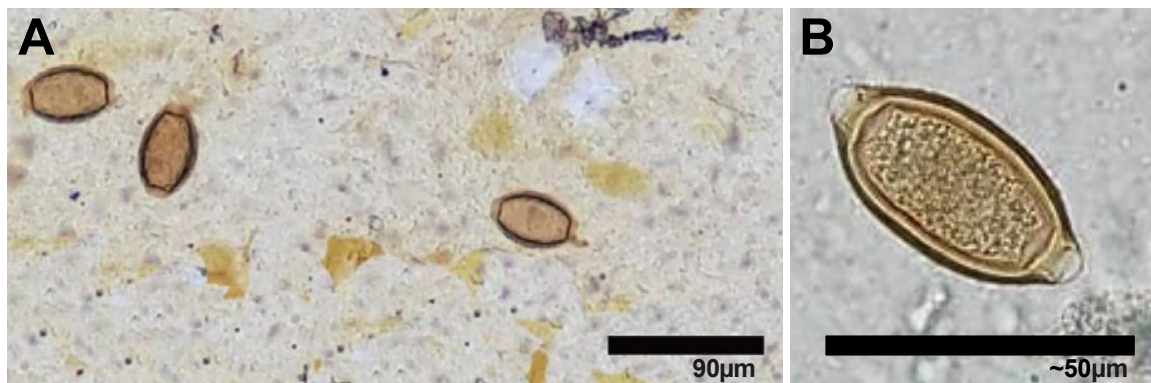


Fig. 3. Microscopic stool sample examination of *Trichuris trichiura* eggs.

'A' depicts eggs found in the Kato-Katz fecal smears of schoolchildren within Yangon Region, Myanmar (as seen in Ryoo *et al.*, 2023). The Kato-Katz technique is the WHO gold standard, used to assess the prevalence and intensity of STHs, allowing for egg quantification, greater sensitivity, cost effectiveness and accessibility compared to other diagnostic methods (Mbong Ngwese *et al.*, 2020). It involves placing a sieved feces sample on a glass slide and creating a thin smear using glycerol-soaked cellophane. Eggs can then be identified and counted per gram of faeces using microscopy.

'B' depicts an egg in greater detail (taken from the CDC, 2024). *T. trichiura* eggs are ovoid, thick-shelled, barrel-shaped, and typically 50-55 by 20-25 micrometers in size. Transparent, bipolar, mucus plugs are also visible.

Scale bars are provided in the bottom right corner for both 'A' and 'B'.

The reduced sensitivity and specificity that microscopy-based parasitological methods provide have given an incentive for the development of molecular-based assays for diagnosis (Else *et al.*, 2020).

The general insensitivity of microscopic methods provides an inadequate gold standard for comparison, but molecular-based diagnostic techniques, namely qPCR, have shown promise with regards to sensitivity (particularly for low intensity infections) and the detection of multiple concurrent infections, when compared with microscopic techniques (O'Connell *et al.*, 2016). However, this method of diagnosis is also limited by costs, and field applications would require training, DNA extraction, time, and pricey equipment for use. To prevent spread effectively, detection would lead to instantaneous point of care treatment, and these methods of detection may realistically take time to relay the outcome, delaying efficient disease control. At present, molecular-based assays are constrained to research, and not for routine endemic use, despite the demand for diagnostics from effected areas which suffer the effects of trichuriasis morbidities. Low cost, field-applicable assays are unavailable at present, but would greatly improve the effectiveness of whipworm control and treatment. Recent parallel studies involved in the search for more efficient/effective diagnostic routes for Leishmaniasis detection suggest that volatile organic compound (VOC) detection has promise to provide a simple non-invasive, field-applicable diagnostic route (Staniek *et al.*, 2019).

1.2 Volatile Organic Compounds

Volatile organic compounds (VOCs) are emitted from the skin, sweat, and other bodily excretions. Importantly, VOC configuration can be modified by changes in the environment, microbiota composition, and immune/infection status, reflecting the individual's metabolic and physiological condition. (Shirasu and Touhara, 2011). The identification and recognition of disease-specific VOCs

could therefore act as diagnostic olfactory biomarkers for several diseases, including infectious, genetic and metabolic ailments. This is an active research area for exploring alternative diagnostic routes, however currently there is little/no available examination into soil transmitted helminth VOC, let alone whipworm, which may benefit from these diagnostic advances.

Both exogenous and endogenous VOCs are exhaled in the breath, however concentrations are often miniscule and hard to distinguish (Dima *et al.*, 2021). Nevertheless, useful biomarkers have been identified that could aid in diagnosis of disease (for example, cancer, diabetes, severe liver disease (Chen *et al.*, 1970, Kaji *et al.*, 1978)). An example of this can be found in Alzheimer's disease (AD), whilst commonly diagnosed at later stages in the disease's progression, AD has demonstrated significant alterations in VOC breath parameters compared to unafflicted controls, with implicated links to AD's pathology (Mazzatenta *et al.*, 2015). This was conducted with a device equipped with a metal oxide semiconductor, allowing for the detection of a wide range of both organic and inorganic volatile compounds correlating with CO₂ levels. Compared to control participants, AD participants had a significantly different relative abundance of VOCs. This could provide a VOC fingerprint belonging to AD, which could be used for earlier diagnosis.

VOC detection may therefore provide a theoretical pathway towards the early diagnosis and management of AD. Further examples of human-derived VOC sources and some evidence for their use have been provided in table.1 below.

Table.1. A summary of primary human-derived sources of VOCs.

VOC Source	Description	Examples of Diagnosis Potential
Skin surface and Hair	VOCs detectable on the skin's surface mainly derive from sweat and sebum, and likely receive contributions from metabolic/hormonal changes, or compounds derived from symbiotic skin surface bacteria's metabolism. Alterations to skin microbiota composition or dysbiosis could be indicative of changes in health status.	Changes in quantity or quality of VOCs emitted by the skin or the skin's microbiome may insinuate either systemic or local disease or infection, ranging from Behet's disease to predicting ulcer development (Duffy and Morrin, 2019, Keerthana <i>et al.</i> , 2024). Hair likewise has previous evidence stating that entrained odour changes with disease state (as seen in leishmaniasis by Staniek <i>et al.</i> , 2019).
Breath	Exhaled VOCs have provided a broad range of volatile analytes that can act as non-invasive biomarkers for several health conditions and pathologies (Moura <i>et al.</i> , 2023). Despite often small VOC concentrations (Dima <i>et al.</i> , 2021), useful biomarkers have been identified that could aid in disease diagnosis.	For example, breath VOCs can be used to identify trimethylaminuria, diabetes, late-stage liver disease (Chen <i>et al.</i> , 1970, Kaji <i>et al.</i> , 1978). Additionally, as previously mentioned, diseases like AD can be detected using breath-derived VOCs as biomarkers (Mazzatenta <i>et al.</i> , 2015).
Urine	Components of urine are substances involved in intermediate or terminal products of many metabolic pathways, many of which carry specific, detectable odours. This allows for VOC patterns to often be prominent and identifiable; however, alterations can often occur due to food ingested and metabolism as opposed to disease (Pelchat <i>et al.</i> , 2011).	Urine profiles are already known to contribute to disease diagnosis (Zlatkis <i>et al.</i> , 1981). VOC and odour differences have been denoted in diseases ranging from lung and prostate cancer to murine hepatosplenic schistosomiasis (Cornu <i>et al.</i> , 2010, Manivannan <i>et al.</i> , 2010, Liu <i>et al.</i> , 2023).

Faeces	VOC profiles from faecal samples elucidate intestinal microbiota and dietary end-products, and as such could be a good non-invasive method of diagnosing gastrointestinal disease. Changes in gut microbiota can often cause or coincide with disease, and provide critical interactions with adaptive immunity (Manos, 2022).	Evidence can be seen concerning <i>Clostridium difficile</i> , <i>Campylobacter jejuni</i> , and <i>Vibrio cholerae</i> infections (Garner <i>et al.</i> , 2007, Garner <i>et al.</i> , 2009). A differentiation of 13 bacterial genera and 29 fecal VOCs were found between early/middle stage AD patients and controls (Ubeda <i>et al.</i> , 2022). VOCs and microbiome composition were shown to coincide stage-specifically with AD development.
Blood	The VOC profiles of blood samples could contribute to disease screening and diagnosis. However, blood samples are more invasive than other listed VOC profile sources, and as such could have reduced accessibility and field use.	Using blood VOCs have been identifiable when looking at diseases like hepatic encephalopathy (Goldberg <i>et al.</i> , 1981) and lung cancer (Deng <i>et al.</i> , 2004), however more study is required for clinical application.

Some VOC sources are described and a few examples of use in disease detection are noted. VOCs can be sourced from other sites (e.g., saliva, lactation, semen), however this table only lists a selection of some of VOC sources studied. Additionally, not all evidence is listed for each of these sources, just a couple of examples demonstrating the use of the source's VOCs as identifiable biomarkers of disease.

1.2.1 VOCs and the Microbiome

The human body is inhabited by a vast quantity of microbial cells, with a greater abundance of genes than the human genome. Individuals harbour unique collections of varying species density, intrinsically linked to health status and disease (Gilbert *et al.*, 2018). The microbiome is likewise heavily interlinked with body odour. Many volatile compounds that contribute to body odour either originate from or are metabolised by the microbiome into odour-contributing volatile compounds. For example, from skin and sweat, Mogilnicka *et al.* (2020)

lists (E)-3-methyl-2-hexenoic acid, (R)/(S)-3hydroxy-3-methylhexanoic acid, 3-methyl-3-sulfanylhexan-1-ol, TMA, ammonia, and methionine as some of the main bacterial metabolites, each of which contribute to the odour profile of this area.

Many instances of malodour prescribed to infection or disease is often caused or is greatly contributed to by resident bacterial flora or specific compositions of microbiota. This is done by promoting/aiding in the production of odours molecules (for example, ammonia or volatile sulphur compounds).

As such, the microbiome is inextricably connected to odour and odour-involved disease detection, and that it is important to note the contribution of the human microbiome has to all the examples of disease detection previously mentioned.

1.2.2 Major Urinary Proteins as a Source of Disease Detection

To name another potential VOC profile contributor, first observed and most extensively understood in mice, pheromone binding proteins, named major urinary proteins (MUPs), are present in some species' urine.

These protein isoform complexes may function as signal modulating agents for pheromones (Edink *et al.*, 2010), responsible for controlling pheromone transport and release via binding and releasing low molecular weight pheromones, providing slow-release mechanisms for VOCs that contribute to scent marks. They could even be functioning as independent chemo signalling molecules, allowing for the communication of scent mark ownership and individual identity (Beynon and Hurst, 2004).

For mice, scent is vital for gleaning complex information from the urine scent marks deposited within their territories. Such information includes an individual's physiological, social, and health status, what food they are consuming, the individual's identity and relatedness, and amount of time passed since the mark was placed (Penn and Potts, 1998¹, Schellinck *et al.*, 1992, Ferkin *et al.*, 1997). When infected or ill, MUPs can signal to other mice the quality of the individuals health, contributing urinary VOC profiles.

MUP expression has already been shown to vary dependent on the infection status and virulence of other diseases, such as Lymphocytic Choriomeningitis Virus (LCMV, Oldstone *et al.*, 2021). Urine odour was shown to change on the fourth day post-rabies and West Nile virus vaccination, during immune activation, too early to correlate to an adaptive immune response (Kimball *et al.*, 2014), as peak antibody production has not been observed until days 14-28 post-inoculation for these viruses (Van de Zande *et al.*, 2009, Smith *et al.*, 2011).

However, parasitic infections, which trigger more adaptive immunity-dominated responses, have been indicated to mediate urine odour changes (Pearce *et al.*, 2006). Parasitic infections have been shown to affect MUP expression, namely schistosomiasis, which showed expression reductions correlating with infection severity (Manivannan *et al.*, 2010). Furthermore, female mice have been shown to distinguish between and be repulsed by protozoan parasite-infected mice when compared to healthy male mice (Kavaliers *et al.*, 1995).

1.2.3 Disease Detection Utilising VOC Detection

Odour can be examined using metabolomics, spectrometry, and other analytical approaches (Cambau and Poljak, 2020). In the past couple of decades spectrometry-based scent analysis instruments were developed for microbial detection, before the standard use of MALDI-TOF-MS for the identification of microbes (Moens *et al.*, 2006, Zhu *et al.*, 2010, Devaraj *et al.*, 2018). More recently, VOC analysis has also been undertaken using gas chromatography-mass spectrometry (GC-MS), secondary electrospray ionization-mass spectrometry (Zhu *et al.*, 2010, Bos *et al.*, 2013) and additionally thermo-desorption gas chromatography mass spectrometry (Koo *et al.*, 2014, Smart *et al.*, 2019).

For diagnostic use, analytical instruments have been limited by the cost and complexity of use (Röck *et al.*, 2008). However, the development of portable VOC analyzers, based on traditional standard VOC analysis, could mitigate these issues and provide an accessible gateway for point of care odour analysis in disease diagnosis. These analyzers benefit from being cost-effective, portable and lack the need for highly skilled operators (Keerthana *et al.*, 2024).

As examples, portable electronic noses have been determined as feasibly detecting lung cancer from the breath samples of patients and healthy controls (van de Goor *et al.*, 2018). These samples were analyzed for patterns using an artificial neural network.

Colorectal cancer could also be detected from samples of the urinary metabolome (Tyagi *et al.*, 2021).

Both GC-TOF-MS and eNose analysis were determined to detect cancer with similar accuracies and specificity, as determined using random forest and neural network models.

Similarly, tuberculosis could be distinguished from breath samples (Coronel Teixeira *et al.*, 2017). When comparing the breath samples of uninfected people using an artificial neural network, sensitivity was 88% and specificity was 92%, with participants exhibiting a high acceptance rate to the eNose.

If this could be utilized for trichuriasis detection, this could mitigate many issues present in the presently used detection methods. VOCs produced from several sources by the host could be potentially utilized for this goal.

Further promise for VOC detection utilization for whipworm is provided through animals identifying and differentiating between disease states through olfaction alone (Cambau and Poljak, 2020), as this supports that VOC profiles are distinguishable by biological detection.

Dog's olfactory sensitivity has been shown to detect *Clostridium difficile* in the faeces of patients, via training using food rewards (Bomers, *et al.*, 2012, Bomers *et al.*, 2014, Taylor *et al.*, 2018). Likewise, dogs have been trained to reliably detect positive samples of human urinary tract infections (Maurer *et al.*, 2016). Dogs may also be able to detect cancer, more specifically malignant tumour odour, first denoted by Williams and Pembroke in 1989. In double blind trails, lung and breast cancer was detected by dogs with high efficiency (McCulloch *et al.*, 2006), and likewise other cancers, such as prostate and colorectal, were successfully detected by dogs from patient urine, stool, and breath samples (Cornu *et al.*, 2010, Sonoda *et al.*, 2011). Sniffer dogs can

detect lung cancer regardless of pathological type, tumour location and staging, suggesting a clinical potential for diagnosis (Liu *et al.*, 2023).

African giant pouched rats have been able to identify *Mycobacterium tuberculosis* from sputum samples with the same sensitivity as smear examination using microscopy (94%), with microscopy being the main diagnostic tool used for diagnosis in low-income countries (Poling *et al.*, 2015, Reither *et al.*, 2015, Mahoney *et al.*, 2011). Rats also increased paediatric tuberculosis detection by 67.6%, where classical smear microscopy diagnosis usually has a lower sensitivity for children relative to adults (Mgode *et al.*, 2018, Cambau and Poljak, 2020).

Further examples include trained bees, which have also been able to identify a variety of conditions, including SARS-CoV-2 in infected minks (Kontos *et al.*, 2022) and signature compounds from *Mycobacterium tuberculosis* and *Mycobacterium bovis* (Suckling and Sagar, 2011). The use of animals as detectors exhibits the potential for odour to be used as a fast, non-invasive diagnostic tool for diseases such as whipworm.

1.3 VOC Utilisation by Vectors

In addition to VOC detection being a useful tool for disease detection, vectors of parasitic disease, such as mosquitoes, depend on environmental and host cues for host selection for bloodmeals (Cator *et al.*, 2012). Such cues include VOC detection, alongside many other factors, such as temperature, volume, coloration, and preening behaviour, however for mosquitoes and sandflies olfactory cues mostly drive host detection (de Angeli *et al.*, 2022).

Physiological/biochemical changes (like those that cause VOC alterations) may

also alter susceptibility of hosts to parasitic infection. All these attractants are determined by several selective evolutionary pressures. Through comprehensive review, Dormont *et al.*, (2021) determined up to 77 volatile compounds, 11 synthetic blends, and 17 organism odours as attractive to mosquitoes, with L-lactic acid, ammonia, and carboxylic acids included as some of the most common attractants.

Further investigation has occurred involving the effects of odours, especially in relation to attraction/repulsion, with the aims to protect against vector-borne disease and biting insects (Lucas-Barbosa *et al.*, 2022, Yan *et al.*, 2021).

1.4 Linking Odour Changes to Immunity Post-Parasitic Infection

Some studies controversially suspect that some parasites manipulate the host and/or vector to increase pathogen success and transmission (Moore, 2002).

This concept supports the parasite manipulation hypothesis, which dictates that mechanisms facilitating transmission through the manipulation of the host could be evolutionarily selected for (Edelaar *et al.*, 2003, Hernandez-Caballero *et al.*, 2022). Theoretically, parasites having a selective advantage to alter infected organisms would increase transmission success (Thomas *et al.*, 2005).

The extended phenotype provides a conceptual framework for host-vector manipulation. First laid out by Dawkins in 1982, it suggests that when favoured by natural selection, manipulation takes place through parasites modifying host behaviour to benefit transmission, utilizing gene expression to induce phenotypic effects on hosts/vectors. This could occur behaviourally, such as the behavioural changes of rodents infected with *Toxoplasma gondii* to increase

chances of predation (Berdoy *et al.*, 2000), or physiologically, such as through odour changes and habitual blood-feeding changes as suspected in malaria transmission (Cator *et al.*, 2012).

VOCs are, for some blood-feeding vectors of parasitic disease, a determinant for host-seeking behaviour, and so therefore would be a suitable target for manipulation, to increase transmission success.

1.4.1 Parasite Manipulation

One of the most well-documented vector-borne diseases in this area is malaria because of its significant global impact and prevalence. *Plasmodium* is transmitted through female *Anopheles* mosquitoes during bloodmeal (CDC, 2020) (Fig.4).

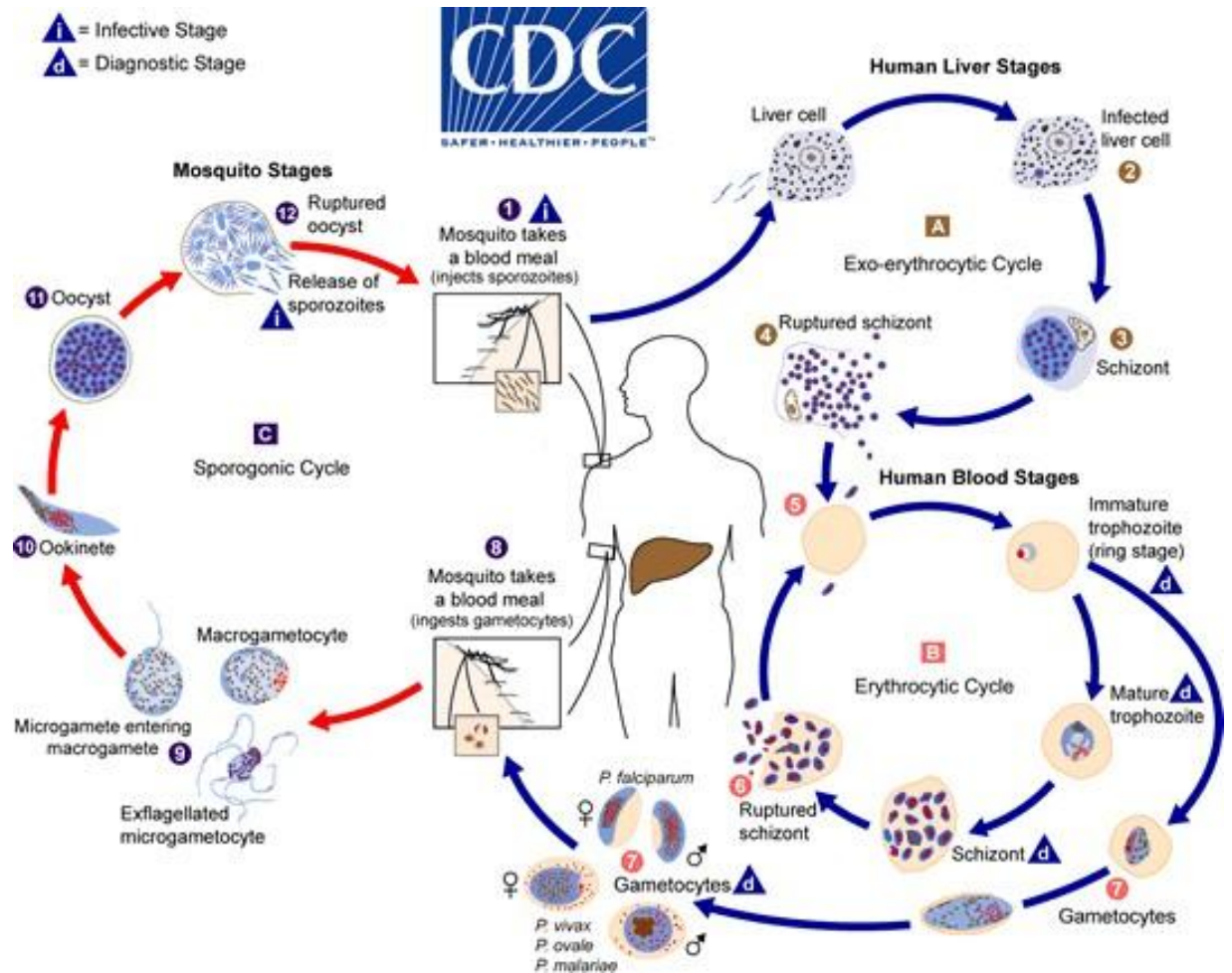


Fig.4. The digenetic lifecycle of the *Plasmodium* genus (Figure from CDC, 2020).

Human host inoculation occurs via sporozoites in a *Plasmodium*-infected mosquito bite, as seen at key 1. Keys 2, 3, and 4 (all encompassed by 'A') marks the exo-erythrocytic cycle, where initial replication occurs in the host's liver.

This cycle advances into the erythrocytic cycle (or erythrocytic schizogony, denoted by keys 5, 6, and 7, under 'B'), where asexual replication occurs within the host erythrocytes.

Differentiation into sexual stages via gametocytes (7) can occur. 'd' denotes clinical manifestation, caused by blood stage parasites. Male gametocytes (microgametocytes) and female gametocytes (macrogametocytes) are transmissible when consumed by a blood-feeding mosquito (8).

The sporogonic cycle occurs within the mosquito vector (keys 9, 10, 11, and 12, under 'C'), where together microgametocytes and macrogametocytes produce zygotes (9). Zygotes give rise to ookinetes (10), which invade the midgut and form oocysts (11). Sporozoite release is catalysed by oocyst rupture (12). These migrate into the salivary glands and infect hosts during vector blood meal (1). Transmissible infection stages are characterised by sporozoite presence (i).

Malaria is infective to many animal species besides humans, including other mammals, reptiles, and birds.

Characteristic alterations and increases in individual VOC emissions are thought to mediate vector attraction. Mosquito behaviour is mainly olfactory-mediated (Takken and Knols, 1999), as long-range host cues are likely detected through differences in the quality or intensity of CO₂ emitted, and/or VOCs acting in conjunction with this (Takken and Knols, 1999, Yan, *et al.*, 2021). Both ammonia alone and synergistically with L-lactic acid were shown to increase *A. gambiae* attraction (Braks, Meijerink, Takken, 2001), and these are both significant components of human sweat.

When Plasmodium is present in the host's blood, VOC changes may facilitate increases the attractiveness of vertebrate hosts to vectors (Cator *et al.*, 2013).

The effect of VOC emissions and the presence of parasite manipulation were also investigated in leishmaniasis, a neglected tropical disease despite high infection rates, morbidity and mortality. This name is an umbrella term, incorporating a spectrum of diseases caused by protozoa in the genus *leishmania* and spread through phlebotomine sandfly vectors during bloodmeal, namely *Phlebotomus* and *Lutzomyia* (Cecílio *et al.*, 2022), as summarized in Fig.5.

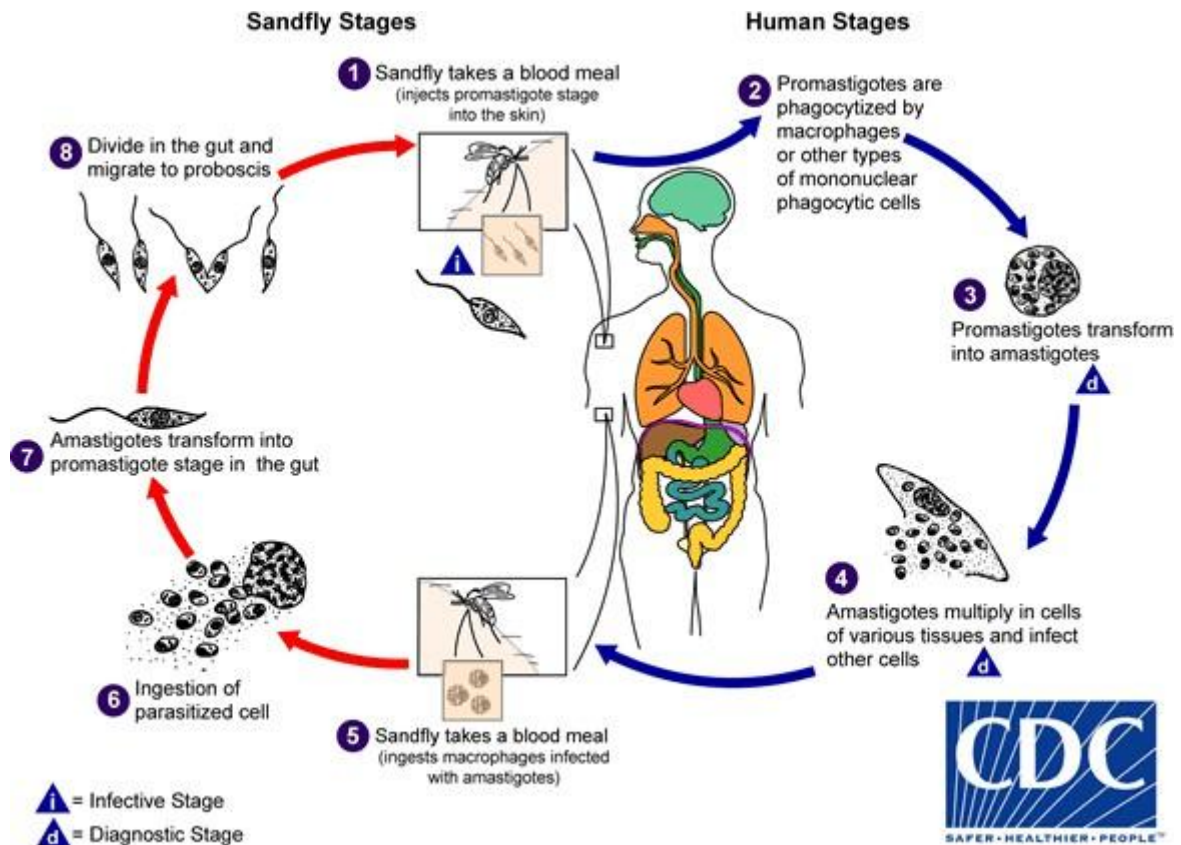


Fig.5. The digenetic lifecycle of the *Leishmania* genus. (Figure from CDC, 2020).

Mammalian host infection with *Leishmania* promastigotes first occurs during infected female phlebotomine sandfly bloodmeal (as seen in key 1). Promastigotes are phagocytised (2), and then establish into intracellular amastigotes (3), which multiply (often in macrophages) and infect other host tissues and cells (4). Determining factors of whether the leishmaniasis infection is symptomatic, visceral, or cutaneous can be determined by both the parasite and host.

When the blood of the mammalian host is fed on, sandflies uptake amastigotes (5, 6). Amastigotes evolve into promastigotes in the infected sandfly midgut (7). Migration into the proboscis (8) allows for the parasite to be injected into a host during blood-feeding. Diagnosis can occur for the host at the stages labelled 'd', (keys 3 and 4), and 'i' denotes when the parasite is infective to the blood-feeding vector.

Leishmaniasis is commonly zoonotic, with the primary reservoirs being canine hosts and the definitive hosts being humans, although other mammals can also experience infection.

Visceral leishmaniasis is the most severe form of disease, with over 90% of cases ending in fatality when left untreated (Alvar *et al.*, 2012), with an annual global prevalence of 50-90 thousand new cases, although only 25%-45% are

estimated to be reported (WHO, 2023). It is commonly caused by *L. infantum* though *L. longipalpis* vectors, with high infection and mortality rates in Brazil, utilizing dogs as a reservoir out of the 70 plus known reservoirs worldwide (Oliveira *et al.*, 2021).

Current control methods rely on early diagnosis, populational awareness, systemic seropositive canine euthanasation, and rapid treatment. Like trichuriasis, VOC recognition and understanding could aid in the diagnosis of this disease.

Investigation into both the direct manipulation of the vector and the indirect manipulation of the host has occurred for both examples (as summarized by Fig.6).

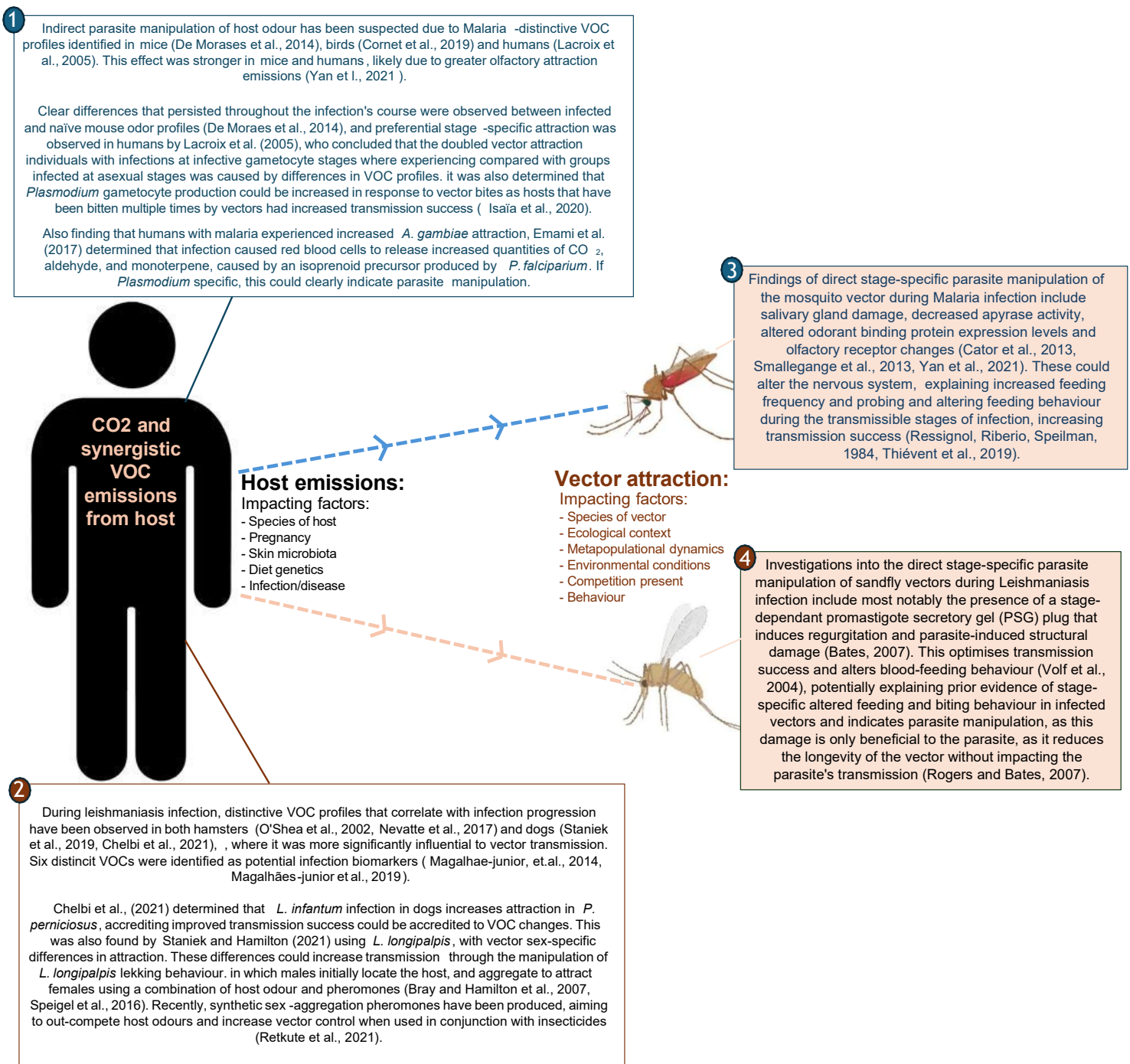


Fig.6. Factors affecting vector attraction to host odour.

Information regarding malaria is denoted in blue (boxes '1' and '3'), whereas information concerning leishmaniasis is represented in black (boxes '2' and '4'). Boxes '1' and '2' summarise current research regarding indirect parasite manipulation (manipulation of the infected host), whereas boxes '3' and '4' summarise current research regarding direct parasite manipulation (manipulation of the infected vector). Figure made with information from Bezerra-Santos *et al.*, (2024) in addition to those referenced within the figure.

1.4.2 Contradictions

Whilst the studies presented in Fig.4 suggest strong evidence pertaining to parasite-specific manipulation, there are contradictions implying that these effects on transmission are instead general consequences of immune response. Current evidence for malaria is debated, with some reporting sensationalism, exaggeration bias, refuting manipulation and some conclusion's validity (Poulin, 2000, Lefèvre, and Thomas 2008, Cator *et al.*, 2012, 2013, Doherty, 2020).

Whilst some studies supported an effect (such as Yan *et al.*, 2021, Cator *et al.*, 2013, and Smallegange *et al.*, 2013), several studies on malaria also contradict, or attest to a lack of effect (such as Nguyen *et al.*, 2017, Cozzarolo *et al.*, 2022, and Stanczyk *et al.*, 2022).

Such contradictions are likely due to the many involved biochemical interactions and compounding factors involved in manipulation, causing an inherent complexity that makes evidence of pathogen-specific manipulation enigmatic and tricky to obtain (Poulin, 1994).

For example, using different species combinations could cause contradicting results by inducing a disproportionate influence of parasite-vector co-evolution, in which selection pressures acting on vectors favor countermeasures against parasites which infect them naturally (Vantaux *et al.*, 2015).

Manipulation mechanisms are an ongoing research area, hoping to differentiate adaptive physiological changes from pathological consequences (Herbison *et al.*, 2018). With current available evidence, a comprehensive understanding of

the occurrence is still out of reach, especially concerning the impact of host-related factors on blood-feeding (Yan *et al.*, 2021).

Conversely, manipulation may not be occurring parasite-specifically, and instead vector attraction could be increased through attraction to general immune responses. Some studies fail to fully acknowledge that the cause of changes in infected organisms could be due to both the parasite infection and its pathological consequences.

Disease/infection, in general, is known to alter the body's emissions, such as VOC profiles (as previously mentioned), microbiota composition, and basal body temperature. This includes factors like CO₂ and temperature, which are common vector attractants (de Angeli *et al.*, 2022, Yan *et al.*, 2021). These changes could be induced, at least in part, by immune challenge or the energetic cost of an infection increasing the chance of transmission success independent of the specific parasite present.

Parasite manipulation is an adaptive fitness strategy which expends energy to reap transmission benefits. If immune challenge already achieves greater transmission success, the evolution of additional direct manipulation mechanisms to exploit this would be unnecessary and costly (Vickery and Poulin, 2010).

In an example supporting this, when stimulating immune challenge without parasite presence, Cator *et al.*, (2013) found that any neurophysical/behavioural changes caused by *Plasmodium* infection could be replicated with striking similarities to the malarial stage-specific alterations that correlate with odorant

receptor responsiveness. In this study, the increased attraction of *A. stephensi* to hosts, which had previously attributed stage-specifically towards *P. yoelii* infection, could be replicated when immune challenge was induced in *A. stephensi* using heat-killed *E. coli* (Cator *et al.*, 2013).

This finding indicates that the presence of malaria parasites does not necessarily facilitate all these changes, and that the explicit extent of *Plasmodium*'s involvement is more ambiguous than previously thought. The involvement of immune response may point to the potential underlying mechanisms for these incidences. Whilst a manipulation mechanism could be inferred through the small quantitative differences found between immune-challenged and malaria-infected mosquitoes in this study, this could instead just be the immune system responding differently to *E. coli* comparatively to malaria. This opens an avenue for research into a better understanding of utilizing VOC profiles for diagnosis, and the causative mechanisms behind them.

The possibility of a causative immune mechanism is further supported by research suggesting that when *Plasmodium*-contaminated blood was ingested by female mosquitoes, mosquitoes that didn't develop sporozoites/oocysts still had significantly different responses from uninfected controls (Stanczyk *et al.*, 2019).

Another demonstration of immune changes linking to indirect odour manipulation can be seen regarding HMBPP ((E)-4-hydroxy-3-methyl-2-allyl pyrophosphate), produced specifically by malaria-infected host blood, increasing mosquito attractiveness (Emami *et al.*, 2017). HMBPP is also a known immune-stimulating molecular pattern (Kabelitz *et al.*, 2007), indirectly

linking changes in odour-post parasitic infection to immune response macroscopically.

Whilst *Plasmodium* has been shown to manipulate the host and the vector, whether this is specific to malaria or a non-specific immunological consequence requires more research. If exactly how the immune system effects VOC emissions were better understood, this knowledge could be incorporated into future treatment plans, diagnosis, and preventive programs for better results and higher success rates.

Concerning leishmaniasis, a similar study to Staniek and Hamilton (2021), which used entrained hair odour from *L. infantum*-infected dogs in y-tube olfactometer bioassays, determined that *L. longipalpis* exhibited preferential attraction to the entrained hair odour of mice infected with *Plasmodium berghei*. *L. longipalpis* is the natural vector of *L. infantum*, however phlebotomine sandflies are unable to transmit *P. berghei*, which is transmitted solely by *Anopheles* mosquitoes on the account of the coevolutionary dynamics of malaria and *Anopheles*' reproductive biology (Mitchell *et al.*, 2015).

This observed preference would therefore indicate an absence of species-specific manipulation, as the manipulating *L. longipalpis* attraction would not benefit *P. berghei* transmission. This is again indicative of attraction being coincidentally beneficial due to general immune response.

This could also imply that the clear differences found between odour profiles of infected and uninfected dogs found by Staniek *et al.*, (2019) correlate to general infection-induced immune response rather than leishmaniasis specifically,

potentially like *Plasmodium*. This could clarify the mechanisms behind disease state-induced VOC changes.

Attraction was seen to parallel immune response. *L. longipalpis* attraction towards entrained *P. berghei*-infected hamster hair odour was positively correlated with the duration of the infection.

Blood-stage gametocyte concentration/malarial infectivity could be thought to be influencing the attraction powers of *P. berghei*, however in later stages of infection gametocyte presence is reduced where immune challenge would remain high. Nevatte *et al.*, (2017) also found that *L. infantum*-infected hamsters were increasingly attractive towards *L. longipalpis* during the progression of the infection.

All this points towards immune response being a major causative agent in the VOC changes caused by parasite infection.

More VOC profiles of hosts infected with *L. infantum* and *P. berghei* could be subject to comparative analysis, to identify any species-specific differences, perhaps using eNose analysis, as indicated by Staniek *et al.*, (2019).

Additionally, flies could be attracted to immune response alone, or a specific type of immune response initiated by disease presence (e.g., Th1 or Th2 immune responses). Immune response is often very specific, involving complex interactions between multiple different immune cell types and cytokines, and so identifying species-specific differences in immune responses and sandfly preference involving these could also be useful.

Manipulation has several active research areas, as it is a multivariate phenomenon made up of highly complex interactions. Specificity is not necessarily required by manipulation to be an adaptive fitness strategy, however non-specific manipulation can be detrimental to transmission success, through increasing the predation of infected hosts or incidences of co-infection (Seppälä and Jokela, 2008). Incurred cost may decrease the adaptive value of the evolution of manipulation.

For example, concerning leishmaniasis and whipworm coinfection, it could be hypothesized that helminth infection could increase susceptibility and morbidity in leishmaniasis infections. In cases where STH infections elicit Th2 immune responses, this would suppress Th1 immune response, causing higher susceptibility for visceral leishmaniasis in endemic regions (Maurya *et al.*, 2012). This is supported by various studies exhibiting detrimental effects of STH-leishmaniasis coinfections causing increased disease severity and poorer therapeutic outcomes compared to solely leishmaniasis-infected individuals (Azeredo-Coutinho *et al.*, 2016).

Conversely, the Th1 immune response has a vital role in decreasing *Leishmania* parasite multiplication (Carvalho *et al.*, 2021), and so it is likely that chronic trichuriasis patients (which elicit susceptible Th1 immune responses) would detriment Leishmaniasis transmission success. However, recently the Hamilton group concluded that chronic *T. muris*-infected mouse hair was more attractive to sandflies as compared to acute infected. This therefore indicates the cause of vector attraction is immune in nature as opposed to parasite mediated. Albeit parasite load differed from high and low dose.

Disputing a link, Tajebe *et al.*, (2017) concluded disease severity in visceral leishmaniasis patients was not greatly impacted by the presence of intestinal parasites, in which a mixed Th1/Th2 immune profile was observed. These results could be due to the high severity of Leishmaniasis used in this study masking such differences.

Regarding malaria and leishmaniasis, there is a geographical overlap between the two, allowing for the occurrence of co-infection (Oliveira-Ferreira *et al.*, 2010, Ornellas-Gracia *et al.*, 2023). A malaria-induced suppressive effect within co-infected patients has been observed, causing increased *Leishmania* load and reduced *Plasmodium* load (van den Bogaart *et al.*, 2013, van den Bogaart *et al.*, 2014): this inhibits malarial transmission, making non-specific manipulation less likely to be evolutionarily selected for in the hypothesized malarial extended phenotype.

Progress into the understanding of this topic falters upon questioning the mechanisms behind potential manipulation, making it harder to distinguish pathological side-effects from adaptive physiological changes (Herbison *et al.*, 2018). Distinguishing between these is important for vector control and disease prevention, as it would illuminate the mechanisms for transmission success and infection. If manipulation occurs, understanding when, where and how it is involved in transmission could greatly advantage diagnostic and preventative methods to reduced infection incidence.

Likewise, if understanding how and what physiological/immunological changes are caused by a disease, diagnostic and treatment methods could be improved.

Whilst the indications of these studies don't exclude any possibility of parasite manipulation, it does imply that immune challenge has a bigger influence over VOC profile changes (and that these are coincidentally beneficial for the parasite). More research involving inducing immune challenge in the host may be beneficial for future study to provide future evidence of immune challenge's involvement into non-specific, indirect manipulation, especially to rule out whether true manipulation really is occurring as opposed to adaptive manipulation (Poulin, 2010). If attraction can be replicated by immune challenge alone, this promotes that parasite manipulation has little/no influence.

Helminth infections have been shown to have unique odour profiles and olfactory preferences (Cevallos *et al.*, 2017).

As previously mentioned, comparison with a parasite that doesn't primarily utilize blood feeding for transmission could also benefit from this, as undertaken using Trichuriasis. This is an ideal model organism, as transmission is not vector dependent and parasite load allows Th1 vs Th2 analysis with the same parasite and host niche. As infected mouse hair was found attractive to sandflies as well, this eradicates any link to a transmission mechanism, confirming the absence of a manipulation mechanism. If levels of attraction are indistinguishable from leishmaniasis-induced VOC profiles, this could identify that one of the main causative agents for VOC changes during infection is immune response.

1.5 Mechanisms of Immune Response

Invading parasites are first affronted with the host's innate immune response, which responds rapidly and non-specifically via the rapid recruitment of immune

cells and local inflammation in response to pathogen associated molecular patterns (PAMPs) detected by pattern recognition receptors (PPRs) (Marshall *et al.*, 2018). The activation and mobility of immune cells such as macrophages, neutrophils, dendritic cells, basophils, mast cells, natural killer cells, eosinophils, and innate lymphoid cells are triggered by the resulting chemokines and cytokines.

Specific acquired immunity is aided by innate immunity, inducing pathogen-specific immunologic effector pathways that eliminate specific pathogens or infected cells through non-self antigen recognition, and the formation of immunologic memory through adaptive T and B cells. Antigen-specific T cells activated by antigen-presenting cells and B cells that differentiate into plasma cells are involved in these functions.

1.5.1 Whipworm as an Immunological Tool

Animals can be used as tractable models for various human diseases, to allow for a better development of understanding, detection and treatment (Phillips and Roth, 2019). *Trichuris muris* in mice has been used to model human trichuriasis for over 60 years, allowing better visualization and understanding of the infection's lifecycle, dose-dependent infection outcomes, and corresponding immune mechanisms (Hubbard *et al.*, 2023). Similar to *P. berghei* use concerning research into malaria, *T. muris* has been a long-standing, useful model, contributing to research into parasite and host responses to human infections, including host susceptibility and resistance, insights into immune responses to infection/challenge *in situ* in a multivariate environment, and informing decisions on anthelmintics and vaccine research for disease control

(Hurst and Else, 2013, Mair *et al.*, 2021). This parasite has also been incorporated as a biomedical tool for research into mucosal inflammation, nematode-secreted immunomodulatory molecules, and Th1/Th2 -mediated immune responses (based on egg infection low/high dose respectively).

T. muris and human-infective *T. trichiura* are very similar species, with approximately 50% of the 10-11,000 predicted gene products identified as one-to-one orthologues with 79% average amino acid identity, as found during genome and transcriptome analyses from Foth *et al.*, (2014). Such analyses have further broadened the base of whipworm knowledge, as exemplified by Tritten *et al.*, (2017) and Shears and Grencis (2022) concerning whipworm Excretory/secretory product composition (aiming to provide a basis of vaccine research) providing greater understanding of host-whipworm interactions and host immunity modulation.

Paired with the array of genetically modified strains of mice and the logistical advantages of mice as laboratory animals, mouse models of *T. muris* are conclusively of great use and importance (Hubbard *et al.*, 2023). *T. muris* in mouse models rarely impacts the hosts' ability to maintain proper hygiene or disrupts eating and sleeping habits, with Giacomini *et al.*, (2018) finding changes such as spatial recognition memory deficits and anxiety-like behavioural phenotypes at 9 months post-chronic infection. These changes are less significant and severe than those that *Leishmania* or *Plasmodium* infection would have on mice, however, which could additionally also involve lethargy, weight loss, significant memory impairment, motor deficits, seizures (Desruisseaux *et al.*, 2009, Portes *et al.*, 2016).

This would make any changes to the host's odour profile more likely infection and the resulting immune response-induced, as opposed to behavioural changes (like diet or grooming activity) that may occur when in research investigating distinctive odour profiles during *Leishmania* or *Plasmodium* infection, especially if the whipworm infection was transient.

1.5.2 Immune Responses to *T. muris* Infection

1.5.2.1 TH1/TH2 Responses

Past studies have identified that Th2 immune responses are vital for parasite expulsion (Fig.7), mechanized by the cytokine production of mainly interleukin (IL)-4, IL-9, IL-5, and IL-13 and the generation of an IgG1 response (a parasite-specific immunoglobulin G1 response) (Mair *et al.*, 2021). Expulsion usually occurs in mice 18-21 days after primary infection, due to the combined efforts of innate and adaptive immunity (Phillips *et al.*, 1974).

Conversely, susceptible mice incur an inappropriate Th1-polarised immune response, in which high levels of IL-12 and IFN- γ are present, and a parasite-specific IgG2 response is generated, enabling chronic infection (Else *et al.*, 1994, Artis, 2006, Hadidi *et al.*, 2012).

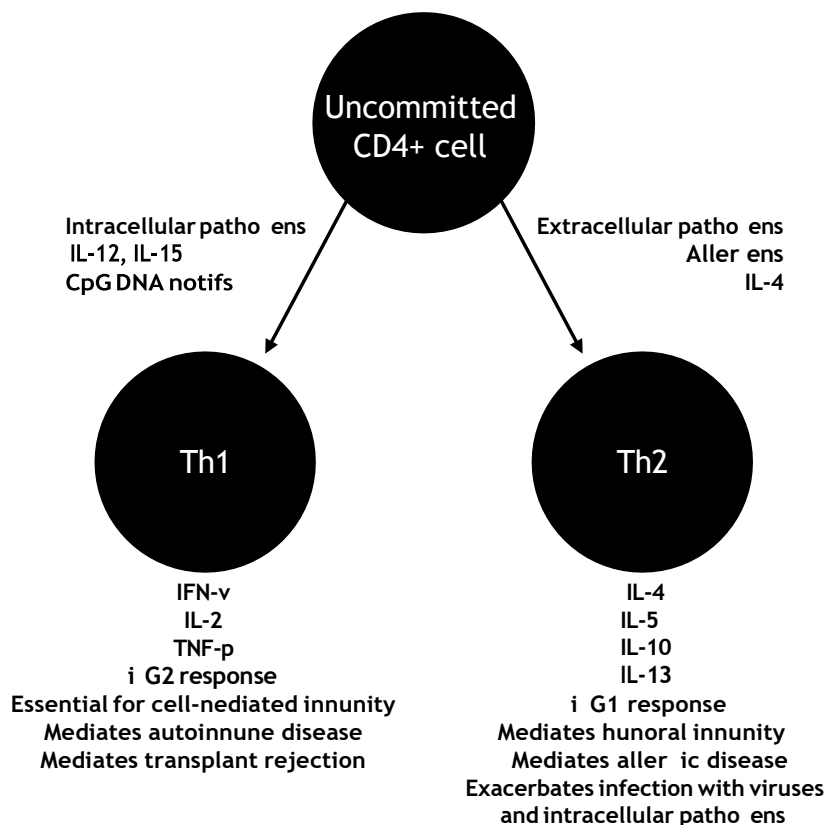


Fig.7. Th1 and Th2 response differentiation (adapted from Umetsu and Dekruyff, 1997)

Type 1 T helper (Th1) cells are induced in the presence of intracellular pathogens, IL-12, IL-18, foreign CpG DNA motifs found on non-vertebrates, and low doses of *Trichuris*, inducing the responses listed above.

Type 2 T helper (Th2) cells are induced in the presence of extracellular pathogens, allergens, IL-4 and high doses of *Trichuris*, triggering the responses listed in the figure.

1.5.2.2 Genetic Predisposition

The genetic background of the host is likely to predispose the susceptibility of the individual to *T. muris* infection. When exposed to high doses, some mice strains are *T. muris* resistant, Balb/C, C57BL/6 resulting in total worm elimination by approximately day 32 post infection via the promotion of a genetically predisposed Th2 dependent immune response, whilst AKR develop a chronic infection. The

remaining mice strains (for example, B10Br, AKR, and C57Bl/6) if infected with a low dose develop chronic infection due to the development of a Th1 dependent immune response (Cliffe and Grencis, 2004).

Predisposed genetic susceptibility particularly concerns differences within the H-2 alleles of mice's major histocompatibility complex (Klementowicz *et al.*, 2012), as in mice with similar genetic background, it has been shown that these can influence CD4+ T cell activation, leading to distinct phenotypic responses to whipworm infection (Else *et al.*, 1990). Additionally, past studies have suggested that resistance can be altered in groups of congenic strains, even when sharing the same H-2 haplotype (Else and Wakelin, 1988).

The H-2 complex can influence parasite expulsion, however the outcome of this infection in mice is determined mostly from genes outside of the MHC complex. Parasites are expelled faster in mice with specific resistant H-2 alleles within the I-A region, of which the influence of these genes are modulated by differences in the D end of the H-2 complex between these strains (Else *et al.*, 1990).

This accounts for how whilst sharing the same H-2k haplotype, BALB/k mice generate a resistant Th2 response, whereas infection in AKR mice becomes chronic, accompanied by a Th1 response (Else *et al.*, 1992).

In addition to modulating predisposition, much evidence has amounted indicating the influence of these genes in the individual odour profiles of mice and rats (Wedekind and Penn, 2000). The influence of MHC in odour has been thought to link to mating preference in order to combat parasites evolving to host MHC genotypes (Penn and Potts, 1999). The MHC control immunological self/nonself recognition. Penn and Potts (1999) state that house mice prefer genetically dissimilar MHC mates, which could be to avoid inbreeding, but also

could submit to an evolutionary pressure that favours the production of MHC heterozygous offspring with enhanced immunocompetence and greater resistance to multiple parasites.

MHC molecules have also been found to occur in sweat and urine (Singh *et al.*, 1987). It is hypothesized that metabolized MHC-bound peptides are made volatile by microbes, hence contributing to odour/VOC emissions (Penn and Potts, 1998²). As previously stated, some vectors could be attracted to different immune responses and likewise could utilise these for pathogen transmission.

1.5.2.3 Infective Dose

In addition, to host genetics and gender, infective dose size can also alter the susceptibility to *T. muris* infection in mice (Klementowicz *et al.*, 2012). The development of Th1 responses is favoured when the infective dose is small. Low dose infections in BALB/k mice (less than 40 eggs as opposed to a high dose of 400 eggs) induced chronic infection through altering CD4+ response (Bancroft *et al.*, 1994). Additionally, resistance to subsequent both low and high dose infections can only be facilitated by a previous high dose infection (Bancroft *et al.*, 2001). The reason behind host response being polarized dose-dependently is unclear- it may be an environmentally influenced genetically set threshold triggered when the cost of the parasite is too great compared to the cost of Th2 response and repair (Colombo and Grecis, 2020).

Hosts *in situ* are repeatedly infected with low doses. When natural infections are modelled in mice using trickle infection as prior described, Glover *et al.*, (2019) found a slow acquisition of immunity took place, mirroring a gradual increase in worm burden prior to partial worm expulsion. Underlying this, the dominating CD4+ T cell response shifted from Th1 to Th2 response, inducing increasing

Th2 cytokine populations. Resistance development following this infection method was linked with the mechanization of worm expulsion. This was confirmed when CD4+ T cell depletion reversed resistance. Trickle infections also induced dysbiotic microbiota, which following resistance could recover alpha diversity. The modes of resistance involved in single-dose vs trickle infection are practically identical, however differences underlie the environment of the initial response, as in trickle infections, Th2 immunity must develop within the context of a mutually antagonistic active Th1 response (Colombo and Grecis, 2020). Trickle infection reflects natural infection conditions, informs about immunity and chronic infection, and confirms the importance of CD4+ T cells.

1.5.2.4 Parasite Genetics

There are three different laboratory-used isolates of *T. muris*; E (Edinburgh), J (Japan), and S (Sobreda), and these can elicit different reactions from the hosts' immune response (Koyama and Ito, 1996).

Chronic infection was established when B10.BR, C57BL/10, and CBA mice, which are resistant to E and J isolates, were inoculated with the S isolate (Koyama and Ito, 1996, Bellaby *et al.*, 1996). S isolate-infected mice in these cases likely established chronic infection due to increased levels of IFN- γ and Th1-associated Ig2a production, promoting a Th1 response, whereas when infected by E or J isolates, Th2 associated IL-5 and higher Th2-associated IgG1 were elicited.

In C57BL/6 mice, which develop chronic infection towards S isolates, but are resistant to E isolates, susceptibility has been correlated to increases Treg

numbers in the gut of S isolate-infected mice (D'Elia *et al.*, 2009), indicating that Tregs promote chronic infection and inhibit protective immunity development.

1.5.3 Components of Immunity

1.5.3.1 Cytokine Involvement

Cytokines are small signalling proteins involved in inflammation and immunity, often expressed in both innate and adaptive immunity. In susceptible models, it is likely that gastrointestinal worms can modulate immune host responses to prevent/delay expulsion, such as by utilizing the inappropriate development of Th1 response to promote chronic infection (Klementowicz *et al.*, 2012).

Susceptible mouse strains produce high levels of Th1 response-associated cytokines, IFN- γ , IL-12 and IL-18 (Cliffe and Grencis, 2004). Supporting this, depletion of these cytokines has rendered normally susceptible hosts resistant (Else *et al.*, 1994, Helmby *et al.*, 2001). Susceptibility did not develop in mice lacking the IL-27 receptor WSX-1 - this is thought to be because Th1 responses are triggered in susceptible hosts via the interaction between IL-27 and WSX-1 at early infection stages (Klementowicz *et al.*, 2012). WSX-1 KO hosts have been shown to experience increased Th2-associated cytokine production and decreased Th1-associated cytokines (Bancroft *et al.*, 2004).

T. muris could produce an IFN- γ homologue that could contribute to host immune regulation in a way which promotes parasite survival, indicative of parasite manipulation (Grencis and Entwistle, 1997). IL-13, critical to worm expulsion, can be neutralized by p43: a single poly-cysteine and histidine tailed protein secreted as over 90% of the total secreted protein of adult *T. muris* (Bancroft and Grencis *et al.*, 2021, Bancroft *et al.*, 2019). This could be indicative of parasite manipulation.

Prolonged inflammatory responses during chronic *T. muris* infection can cause host-detrimental immunopathology to develop, exacerbating immune system responses to other agents. Systemic up-regulation of pro-inflammatory mediators during chronic infection have led to detrimental impacts in mice (Dénes *et al.*, (2010), which supports the extended phenotype theory. Th1 Inflammatory response could alter the host's VOC production long term, differentiating host odour from naïve counterparts.

Concerning acute infection, resistance-associated cytokines induce parasite expulsion by establishing a Th2 immune response, usually against high dose whipworm infection. Major cytokines of note include IL-4 and IL-13 (Grencis, 2001), as mice deficient in either are liable to chronic infection (Bancroft *et al.*, 1998). Additionally, IL-13 neutralisation can convert female BALB/c IL-4 KO mice to a *T. muris*-susceptible phenotype. This indicates a dominant role for IL-13 regarding *T. muris* immunity.

Additionally, tumour necrosis factor- α (TNF- α) -treated susceptible IL-4 KO mice can prevent chronic infection (Artis *et al.*, 1999). However, TNF- α is thought to enhance ongoing immune response in either Th1 or Th2, and is a non-essential component of immunity development, as TNF- α can also promote stronger Th1 responses in previously susceptible mice (Hayes *et al.*, 2007). It is likely that IL-4 and/or IL-13 in combination with a range of Th2-related cytokines alter the intestinal environment in such a way that allows for efficient *T. muris* expulsion (Klementowicz *et al.*, 2012).

Also of note, IL-9 could have early protective immune response involvement (Faulkner *et al.*, 1998), as evidenced through acute infection models and neutralisation experiments (Richard *et al.*, 2000).

The IL-10 receptor family and IL-10 signalling have also been known to promote Th2 immunity and modulate intestinal inflammatory responses to limit/regulate immunopathology (Duque-Correa *et al.*, 2019, Schopf *et al.*, 2002). There are inter-specific differences concerning IL-10's involvement in Th1/2 responses between mice and humans, as in mice IL-10 is regarded as a Th2 cytokine, but it can be secreted during both Th1 and Th2 responses in humans (Rasquinha *et al.*, 2022), and so corresponding differences may be seen between *T. muris* and *T. trichuris* infection models.

Early immune events are likely important for combating trichuriasis, especially with past studies indicating that novel innate cell populations (primarily those interacting with/secreting the alarmin cytokines IL-25 and IL-33, for example: tuft cells (Myhill *et al.*, 2018)) initiate Th2 immunity during gastrointestinal parasite infections (Neill and McKenzie, 2011).

IL-25 and IL-33 help induce innate lymphoid cells and facilitate resistance (Humphreys *et al.*, 2008, Saenz *et al.*, 2010²). IL-25 can induce Th2-promoting GALT-specific MMP^{type2} cells (now characterised as ILC2s), and IL-33 can stimulate Th2-associated IL-4, IL-9 and IL-13 production (Saenz *et al.*, 2010¹). Th2 immunity has been linked to IL-33 through its involvement in the activation of NF-κB and MAP kinases via the IL-1 receptor ST2, commonly expressed on mast and Th2 cells (Harris, 2017, Schmitz *et al.*, 2005). IL-33-mediated resistance appears T cell-dependant as despite increased production as early

as day 3 post-infection, this treatment does not result in worm expulsion later during chronic infection, and IL-33 treated SCID mice remain susceptible despite increasing pathology (Humphreys *et al.*, 2008).

Humphreys *et al.*, (2008) also found increased IL-33 production during early infection in resistant mice strains synced with increased TSLP (Thymic stromal lymphopoietin) production. TSLP is an important Th2-inducing intestinal epithelial cell-derived alarmin cytokine that acts on a wide range of immune cells, as evidenced by the impaired Th2 cytokine production and increased *T. muris* susceptibility caused by disrupted TSLP-TSLP receptor (TSLPR) interactions (Massacand *et al.*, 2009). Taylor *et al.*, (2009) found that the ineffective parasite expulsion phenotype brought on by these induced disruptions had causative links to gut inflammation and pro-inflammatory cytokine production (such as IL-12/23, IFN- γ , IL-17A). TSLP was implicated in early immune priming and Th2 response against *T. muris*, through IFN- γ neutralisation and resistant phenotype restoration in TSLPR KO mice.

1.5.3.2 Innate Immune Cell Involvement

Innate lymphoid cells (ILCs) are abundant at non-mucosal and mucosal barriers in addition to lymphoid and non-lymphoid tissues (Darlan *et al.*, 2021). Th2-associated response and anti-helminth control is supported by ILC2s, which can be stimulated in response to epithelial cell-derived alarmin cytokines like IL-25, IL-33, and TSLP (Artis and Spits, 2015). In turn, this facilitates the production of IL-4, IL-9, IL-5, IL-13 and amphiregulin (Kumar, 2014). MHC class II presence on ILC2s allows for communication between ILC2s and CD4⁺ T cells to further promote Th2 immunity (Oliphant *et al.*, 2014). ILC2s may not be essential for

clearance however, as *T. muris* expulsion in iCOS-T mice was not affected by lack of ILC2s (that was induced by diphtheria toxin treatment) (Glover *et al.*, 2019).

Depletion in other innate cell groups like FcεRI⁺ reduced intestinal Th2 responses and correlated with increased *T. muris* worm burden (Perrigoue *et al.*, 2009).

Basophils fortify defensive immune response during infection (Yousefi *et al.*, 2021). Upon immune activation, basophils express MHCII and produce Th2-inducing cytokines (e.g., TSLP, IL-4), directly inducing Th2 defences and assisting dendritic cell (DC)-mediated Th2 differentiation (Perrigoue *et al.*, 2009, Sokol *et al.*, 2008, Sokol *et al.*, 2009, Wynn, 2009). Worm expulsion was also impaired when basophil-specific notch inhibition was induced (Webb *et al.*, 2019). During acute infection, reduced basophil numbers were linked to reduced IL-5, IL-13, and worm expulsion in TSLP receptor KO mice (Siracusa *et al.*, 2011). However, whilst worm burden was reduced, expulsion was still delayed relative to controls when adoptive basophils were transferred into these mice models, suggesting an indirect involvement. Th2 response development was not inhibited in basophil-deficient mice with other helminths infections, (*Nippostrongylus brasiliensis*, and *Schistosoma mansoni* (Kim *et al.*, 2010, Phythian-Adams *et al.*, 2010, Sullivan *et al.*, 2011)), prompting further investigation into basophil involvement concerning *T. muris* infection.

Mast cells also exhibit crucial roles in host defence against numerous parasites, activating and accumulating at infection sites. Elevated mast cell numbers have been discerned during *T. muris* infection (Lee and Wakelin, 1982), and are

linked to Th2 immune activation, with such accumulations remaining at the site of *T. muris* infections up to several months post (Sorobetea *et al.*, 2017). In susceptible mice (where Th1 responses dominate) mast cell accumulation cannot be seen. As shown by Lee and Wakelin (1982) using NIH mice, mast cell presence at the infection site doesn't always correlate with worm expulsion, however when IL-9-secreting T cells are transferred into *T. muris* infected mice, mast cell numbers increase at the site of infection and correlate with elevated mMCP-1 (mouse mast cell protease 1) serum levels, causing faster worm expulsion (Faulkner *et al.*, 1998).

Mast cell-derived proteases have indicated to maintain barrier integrity through epithelial permeability (Sorobetea *et al.*, 2017). Aside from any potential links to expulsion, it could also be indicative of long-lasting impacts within the gut environment and on intestinal-barrier integrity, in turn potentially altering microbiome compositions and therefore fecal VOCs during trichuriasis infection. Despite all of this, it is likely that mast cell involvement for protective immunity against this parasite is minor, despite naturally mast cell-deficient mice experiencing delayed expulsion, because wild-type counterparts can undergo expulsion with no indication of mastocytosis (Koyama and Ito, 2000). Antibody neutralization of stem cell factor receptors (c-kit receptors) (vital for mast cell development) had no effect on expulsion, supporting a dispensable role (Betts and Else, 1999). Further study into the mast cells is needed to clarify the extent of this involvement.

Significantly higher levels of colonic epithelial chemokines such as CCL2, CCL3, CCL5, and CCL20 can be found during early infection in resistant mice

compared to susceptible mice. Such chemokines induce DC recruitment to the large intestine (Cruickshank *et al.*, (2009). Susceptibility/resistance to trichuriasis infection may be linked to differences in DC phenotype, with the different responses garnering differing DC kinetics (Harris, 2017).

Resistant mice (when compared to susceptible mice) experience faster DC mobilization to the infection site, and DCs seem to mature faster, displaying higher expression of CD80/86, MHCII and CCR7, and lower endocytic activity (Cruickshank *et al.*, 2009, MacDonald and Maizels, 2008). Colonic DCs form transepithelial dendrites in resistant mice, uncommon in controls, directly supply luminal *T. muris* antigens to naïve T cells. Antigen transfer via pinocytosis in colonic epithelial cells can be assisted by DCs to facilitate more efficient antigen uptake and immune response. As this is not observed in control mice, this likely has a significant impact on resistance development.

Perrigoue *et al.*, (2009) found that restricted MHC class II (MHCII) expression to DCs was not enough to generate a Th2 cytokine production and prevent parasite expulsion, suggesting the generation of Th2 responses during *T. muris* infections does not entirely require DCs. Restoration of the resistant phenotype using DC-restricted MHCII treatment and IFN- γ neutralizing antibodies suggested that Th2 responses can be triggered by DCs during infection if Th1 responses are repudiated. In other studies involving alternative parasite infections and alternative strategies for basophil and DC nullification, DCs were crucial components for parasite-induced Th2 defences (Kim *et al.*, 2010, Ohnmacht *et al.*, 2010, Phytian-Adams *et al.*, 2010, Sullivan *et al.*, 2011), so it is possible that this observation is either specific to *T. muris* or specific to Perrigoue *et al.*, (2009). Despite limited knowledge on any initial immune

regulation regarding *T. muris* response, it remains likely that at initial stages of infection DCs play a significant role in generating and determining effective immune responses, as in resistant mice the initial recruitment of DCs occurs days prior to adaptive immune response production (Cruickshank *et al.*, 2009, Little *et al.*, 2005, Else *et al.*, 1994).

Another professional antigen-presenting cell, macrophages, an important antigen presenting cell (APC) for both Th1 and Th2 responses, is thought to have a critical role in the immune response to gastrointestinal helminths.

Alternatively activating macrophages (AAMs) also have a suspected involvement concerning tissue repair, as AAM populations increase post worm expulsion (Little *et al.*, 2014, Sorobetea *et al.*, 2018).

Despite this, the absence of mannose receptors on AAMs did not deter parasite expulsion, and so these receptors are likely non-essential for immune response generation (De Schoolmeester *et al.*, 2009). Deficiencies in the enzyme arginase-1 (a key effector and marker within particularly the Th2-associated M2 subset) also had no effect on expulsion and immune response (Bowcutt *et al.* 2011). It is therefore likely that despite being involved in immune response, macrophages seem to be not directly necessary for worm expulsion.

Elevated numbers of eosinophils (another important APC for Th2 responses) in the colon and mesenteric lymph nodes (MLNs) during *T. muris* infection were found to be present in resistant mice (Dixon *et al.*, 2006, Svensson *et al.*, 2011). This is likely caused by IL-5 and the chemokine CCL11, which synergistically recruit eosinophils to the colonic mucosa during *T. muris* infection, as shown by Dixon *et al.*, (2006) in CCL11 KO mice models (which reduced numbers in the

colon), and CXCL11 and IL-2 double KO mice models (in which eosinophilia is entirely absent). Additionally, using anti-IL-5 antibodies to neutralize eosinophils dropped recruitment to infection sites (Betts and Else, 1999).

Research conducted by Svensson *et al.*, (2011) indicates that these cells contribute to Th2 response-associated resistance, as an activated phenotype that can produce IL-4 was discovered in eosinophils and was found in the MLNs of resistant mice, initiated during the second week post-infection and peaking during worm expulsion. This is likely dispensable for protective immunity however, as expulsion and the Th2 response were found to be independent of the reduction/depletion of eosinophils during trichuriasis. Several papers have indicated that neutralizing IL-5 and decreasing eosinophil populations did not restrict *T. muris* reproduction, elimination or survival (Betts and Else, 1999, Dixon *et al.*, 2006, Svensson *et al.*, 2011, Sorobetea *et al.*, 2017).

Natural killer (NK) cells are another extension of innate immunity, and initiate defence through antibody-dependent cellular cytotoxicity and exhibiting APC qualities. Whilst CD4+ T and DX5+ NK cells can source IL-13 in IL-4 KO mice, only DX5+ NK cell depletion results in the inability to clear parasites (Hepworth and Grecis, 2009). NK cell-deficient mice models have exhibited delayed worm expulsion (Krauss, 2018), with gender-based differences in immune response, and expulsion is often linked to NK cells (Martín-Fontecha *et al.*, 2004, Wald *et al.*, 2006).

1.5.4 Adaptive Immune Cell involvement

T cells are major components of the cell-mediated adaptive immune response and have been known to moderate *T. muris* expulsion since 1983 (Lee *et al.*), when the transfer of T cell-enriched populations from infected hosts into naïve recipients conferred immunity and parasite expulsion. This is supported by the apparent susceptibility of athymic mice (which lack T cells), where a resistant phenotype could be restored through transfer of mesenteric lymph node cells (Ito, 1991). It is therefore likely that T cells and gut-homing T cells play an indispensable role in whipworm expulsion (Hammerschmidt *et al.*, 2008).

Protective immune responses against *T. muris* seem to be mainly regulated by helper T cells, as the use of neutralising antibodies for CD4+ T cells but not for CD8+ T cells resulted in an immune response associated with susceptibility (Koyama *et al.*, 1995, Humphreys *et al.*, 2004, Koyama, 2002). Resistant infected BALB/c mice were shown at the time of expulsion (approx. day 21 post infection) to have increased CD4+ intraepithelial lymphocytes (IELs), whereas susceptible AKR mice were shown to have majority CD8+ during IEL analysis of the large intestine (Little *et al.*, 2005).

The depletion of CD4+ T cells resulted in susceptibility, whereas NK1.1+ natural killer cells with neutralizing antibodies or CD8+ T cells did not (Koyama *et al.*, 1995, Koyama, 2002, Humphreys *et al.*, 2004). Past studies have revealed that the development of *T. muris* protective immunity is likely almost exclusively dependent on CD4+ T lymphocytes and the related cytokines, and that this involvement may be an involved factor in infection-induced VOC changes.

Further evidence for the importance of CD4⁺ cells has been provided by Else and Grecis (1996), where adoptive transfer of BALB/c mice's CD4⁺ T cells into susceptible severe combined immunodeficiency (SCID) mice resulted in parasite expulsion, however expulsion failed when this transfer occurred on day 34, linking how CD4⁺ T cells likely mediate expulsion at the larval stage of the parasite.

When at larval stages, CD4⁺ T cells acting locally at the infection site are the most effective at promoting expulsion, as inhibiting β 7 and α E integrins (gut homing receptor and MAdCAM-1 (a gut homing ligand)) prevented parasite explosion that would otherwise occur when transferred CD4⁺ T cells are transferred into SCID mice (Betts *et al.*, 2000, Svensson *et al.*, 2010).

Interestingly, Svensson *et al.*, (2010) found that inhibiting the chemokine receptors CCR6 and CXCR3 did not prevent parasite expulsion, despite these receptors being considered the most

abundant chemokine receptors expressed by CD4⁺ T cells in mesenteric lymph nodes and vital for gut homing by T cells (Klementowicz *et al.*, 2012).

Additionally, age decreases stimulation and the ability of CD4⁺ T cells to polarize into a Th2 response, making usually resistant mice increasingly susceptible (Humphreys and Grecis, 2002). VOC profiles can also be altered by characteristics like age.

Whilst at least one of the key Th2-associated cytokines (e.g., IL-4, IL-5, IL-9 and IL-13) are secreted by the aforementioned innate immune cells (basophils, eosinophils, mast cells), they are often sourced more majorly from ILC2s and CD4⁺ Th2 cells (Yousefi *et al.*, 2021). More specifically, when mice were

deficient in IL-4, which stimulates mucin production in enterocytes, and in IL-13, which causes goblet cell hyperplasia (both beneficial for expulsion), this conferred a susceptible phenotype (Darlan *et al.*, 2019, Sharba *et al.*, 2019). IL-9, a pleiotropic cytokine with studied links to Th2 responses, is mainly secreted by a subset of distinct CD4⁺ T cells (Th9 cells). IL-4 and TGF- β (transforming growth factor β) together can reprogram CD4⁺ T cells into Th9 cells (Dardalhon *et al.*, 2008, Veldhoen *et al.*, 2008). TGF- β alone is important, as shown through CD4-dnTGF- β RII mice (in which CD4⁺ T cells' ability to respond to TGF- β has been stunted by a truncated TGF- β receptor) (Veldhoen *et al.*, 2008). These mice displayed increased worm burden, decreased levels of IL-4 and IL-9, but normal IL-13.

IL-9 was likewise proved critical through the utilisation of neutralising antibodies by Khan *et al.*, (2003).

Regulation of parasite burrowing-induced intestinal inflammation is vital in chronic infection to prevent sepsis, and in *T. muris* IL-10 and T regulatory (Treg) cells (a subpopulation of CD4⁺ cells) prevent *T. muris*-induced intestinal damage through Th2 response cytokine inhibition, facilitating worm survival (Schopf *et al.*, 2002). The depletion of Tregs at early and late infection stages caused low dose infected mice to experience different immune outcomes. Early depletion led to an enhanced Th2 response and a stunted Th1 response, accelerating expulsion rates. Conversely, late depletion after the establishment of infection increased worm burden. This provides evidence that Tregs inhibit Th2 cell expansion during whipworm infection prior to T cell polarization establishment (Sawant *et al.*, 2014). D'Elia *et al.*, (2009) found parasite

expulsion of the S isolate could be enabled when Treg cells were reduced through treatment with anti-CD25 antibodies, but these cells were still vital for protecting against intestinal pathology.

Concerning IL-10, a key cytokine produced by Tregs, deficient mice infected with high doses experienced worse colitis and heavier worm burden than controls, inferring that IL-10 not only contributes to the Th2 immune response, but also regulates IFN- γ -induced inflammation (Grencis *et al.*, 2014, Schopf *et al.*, 2002).

Regarding humoral adaptive immunity, B cells can act as APCs and secrete cytokines. B cells have been shown to produce VOCs, selected by MHC alleles, resulting in cell-specific 'odour fingerprints' distinguishable by GC-MS (Aksenov *et al.*, 2012). Already involved in determining VOC profiles, these cells could also be involved in infection-induced odour changes, alongside cells such as ILC2 and ILC3 and basophils, which also exhibit MHC but thus far have no current established research into these cells concerning cell-specific odour. The antibodies (Ig) B cells produce have an involvement with protective immunity generation against *T. muris* (Koyama *et al.*, 1995, Blackwell and Else, 2001). The relative concentration of antigen present likely correlates proportionally to parasite burden (Colombo and Grecis, 2020). IgA- and IgG-producing cells have been seen in MLNs beyond days 14 and 21 post infection (Koyama *et al.*, 1999, Blackwell and Else, 2002). IgA and IgG1 transfer from resistant mice caused a partial restoration of the resistant phenotype in susceptible mice, likely due to antibody-mediated neutralization of parasitic antigens and antibody-induced larval trapping (Sorobetea *et al.*, 2018). Elevated

IgG1 levels have been denoted in resistant animals, correlating to the development of the Th2 response, and likewise has been noted for elevated IgG2 levels in susceptible mice, linking to Th1 immunity.

B cells have been deemed nonessential for the generation of an efficient Th2 response, although they seem to aid in Th2 response enhancement (Sahputra *et al.*, 2019). Successful parasite expulsion has been observed independent of B cells through the adoptive transfer of CD4+ T cells into SCID mice (Else and Grecis, 1996) indicating this. However, B-cell deficient μ MT mice have been shown to be *T. muris* susceptible, and that resistance can be restored through adoptive B cell transfer or IgG administration from infected resistant mice (Blackwell and Else, 2001). Due to such contradictions, the function of B cells and antibodies concerning *T. muris* infection necessitate further study.

1.5.5 Expulsion

The expulsion of *T. muris* is initiated by Th2 response, and incorporates intestinal epithelial cell turnover, goblet cell/mucin production, and hypercontractility of the smooth muscle (Fig.8).

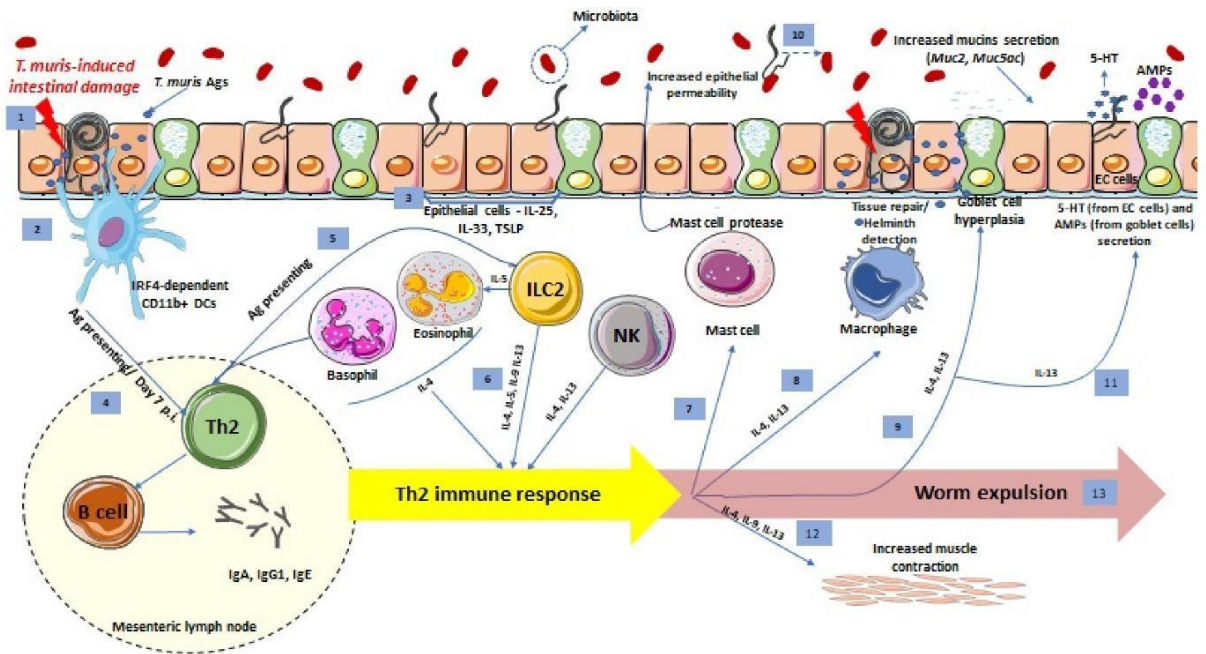


Fig.8. A representative schematic of the Th2 Intestinal immune response and subsequent expulsion of *T. muris* infection, as seen in Yousefi *et al.*, (2021).

(1) *T. muris* larvae breach the intestinal epithelium, and *T. muris* antigens are released. (2) *T. muris* antigens are taken up by IRF4-dependant CD11b+ dendritic cells. (3) Alarmin production is initiated by Intestinal epithelial cells to recruit immune cells. (4) At day 7 post-infection, dendritic cells present *T. muris* antigens to adaptive immune cells present in the mesenteric lymph node, activating Th2 cells, the central source of Th2 cytokines. B cells are stimulated by these Th2 cells, causing the synthesis and secretion of IgA, IgE, and IgG1. (5) Innate immune cells also present antigens to adaptive immune cells in the mesenteric lymph node. (6) Th2 cytokines are released by basophils, eosinophils, ILC2s and NK cells (innate immune cells), promoting a Th2 response. A Th2 response is indicative of; (7) mast cell activation to release mast cell protease, increasing the permeability of epithelial cells, (8) alternatively activated macrophage development, allowing for tissue repair and helminth detection, and (9) goblet cell hyperplasia and increased mucin (namely Muc5ac and Muc2 secretion). (10) Microbiota composition is affected by *T. muris*, which can influence barrier function and mucin secretion, (11) increase 5-HT and AMP production from enterochromaffin cells and goblet cells respectively, and (12) increase the contraction of the smooth muscle. (13) all the aforementioned Th2 responses result in *T. muris* expulsion.

1.5.5.1 Intestinal Epithelial Cell Turnover

Particularly during early *T. muris* infection, epithelial cells indulge in important roles. The parasite can be driven from its intracellular epithelial cell niche through increased epithelial cell turnover (Cliffe *et al.*, 2005). This occurrence can be visualized as an epithelial escalator between the proliferation zone of the crypt and shedding zone of the lumen, shedding the embedded parasite with cast off cells. Differences in epithelial turnover speed is linked to the immune response and cytokine profiles of resistant and susceptible hosts, with Th2 and Th1 responses corresponding to epithelial turnover speed up- and down-regulation respectively. Stimulation of intestinal epithelial cells are needed to initiate effective immune response generation and worm expulsion, as demonstrated by Zaph *et al.*, (2007) using deficient nuclear factor- κ B signalling. Increased turnover may alter the gut microbiota, altering the VOCs present in faecal contents in ways indicative of a protective immune response.

IL-25, IL-33, and TLSP are vital to Th2 immune activation and are secreted from these cells (Harris, 2017). Other cytokines are also involved, such as IL-4 and IL-13 (Bancroft *et al.*, 2000). Epithelial cell turnover upregulation has been found to be IL-13 dependent but IL-4 independent, whereas downregulation has been linked to TH1-associated IFN- γ (Cliffe *et al.*, 2005). In chronic infections, IFN- γ has been linked to crypt hyperplasia, epithelial cell apoptosis and proliferation regulation (Cliffe *et al.*, 2007, Artis *et al.*, 1999), potentially alongside indoleamine 2,3-dioxygenase (IDO) (Bell and Else, 2011), SETD7 (SET domain-containing 7 histone lysine methyltransferase) (Oudhoff *et al.*, 2016), and Mina (Myc induced nuclear antigens) (Pillai *et al.*, 2019).

1.5.5.2 Goblet Cells/Mucus Production

A viscoelastic mucus layer, caused largely by goblet cells, coats the gastrointestinal epithelium, acting as a physical barrier of defence against pathogens (Dharmani *et al.*, 2009). Goblet cells and mucin production, already a vital element of innate defences, are driven by Th2 effector responses to significantly expel parasites (Hasnain *et al.*, 2010, Hasnain *et al.*, 2011¹). Primarily believed to be regulated by Th2 cytokines (McKenzie *et al.*, 1998, Khan *et al.*, 2001), goblet cell hyperplasia has also been witnessed through IL-4/IL-13 independently (Marillier *et al.*, 2008). IL-13 also stimulates the expression of secretory mucins into the mucus layer through GABA- α 3, increasing mucin expression and thickening the glycocalyx during acute infection (Hasnain *et al.*, 2011). This allows for worm motility impairment, trapping the worms in the mucus and inhibiting the worm's feeding capacity, complementing expulsion (Kim and Khan, 2013).

Whilst both resistant and susceptible models may experience goblet cell hyperplasia and the upregulation of cell surface mucin secretion (Artis *et al.*, 2004), there are significant variations between the type of mucin produced between the two phenotypes (Hasnain *et al.*, 2010, Hasnain *et al.*, 2011¹, Hasnain *et al.*, 2011²). Hasnain *et al.*, (2010) found that the mucin Muc-2 was only up-regulated in resistant animals, caused by IL-13 (a Th2 cytokine) and linked to expulsion. Furthermore, delayed parasite clearance was observed in Muc-2-deficient mice relative to wild-type mice.

Alongside Muc-2, Muc5ac, typically only produced in the stomach and airways, was found in the intestine of resistant animals prior to expulsion, and animals deficient in Muc2ac displayed susceptibility and inhibited expulsion despite strong Th2 response and neutralizing IFN- γ antibody treatment to further promote Th2 defence (Hasnain *et al.*, 2011²). This could be because mucins have damaging effects on worms, as *T. muris* worms treated with human Muc5ac exhibited reduced worm viability based on monitored ATP levels. Other goblet cell secretory products, like resistin-like molecule β (RELM β) has been found at higher relative concentrations in resistant phenotypes and has henceforth been linked to whipworm immunity (Artis *et al.*, 2004). Th2 cytokine production correlates with RELM β induction, and it was determined using KO models that IL-13 but not IL-4 may have a significant role in inducing RELM β production. Artis *et al.*, (2004) also brought up the possibility that RELM β could have a direct negative impact on worms by impairing chemotaxis caused by alterations to chemosensory apparatus, however since RELM β KO mice experienced expulsion in acute infections normally, RELM β may be dispensable for helminth-resistant Th2 responses, and is instead limited to environments where Th2 responses dominate (Nair *et al.*, 2008).

1.5.5.4 Muscle Hypercontractility

Muscle hypercontractility and smooth muscle function may also play a significant role in gastrointestinal parasite expulsion. Increased intestinal smooth muscle contractility has been associated with parasite expulsion in another intestine-dwelling helminth, *Trichinella spiralis*, attributed to CD4⁺ T cell involvement (Khan *et al.*, 2001, Khan *et al.*, 2005, Vallance *et al.*, 1999).

Similar to this parasite, *T. muris* has exhibited that Th1 responses cause reduced muscle contractility and excitatory innervation, inhibiting successful expulsion (Khan *et al.*, 2001). Such impairments could be partially restored through dexamethasone treatment and persisted after expulsion in susceptible AKR mice (Motomura *et al.*, 2010), indicating that chronic TH1-biased parasite infection could be a causative agent of underlying inflammation, gut disorders, and dysfunctional muscle contractility (like IBD) in countries that experience endemic parasitic infections (Yousefi *et al.*, 2021).

Increased resistance to *T. muris* has also been found to correlate with increased muscle contractility, likely controlled by IL-9, as shown by Khan *et al.*, (2003) using anti-IL-9 antibody treatment and immunization to induce reduced expulsion and muscle contractility. Supporting this, in transgenic infected mice overexpressing IL-9, faster worm expulsion was witnessed relative to uninfected controls (Faulkner *et al.*, 1998). It was also recently demonstrated by Chen *et al.*, (2021) that enterochromaffin cells could be stimulated by IL-33-ST2 signalling to secrete and synthesize 5-HT, activating enteric neurons and promoting gut mobility in ways beneficial to *T. muris* expulsion.

It is therefore likely with the prior supporting evidence that muscle contractility is an immune-mediated expulsion mechanism of *T. muris*, alongside increased mucus production and epithelial cell turnover.

1.5.6 Microbiome and Immune Response

Interrelations between the host immune system, *T. muris*, and the gut microbiome hold great importance on the impacts and outcomes of trichuriasis.

Intestinal microbiota in healthy conditions are complex and diverse bacterial communities, and major components in forming the local intestinal environment, in addition to immunity, inflammation, homeostasis and metabolism (Holm *et al.*, 2015). Interactions between parasites and microbiota can push host immunity down inflammatory or anti-inflammatory routes, and conversely the microbiota can alter the parasite's colonisation, infectivity and reproduction, even potentially allowing for mutualism (Yousefi *et al.*, 2021).

Persistent interactions with whipworm and intestinal microbiota have been inversely correlated with immune-associated disease incidence, such as allergies, IBD, type 1 diabetes, and rheumatoid arthritis (Molodecky *et al.*, 2012, Kondrashova *et al.*, 2013, Kramer *et al.*, 2013). Any downstream effects on the immune system are still somewhat unclear.

Distinct mucosal sites like the lung and the intestine can engage in immunological crosstalk (Keely *et al.*, 2012), for example regarding intestinal microbiota modulating susceptibility to asthma in later life, (Penders *et al.*, 2007, Russell *et al.*, 2012). Chenery *et al.*, (2016) determined that low dose *T. muris* infection in the intestines initiates the production of Th1 cell-dependant IFN- γ and myeloid cell-derived IL-10 in the lungs without initiating any direct airway pathology, suppressing type 2 airway inflammation. It is speculated that Tregs and the subsequently secreted IL-10 and TGF- β contribute to the beneficial effects of helminths in inflammatory conditions (Sakaguchi *et al.*, 2008), however conflicting results involving IL-10 KO mice suggest further research is required into this topic (Wilson *et al.*, 2011).

Contemporary methods have elucidated that gut microbiota can attach terminally to the eggs and facilitate *T. muris* egg hatching, directly favouring worm establishment (Hayes *et al.*, 2010). In fact, it was established using germ-free mice that intestinal microbiota is essential for successful *T. muris* infections (White *et al.*, 2018). Gut microbiota facilitates chronic infection development and long-term parasite survival by reducing diversity, preventing the eggs of second infection doses from hatching and controlling *T. muris* numbers, preventing infection level from initiating protective immunity induction (Colombo and Grecis, 2020). This is further aided by the selection and acquisition of specific intestinal bacterial subsets in the gut environment by *T. muris* to facilitate survival (White *et al.*, 2018).

Utilising 16s ribosomal-RNA gene-based sequencing, Holm *et al.*, (2015) determined that *T. muris* enforced a dramatic impact on large-intestinal microbiota, characterised by a large diversity decrease, and a marked surge in the genus *Lactobacillus*, where chronic infection pushed a shift from favouring regulatory T cells to inflammatory T cells. This is supported using DGGE, 454 pyrosequencing, and metabolomics, by Houlden *et al.*, (2015), who observed significant changes in the α and β -diversity of faecal microbiota between 14-28 days post-infection. Particularly, this concerned a reduced diversity and abundance of *Bacteroidetes*, most notably *Prevotella* and *Parabacteroides*. These changes could be reflected in faecal VOCs, which could be worth examining to better understand VOC alterations under disease pressure. At day 41 post-infection, metabolic differences concerning essential amino acids and dietary plant-derived carbohydrates were also witnessed by this study, resulting in reduced weight gain in infected mice comparative to controls. Such changes

were parasite-presence dependant, as following parasite clearance microbiota changes transitioned back to indistinguishable from control mice.

Physical alterations induced by *T. muris* can also impact gut microbiota, such as the aforementioned changes in the mucus layer and mucin production (Hasnain *et al.*, 2010, Hasnain *et al.*, 2011, Leung *et al.*, 2018). Such changes can alter nutrient accessibility and impair microbiota attachment, benefiting *Mucispirillum* and *Clostridiales*, which are abundant during *T. muris* infection (Holm *et al.*, 2015, Houlden *et al.*, 2015, Ramanan *et al.*, 2016).

Regulation of the secretion and synthesis of antimicrobial peptides (AMPs) may alter the structure and composition of gut microbiota. AMP expression has also been linked to *T. muris* expulsion, which are generated by goblet cells (Forman *et al.*, 2012, Bell and Else., 2011).

Increased Ang4 expression having been found in resistant mice, linking to helminth expulsion, however the mechanism behind this is unclear (D'Elia *et al.*, 2009). It is suspected that Ang4 either incites a direct toxic effect on *T. muris* like on *T. spiralis* (Hamann *et al.*, 1987), or induces changes in the microbial composition, instigating changes in the host immune response (Leung *et al.*, 2018).

It is likely that the dominating immune response countering resistant/chronic whipworm infection and any intestinal microenvironment changes may hold importance in host microbiota alterations (Durque-Correa *et al.*, 2019). For example, Th2 immunity caused an increase in beneficial bacteria, such as *Clostridiales*, which outcompetes *Bacteroides vulgatus*, a colitogenic. This

capped colitis severity and reducing intestinal pathology (Ramanan *et al.*, 2016).

However, the consequences of microbiota-induced physical changes within the gut during *T. muris* infection outcomes have not yet been studied sufficiently enough for any definitive conclusions (Cortes *et al.*, 2019).

Likewise, microbiota and the immune system in relation to disease detection through odour and determining the mechanisms behind this have been insufficiently studied using urine and faeces concerning trichuriasis.

1.6 Aims

If the underlying mechanisms that outline specific odour profiles can be identified, then therapeutic targets could be better distinguished. This project aims to scrutinize the influence that *T. muris*-induced immune challenge has on urine odour using a well-studied C57BL/6 mouse model and determining if its' odour profile would be sufficient for whipworm detection using portable VOC analyser and sandfly attraction, aligning with previous research conducted using mouse hair.

Urine holds promise as good target for VOC detection. Prior research on this project has determined that the skin and hair VOCs of infected mice were distinguishable from uninfected controls. As previously mentioned, mouse urine is an intraspecific communication method- abundant in MUPs which can convey health status. These may allow for detectable odour changes specific to *T. muris* infection, that can be identified through changes in MUP expression or by using portable VOC analyser.

This will be examined using infected vs uninfected urine, as if infection in urine can be detected, VOC detection could be utilised as a quick, non-invasive diagnostic procedure. This examination will also include both low dose and high dose infections, as chronic Th1 and acute Th2 immune responses lead to different infection outcomes and may influence any odour changes detected using a portable VOC analyser.

T. muris-induced changes in VOC profile can also be examined through biological detection in the form of sandfly attraction, as sandflies have been shown to be attracted to infection-induced odour changes (Staniek *et al.*, 2019). It would be useful to determine which specific feature of immune response is attractive to sandflies, as this could indicate a mechanism behind sandfly attraction, and give some insight into how immune cells control odour. As sandflies have been previously shown to uphold attraction to immune responses using hair and skin, where microbial communities thrive, it could be useful to determine whether the appeal of infected odour recorded by these insects previously are entirely immune-induced, or if microbial interactions are required to this enforce attraction.

Additionally, it is difficult to determine the extent at which the microbiome interacts with VOC profile, especially in the case of infection. Testing urine, an area with a sparse microbiome, when compared with faeces, which is widely accepted to have a vast microbiome, could be useful for determining the extent of which the involvement of the microbiome and which microbiota is at play.

Testing individual cytokines for differences in sandfly attraction could also achieve an idea of how involved the microbiome is in relation to attraction. By

using specific Th1 and Th2 cytokines, it could be determined if these individual immune cells are causative to sandfly attraction.

An understanding of disease-specific VOC emissions and uncovering the molecular mechanisms behind disease-induced odour changes could progress the investigation and understanding of the pathophysiological mechanisms behind specific diseases (Shirasu and Touhara, 2011). This would aid in the development of diagnostic tools and the successful treatment of trichuriasis in human populations, especially in areas where whipworm is both most prevalent and diagnostic methods are the most inaccessible.

Chapter 2: Methods

2.1 Sample Collection

2.1.1 Animals

C57BL/6 mice, housed at Lancaster University, were kept on a 12-hour light/dark cycle ($22 \pm 1^\circ\text{C}$, 65% humidity) in individually ventilated cages. All procedures were in accordance with the Home Office Science Act (1986) and were carried out using 6–12-week-old littermates after 1 week acclimatisation. All experiments conformed with the Lancaster University Animal Welfare and Ethical Review Body (AWERB) and ARRIVE guidelines. All experiments carried out at Lancaster University were carried out under the project licence PP4157153.

2.1.2 *T. muris* Infection

Female mice were infected with *T. muris* on day 0 of the experiment. Infection was established using a single low dose (~30 eggs in 200 μL PBS (Gibco™)) to promote susceptibility or a single high dose (~200 eggs in 200 μL PBS) to promote resistance and helminth expulsion. This was done via oval gavage with a blunt needle.

Samples were taken of hair, urine and faeces on days 0, 7, 14, 21, 25, 28, and 42 of infection. Samples were collected in Eppendorf™ tubes (Fisher Scientific™) and Mylar resealable foil bags (for hair samples) and kept in -80°C storage conditions with a minimal freeze-thaw cycle until use (Holbrook *et al.* 2023).

2.2 Y-Tube Olfactometer Bioassays

Bioassays were conducted using a Y-tube olfactometer to assess the response of female sandflies to the odour of *T. muris*-infected mice urine. Samples from mice infected with high doses, low doses and non-infected controls from the same time points post-infection were paired in a series of Y-tube olfactometer choice experiments (Fig. 9).

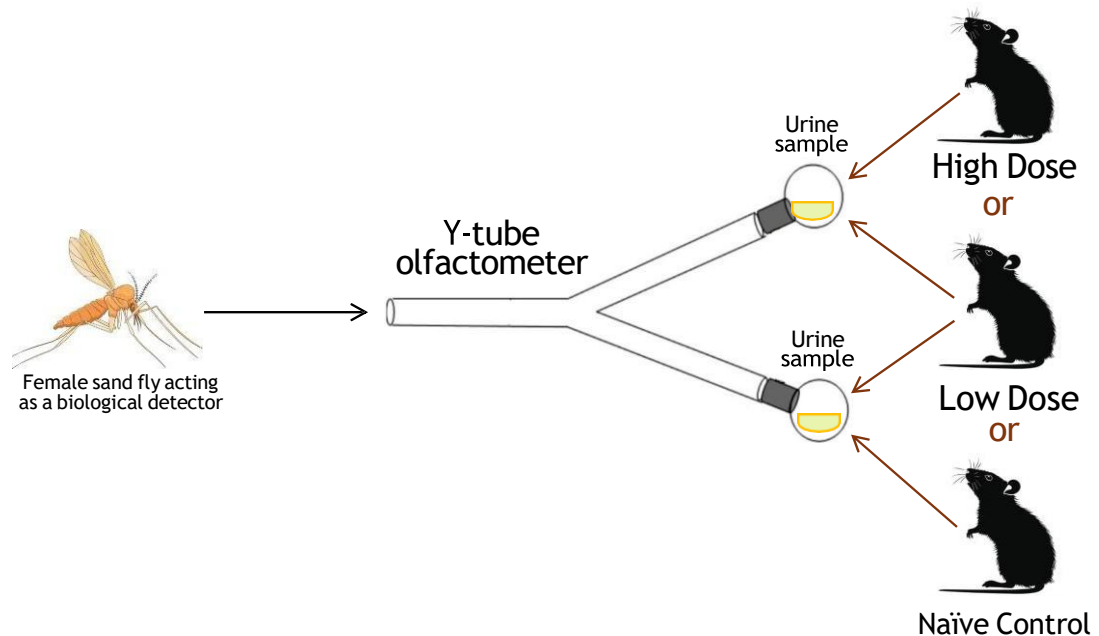


Fig.9. A simplified visual representation of Y-tube olfactometer choice experiments, in which the urine of C5BL/6 mice infected with high doses, low doses, or naïve controls from the same time periods post-infection were subject to sandfly preference.

The sandfly acts as a biological detector for *T. muris*-induced changes in VOC profiles. Sandfly responses to mouse urine infected with high dose *T. muris* against low dose *T. muris* were examined, in addition to high dose against naïve mouse urine, and low dose against naïve mouse urine.

Equal amounts of these samples were placed in airtight short necked round bottomed flasks, and female sandflies were introduced to the olfactometer and had their position recorded after three minutes. Presence in one of the olfactometer arms suggested an odour preference.

2.2.1 Experimental Set Up

L. longipalpis sandflies from a Lancaster University colony (established from individuals collected from Campo Grande, Brazil) were raised by methods chronicled by Lawyer *et al.* (2017).

Sandflies were contained during a 12:12-hour photoperiod at (~25-29°C range; 95% relative humidity) within Nylon Barraud cages, and blood-fed with sheep blood (TCS Biosciences Ltd, Buckingham, UK) through a chicken skin membrane prior to oviposition (Moraes *et al.* 2018). Post-emergence, sandflies were kept in cages covered with plastic bags to regulate temperature and humidity for 5-7 days prior to bioassay. sandflies were fed with 60% sucrose solution *ad libidum*, cut two days prior to the bioassay. sandflies were allowed time to acclimate in the bioassay room 45 minutes prior to the bioassay (mean temperature 25.51°C (\pm 1.33°C), range 21.3-28.8°C: mean humidity 35.23% (\pm 6.04), range 24-49%). After bioassays were conducted, flies were blood fed.

Through the apparatus, a clean air flow (ZeroGrade; BOC, Lancaster, UK) was controlled by a two-stage cylinder regulator valve (BOC Series 8500 Air Regulator BOC) and a rotameter (Sigma-Aldrich Company Ltd, UK) adjusted to 5ml sec⁻¹. This was confirmed using a bubble meter. All connections were sealed airtight using RS Pro Teflon tape (RS Components Ltd, UK). Fabric netting was used to prevent sandfly escape.

All Teflon tubing and glassware was cleaned using 10% Teepol™ multipurpose detergent solution, distilled water and acetone (Fisher Scientific™). Glassware was then baked for an hour in 180°C, whereas Teflon tubing was allowed to airdry, ready for the next use.

2.2.2 Conducting Bioassays

Bioassays were conducted utilising a horizontal y-tube olfactometer on a steady bench, which was connected to airtight Teflon tubing and sealed with Teflon tape, similar to the y-tube olfactometer assays conducted by Staniek *et al.* (2021). This allowed the sample odour to permeate into the air flowing through the tubing attached to each olfactometer arm, allowing for attraction preference to be determined. A 20cm maximum distance was available for a sandfly to travel if they were attracted. To reduce spatial bias the arms were rotated 180° for every 20 sandflies tested. For each experimental replicate 80 female sandflies were used, as past research dictates only blood-seeking female sandflies display preferential attraction (Staniek *et al.*, 2021).

Mouth aspirators were used to remove individual female flies from the holding cage and for release into the open stem of the Y-tube. sandfly position was then recorded after three minutes as attracted to one sample, attracted to the other sample, or with no response (in neither arm of the Y-tube olfactometer).

For urine, samples from the same time point post-infection of equal quantity (10-30µl, dependant on the amount of urine produced) were introduced into 50ml short neck round bottom flasks (Pyrex Quickfit), which were attached with Teflon tape to the tubing connected to each arm.

For testing sandfly attraction to Th1/Th2 cytokines, 20 µl of cytokine diluted to 1pg/µl was introduced into the 50ml short neck round bottom flask (Pyrex Quickfit) on one arm of the y-tube olfactometer. In the other arm, 20 µl of the relevant diluent was introduced. IL-4 was used as a Th2-associated

cytokine, diluted in PBS. IFN- γ was used as a Th1-associated cytokine, diluted with Assay diluent from BD™ Cytometric Bead Array (CBA) Mouse IFN- γ Flex Set. Samples were stored in -20°C and mixed before use.

2.2.3 Bioassay Blind Control

To ensure the validity of this experimental method, a blind control was conducted using a total 80 virgin female sandflies. Hexane extract of the sex-aggregation pheromone, which was made up of 1000 4.5-day old male Campo Grande *Lutzomyia longipalpis* sandflies, was used for as a positive control in this experiment (1 male equivalent/ μ l), produced in a similar manner to what was described by Bray and Hamilton (2007). Hexane (Fisher Chemical™) was used as the negative control. 1 μ l was used per sandfly.

2.3 VOC Analysis

VOC analysis was performed using a portable VOC analyser (Model 720, Roboscientific Ltd, Leeds, UK), similar to Staniek *et al.* (2019).

24 semi-conducting polymer sensors gave a total of two readings per sensor.

Each sensor had semi-selectivity to a different group of volatile chemicals (such as alcohols, aldehydes, ketones, organic acids), allowing for the creation of a digital footprint of VOC emissions through voltage and resistance over time.

2.3.1 VOC Sample Preparation

An equal amount from each urine sample (Approx. 20 μ L) was sealed in foil bags, with an additional seal added just below the incorporated seal of the sample bag, using a heat sealer.

The sample bags were then inflated via the insertion of needle attached to diaphragm pump for around 5 seconds. Removal of the syringe was then followed swiftly by sealing the puncture with PVC electrical tape at the location of the puncture, resulting in airtight, sealed, inflated sample bags. These were left for 5 minutes to ensure that the bags did not leak.

Samples were then incubated in an oven at 50°C for at least 15 minutes and then left for five minutes to cool to room temperature. For faecal samples, the faeces were placed in the bag and after inflation, approx. 20 µL of qH₂O were injected into the bags prior to incubation.

These samples were then analysed using the VOC analyser.

2.3.2 VOC Sampling

The samples were taken by inserting an 18-gauge needle attached to a PTFE sample tube into the side of each foil bag (Fig.10). The tip of the needle was placed in the headspace of each bag.



Fig.10. Representative visualisation of VOC sampling using portable VOC analyser as described.

Image was created in <https://BioRender.com>.

The analyser ran through baseline, absorb, desorb, flush and then the whole cycle again, producing 2 readings for each individual sample.

Once finished the needle was removed, and these processes were repeated for the next sample.

2.4 qPCR

2.4.1 RNA Extraction

Post-extraction from C57BL/6 mice, liver samples were stored in Eppendorf™ tubes containing 1mL TRIzol® (Invitrogen™) under -80°C until use.

These were homogenised using a homogeniser that was sequentially rinsed with DEPC water (Promega©) in between samples, then left for 10 minutes to warm to room temp. 0.2mL of chloroform (Fisher Chemical™) was then added to each tube and they were vigorously shaken for 15 seconds until cloudy, then incubated at room temperature for a further 3 minutes and centrifuged at 4°C, 12000 x g for 15 minutes in a SIGMA 1-14K refrigerated centrifuge. The colourless upper aqueous phase was carefully removed from the white protein interphase and the red DNA organic phase and precipitated with 0.5mL isopropanol (Sigma Aldrich™), inverted to mix. This was stored at -80°C for at least 2 hours.

Following this, the samples were centrifuged again (12000 x g, 10 minutes, 4°C) and the supernatant was poured off. The residual was extracted using a pipette, and the pellet was washed with 75% ethanol (Fisher Chemical™), vortexed and then spun (7500n x g, 5 minutes, 4°C). Ethanol was then poured off and the samples were left to dry for 10 minutes at room temperature. The remaining pellet was then resuspended in 30-50 µL RNase/DNase free water (QIAGEN) and stored at -80°C.

2.4.2 Reverse Transcription of T cell cDNA

1µL oligoDT (Promega©) and 4µL of the extracted RNA mentioned above were dispensed into PCR strip tubes, then this was kept at 70°C for 5 minutes, then kept on ice.

A buffer mixture was made containing a ratio of 6µL 5x ImProm-II™ reaction buffer(Promega©), 3 µL deoxynucleoside triphosphates (dNTP mix., Promega©), 0.6µL RNAsin® Ribonuclease inhibitor (Promega©), 1.5µL

ImProm-II™ Reverse Transcriptase (Promega©, A3602), 3.6µL MgCl₂, and 14.3 µL Nuclease-free water (ImProm-II™ Reverse Transcription System (A3602), Promega©).

29µL of this mixture was then added to the samples and these were incubated at 25°C (5 minutes), 40°C (60 minutes), and 70°C (15 minutes) facilitated by a T100 Thermocycler, then stored at -20°C.

2.4.3 RT-qPCR Analysis

A mixture with the ratio; 12.5 µL SYBR™ green universal master mix (Roche™), 1 µL forward primer (Sigma®), 1 µL reverse primer (Sigma®) and 8 µL of nuclease-free dH₂O (Promega©) was made up with the primers relevant for each gene of interest (table 2), in addition to the primers for the hypoxanthine-guanine phosphoribosyltransferase (Hprt) housekeeping enzyme, which was used as a control.

Table. 2. Primers used to identify MUP expression.

Gene Name	NCBI Gene ID	Forward Sequence 5'>3'	Reverse Sequence 5'>3'
MUP 1	17840	GAAGCTAGTTCTACGGGAAGGA	AGGCCAGGATAATAGTATGCCA
MUP 5	17844	ATGGAGCTCTTTGGTCGA	TGTATGGAAGGGAAGGGATG
MUP 15	100039150	GTGGAGTGTAGCCACGATCA	CAGCAGCAACAGCATCTTCA
MUP 16	100039177	AGAAAAGATTAATGGGGAATGGCA	ATTCGGAGCACTCTTCATCTCT
MUP 18	100048884	GAAGCTAGTTCTACGGGAAGGA	ACGTCACAGAATATTCACCAG
MUP 20	381530	ATGAAGCTGCTGGTGCTG	TTGTCAGTGGCCAGCATAATAG
MUP 21	381531	AGTCTGTATCCAGGCAGAAGAA	TCTCCAAGACAGTGATGTTTTCC

It is worth noting that the primer for MUP 1 could also target other MUPs (MUP 2, 7, 8, 9, 10, 11, 12, 13,14, 17 and 19) as MUPs are known to be highly related (Logan *et al.* 2008).

22.5 µL of this mixture was added to the relevant wells of a 96 well PCR plate (Biolegend®), with 12 wells used for each gene of interest. 2.5 µL of cDNA from reverse transcription reaction was added to this, diluted at a 1:5 ratio using dH₂O. The plate was then sealed using an Microseal 'B' adhesive sealing film (BioRad™) and briefly centrifuged, before qPCR analysis was run on a BioRad CFP Opus 96.

2.5 Flow Cytometry

2.5.1 Single Colour Compensation Controls

Single colour compensation controls were performed prior to flow cytometric analysis of the sample, to determine the levels of compensation and correcting fluorescence spillover.

One Invitrogen Ultracomp Ebeads™ Plus Compensation Bead was added to ten Eppendorf™ tubes. This was pulse-vortexed prior to being dispensed. Tubes were then labelled and 1 test of antibody conjugate (Table 3) was added to each tube.

Table 3. Antibody conjugates used for single colour compensation controls.

Antibody	Antibody Conjugate	Manufacturer	Clone
Ly-6G	FITC	eBioscience™	1AB-Ly6G
IL-5	PE	eBioscience™	TRFKs
TCR (γδ)	Pe-Cy7	BioLegend®	GC3
CD64	PercP	BioLegend®	X54-5/7.1
(ST2) IL-33R	APC	eBioscience™	RMST2-33
CD4/L3T4	APC-Cy7	Life Technologies™	GK1.5
CD3/MHC II	AF700	eBioscience™	M5/114.15.2
Ly-6C	E450	eBioscience™	HK1.4
CD8α	PE-CF594	BD Horizon™	53-6.7
CD45	565	eBioscience™	30-F11

Tubes were then incubated in the dark for 15-30 minutes, then suspended in phosphate buffered saline (PBS, ~200 µL). This was centrifuged at 400g for 5 minutes then the supernatant was resuspended in ~200 µL PBS.

These controls were then pulse-vortexed before analysis then ran on the cytometer.

2.5.2 Enzymatic Digestion of the Liver and Bladder

Enzymatic digestion proceeded following steps 8-10 from the protocol described by Way *et al.* (2023).

Digestion buffer (liberase (5mg/mL), 1% HEPES, 200 µg/mL deoxyribonuclease I, sterile foetal bovine serum (Gibco™) and HBSS).

Once isolated, livers and bladders are finely chopped. The samples are then transferred into a 50mL conical tubes (Corning®) containing 10mL digestion buffer.

The samples are then kept in a rolling incubator at (37°C, 100 rpm, 40 minutes) to allow for digestion.

2.5.3 Preparation for Flow Cytometry Staining

Preparation commenced again following steps 11-16 from the protocol described by Way *et al.* (2023).

Samples were removed from the incubator and manually ground through at 70 µm tube top cell strainer (Corning®) into a 50mL conical tube with ice-cold PBS. The pellet of both liver and bladder samples was isolated after they were span (400xg, 5 minutes, 4°C). For liver samples, pellet was resuspended in HBSS and then spun at (30xg, 5 minutes, 4°C). The resulting supernatant was spun further at 400xg.

Residual red blood cells (RBCs) were then removed using the addition of 1mL of RBC lysing buffer Hybi-Max™ (Sigma® Life Science). Samples were then

shaken for 60 seconds, then span again with 1mL of HBSS for 5 minutes for as many times as necessary.

Pellets were resuspended in 200µL HBSS.

1X fix perm was produced using 200µL fixation/permeabilization concentrate (Invitrogen™) for every 600µL of Invitrogen eBioscience™

fixation/permeabilization diluent. The pellet was cleaned using 200µL HBSS and resuspended using 200 µL fix perm for bladder samples and 600 µL for liver samples for 15 minutes.

2.5.4 Staining for Flow Cytometry

1x perm was used for subsequent steps (10x stock diluted with qH₂O). 200 µL was added to each sample and then this was spun at 400xg. 2 µL of anti-mouse CD16/32 FC block (BioLegend®) was added to every 400 µL 1x perm. and kept on ice for 15 minutes.

Antibody mixes were prepared using individual antibodies and 1x perm buffer. Samples were then split to test for both myeloid and lymphoid cells. This was done using the individual antibodies listed in Table 4 and Table 5 respectively.

Table.4. Myeloid antibody panel for cell staining

Antibody	Manufacturer	Fluorophore	Clone
CD45	eBioscience™	e506	30-F11
CD11b	eBioscience™	APC	M1/70
CD11c	eBioscience™	PE/Cy 7	N418
Ly-6G	eBioscience™	FITC	1AB-Ly6G
Ly-6C	eBioscience™	e450	HK1.4
MHC II	BioLegend®	AF700	M5/114.15.2
CD64	BioLegend®	PercP-Cy5.5	X54-5/7.1
SIGLEC-F	eBioscience™	AF600	1RNM44N

Table. 5. Lymphoid antibody panel for cell staining

Antibody	Manufacturer	Fluorophore	Clone
CD45	eBioscience™	e506	30-F11
CD3	eBioscience™	AF700	17A2
CD4	Life Technologies®	APC-Cy7	GK1.5
CD8α	BD Horizon™	PE-CF594	53-6.7
GATA3	BioLegend®	PerCP-Cy5.5	16E10A23
T-bet	eBioscience™	e660	eBio4B10 (4B10)
CD45RB	BioLegend®	PE	MEM-55

100 µL of stain cocktail was added to each pellet these were left for 30 minutes on ice.

After staining, samples were centrifuged (400xg, 5 minutes) and the pellets were resuspended in 200µL PBS and kept at -4°C until they could be run on the Beckman Coulter Cytotflex flow cytometer.

2.5.5 Gating Strategy

Data produced from flow cytometry was processed and presented using FlowJo v11, using the gating strategies depicted on Fig.11 and Fig.12.

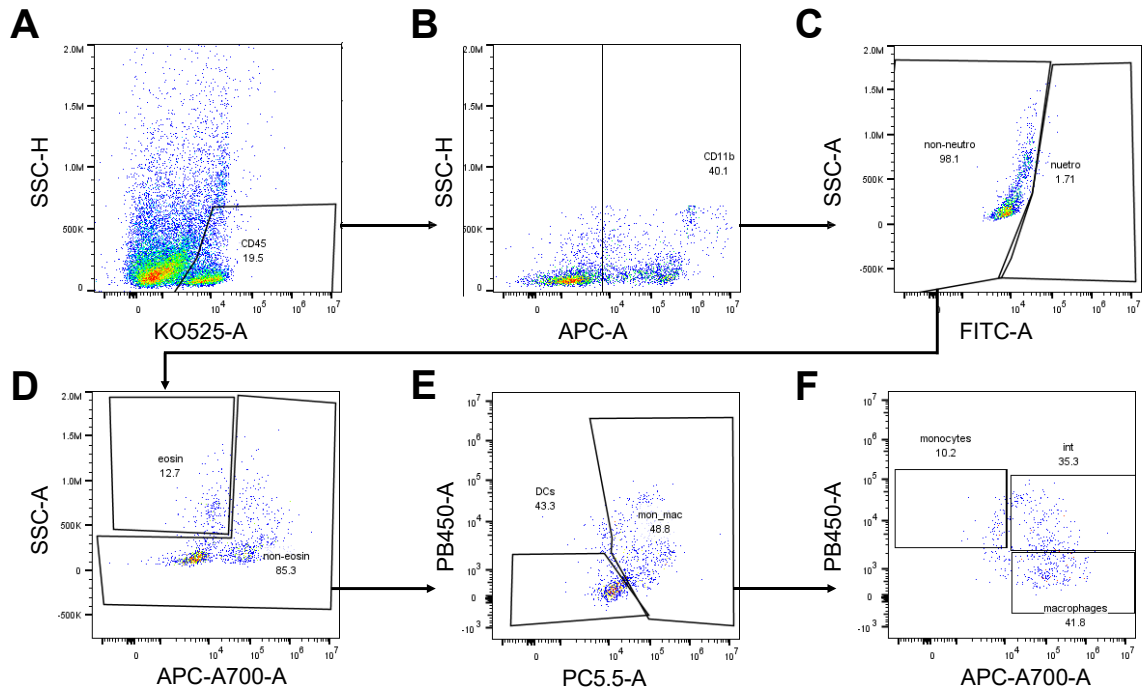


Fig.11. Gating strategy for myeloid cells.

Gating strategy was based off those outlined by Scott *et al.* (2017). Data was produced using flow cytometry and processed and presented using FlowJo v11.

(A) CD45⁺ immune cells were gated using SSC-A against e506 (KO525-A). (B) From the CD45⁺ gated immune cells, CD11b⁺ cells were gated using SSC-A against APC (APC-A), providing a selection of the total myeloid compartment. (C) Ly6G⁺ neutrophils were excluded by gating the CD11b⁺ cell population using SSC-A against FITC (FITC-A).

(D) From the gated CD11b⁺ Ly6G⁻ cells, MHCII⁻ eosinophils were excluded by gating using SSC-A against AF700 (APC-A700-A). (E) A selection of CD64⁺ monocyte-macrophages where then separated from dendritic cells from the MHCII⁺ cell population by gating using e450 (PB450-A) against PERCP (PC5.5-A). (F) the monocyte waterfall was then revealed from CD11b⁺ CD64⁺ cells by gating SSC-A against AF700 (APC-A700-A). This depicts the sequential process of differentiation from monocytes into activated mature macrophages, whereby monocytes display Ly6C⁻MHCII⁺; intermediate stages show Ly6C⁺ MHCII⁺; and macrophages exhibit Ly6C⁺MHCII⁻.

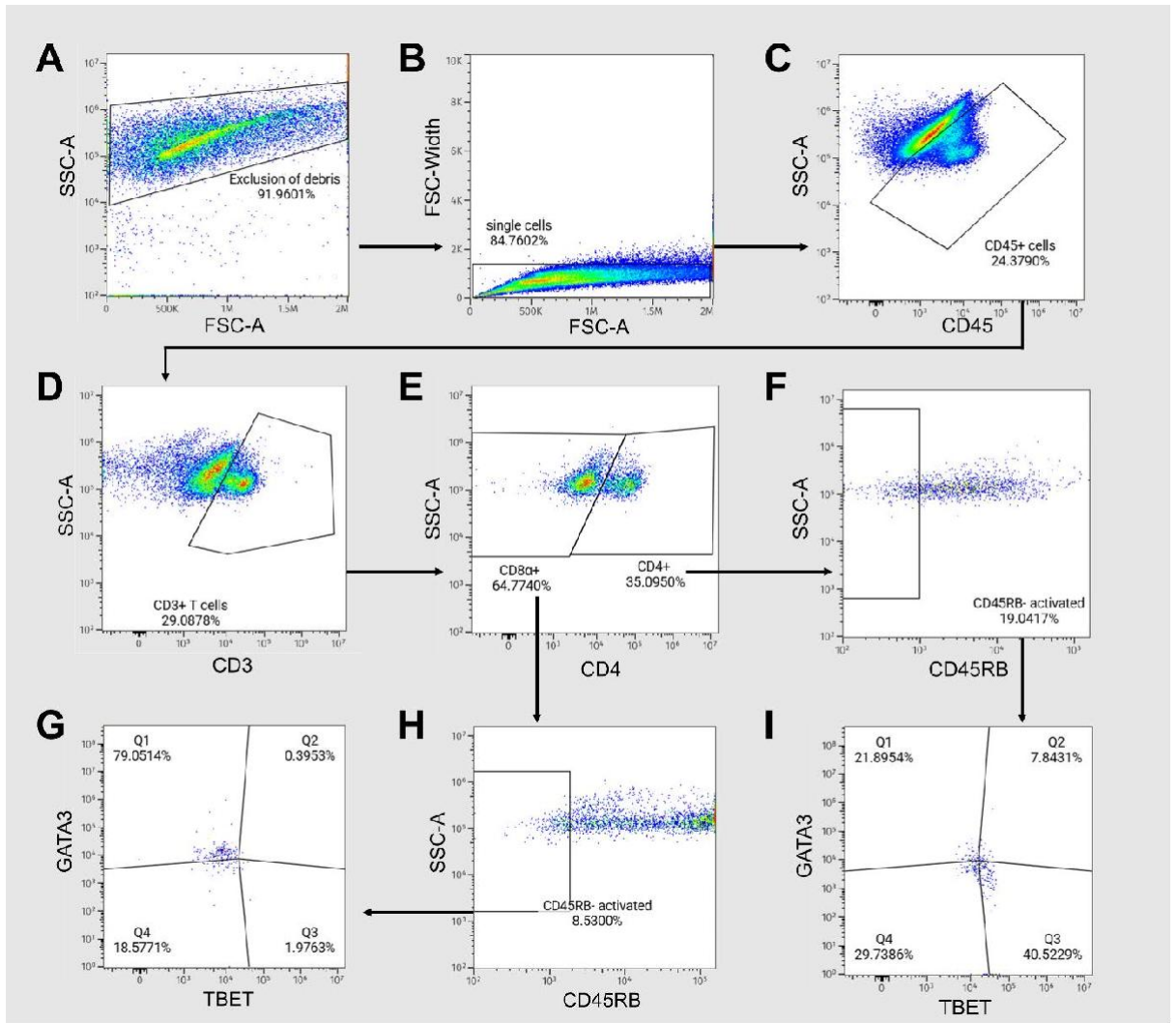


Fig.12. Gating strategy for T cells.

Data was produced using flow cytometry and processed and presented using FlowJo v11.

(A) Debris was excluded using SSC-A against FSC-A. (B) Single cells were then gated using FSC-width against FSC-A. (C) CD45+ immune cells were gated using SSC-A against e506 (KO525-A). (D) From the CD45+ gated immune cells, CD3+ cells were gated using SSC-A against AF700 (APC-A700-A). (E) CD4+ T helper cells and (CD4-) CD8 α + cytotoxic T cells were gated from the CD3+ population using SSC-A against APC-Cy7 (APC-A750-A, marking for CD4). (F) From the gated CD4+ T helper cells, CD45RB- activated cells were gated using SSC-A against PE-A. (I) CD45RB- GATA-3+ Th2 cells and CD45RB- T-bet+ Th1 cells were then gated using PercP (PC5.5-A, marking for GATA-3) against 660 (APC-A, marking for T-bet). GATA-3+ Th2 cells can be seen in zone 'Q1', and T-bet+ Th1 cells can be seen in zone 'Q3'. 'Q4' and 'Q2' segregate double negative and double positive cells respectively. The same gating using in (F) and (I) on CD4+ cells were used in (G) and (H), but on the identified CD8 α + cells.

2.6 Data Analysis and Statistics

GraphPad Prism v10.4.1 was used to produce figures, with results presented using mean (\pm SEM). Statistical analysis was also conducted utilising GraphPad Prism. P values of <0.05 were determined statistically significant ($P<0.05=*$, $P<0.01=**$, $P<0.005=***$).

When comparing two experimental groups, paired T-tests were used. For three or more groups, ANOVA with Bonferroni or Šidák's multiple comparisons were used. When data did not follow normal distribution (assessed using Shapiro-Wilk), Mann-Whitney U tests were used instead.

All statistical analysis and graphical figures were completed using GraphPad Prism v10.4.1.

VOC analysis was examined using principal component analysis, using all the 24 extracted divergencies/peak heights and areas.

Further analysis following this was conducted using machine learning model analysis. This was conducted on Ubuntu 20.04, using the programming language Python 3.8, as it is widely recognized in data science for its extensive ecosystem of libraries and suitability for both machine learning and deep learning tasks (Géron, 2019). Several third-party libraries were installed via pip, including NumPy, Pandas, Scikit-learn, TensorFlow/Keras, Matplotlib, and Seaborn, to maintain consistency and facilitate tasks such as numerical computation, data manipulation, model development and evaluation, deep learning model training, and visualization of results.

Data preprocessing was carried out using Pandas for data loading and cleaning. Missing values were addressed by imputing the mean of the respective feature, while categorical variables were converted into numerical representations through One-Hot Encoding. StandardScaler from Scikit-learn was used to standardize the numerical features and improve model performance, ensuring that each feature had a mean of 0 and a variance of 1. The data was subsequently split into training and test sets, with 80% allocated for training and 20% for testing (Pedregosa *et al.*, 2011).

For machine learning tasks, a variety of algorithms from Scikit-learn were utilized. Models were trained on the training data, and performance was evaluated on the test set using the accuracy score metric (Pedregosa *et al.*, 2011). Furthermore, TensorFlow/Keras was employed to develop deep learning models, such as a multi-layer perceptron (MLP), for binary classification. The MLP comprised of three fully connected layers, with ReLU activation functions applied to the first two layers and a sigmoid activation function used for the output layer (Abadi *et al.*, 2016).

Concerning model training and evaluation, in the deep learning models like MLP, the Adam optimizer was used in conjunction with binary_crossentropy as the loss function. During the training process, both training and validation loss were monitored across epochs until convergence was achieved. Model performance was evaluated using standard metrics, including accuracy and F1 score. All experiments were conducted within the Ubuntu 20.04 environment to ensure reproducibility and transparency.

Chapter 3: Results

3.1 Expression of MUP-related genes are altered during chronic *T. muris* infection

To investigate the mechanisms of odour change during *Trichuris muris* infection we first examined potential changes in major urinary proteins (MUP). These molecules are involved in chemo signaling and have been previously shown to be modulated by infection. (Oldstone *et al.* 2011) determined that changes in MUP 10, 9, 7, and MUP 20 when afflicted by LCV, however this has not been thoroughly examined concerning helminth infection, namely Trichuriasis.

T. muris-induced changes in MUP expression could indicate differences in urine odour, allowing for distinctive infection-induced odour profile differentiation.

Liver samples were therefore taken from mice with chronic *T. muris* infections for RT-qPCR analysis to examine MUP related-gene expression (Fig.13), as the liver are the site of MUP production in mice (Flower *et al.* 2000).

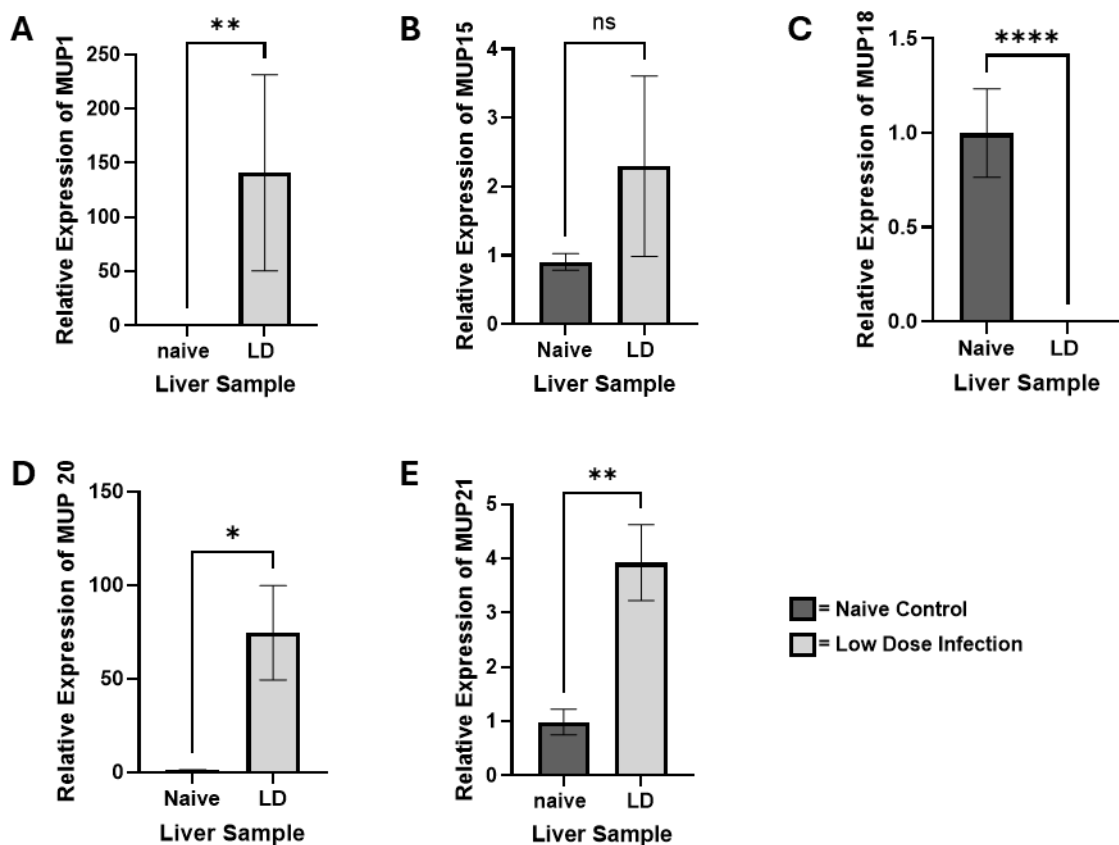


Fig.13. Chronic *T. muris* infection increases the expression of MUP 1, 20 and 21, and decreases the expression of MUP 18 in infected mice.

C57BL/6 mice infected with ~30 *T. muris* eggs and were culled and dissected on day 35 post-infection. A large segment of liver was collected, placed in TRIzol®, and frozen at -80°C prior to use. Following RNA isolation and RT-qPCR analysis, the data collected underwent $2^{-\Delta\Delta CT}$ analysis. Plotted data (n=6-8 mice per group) displays the relative expression of (A) MUP1, (B) MUP 15, (C) MUP 18, (D) MUP 20 and (E) MUP 21, and are from 2 independent experiments, presented as mean \pm SEM. As these results did not follow normal distribution via Shapiro-Wilk, Statistical analysis was completed using Mann-Whitney U tests (* = $p < 0.05$, ** = $p < 0.01$, *** = $p < 0.001$, **** = $p < 0.0001$).

The relative hepatic expression of MUP1 in low dose subjects (140.9, \pm 90.45) was significantly greater than naive counterparts (0.8763, \pm 0.2718, Mann-Whitney U test; $p = 0.0022$). This increase in relative expression was also seen in both MUP20 (naïve=1.071, \pm 0.3964, low dose= 74.50, \pm 25.14; $p = 0.0286$), and

MUP21 (naïve=0.9868, \pm 0.2347, low dose=3.925, \pm 0.6970; $p=0.0025$) with significantly greater increase than naïve counterparts.

However, this was not the case for all MUPs examined, as the relative hepatic MUP15 expression of low dose subjects (2.299, \pm 1.310) was not significantly different from naïve counterparts (0.9089, \pm 0.1198).

Moreover, MUP18 had significantly lower relative expression when comparing naïve (0.9987, \pm 0.6644) and low dose-treated subjects (9.69×10^{-4} , $\pm 8.795 \times 10^{-4}$; $p < 0.0001$).

These data demonstrate that a chronic *T. muris* dose produces infection-induced changes in MUP expression, suggesting such differences could be the responsible mechanism for the observed odour change.

3.2 *T. muris* Infection Does Not Influence the Innate or Adaptive Profile of Liver Immune Cells in Both the Chronic and Acute State

As immune challenge and inflammatory responses are thought to be a significant contributing factor to both MUP expression in mice and odour changes in infected patients (Oldstone *et al.* 2021, Wedekind and Penn, 2000), the liver, as the site of MUP production, would be useful to examine to see if and what causative immune response could be present in infected mice that would induce MUP changes in expression. Therefore, we conducted liver digests and flow cytometry immune profiling of both chronic and acute infected versus naïve mice to visualise any potential difference in immune profile caused by infection.

3.2.1 Analysis of Myeloid Cells in the Liver

Eosinophils have a significant role in immune responses towards parasitic and helminth infections, such as whipworm, whereas neutrophils can contribute to the initial response to infection (Dixon *et al.*, 2006). As such, comparisons were made between the identified proportions of eosinophil and neutrophil subsets within the liver (Fig.14).

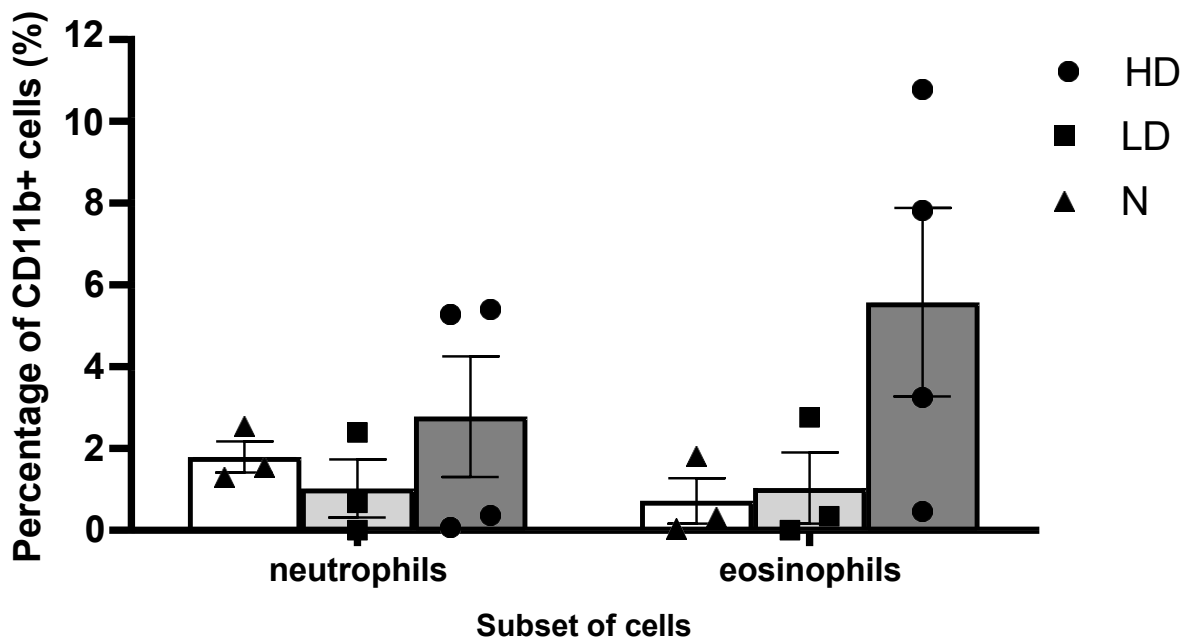


Fig.14. No significant differences were found concerning neutrophil and eosinophil subsets in the livers of mice infected with high doses or low doses of *T. muris*.

Mice were infected with high (~200eggs) or low (~30 eggs) doses of *T. muris* and then culled at days 25 and 27 post-infection, where livers were removed digested in liberase before cell populations were examined via flow cytometry.

N=3-4 mice per group are from 4 Independent experiments, presented as mean \pm SEM. Statistical analysis was completed using ANOVA with Šidák's multiple comparison tests.

On comparison, neither a Th2 inducing high dose or Th1 inducing low dose infection had a significantly different percentage of neutrophils from the respective naïve group (1.257%, $\pm 0.5338\%$, $P=0.9516$ and 0.9805 for high and low dose respectively). In addition, the proportion of neutrophils present as a percentage of CD11b+ cells in high dose treatment (3.68%, SEM $\pm 0.909\%$) were not different from low dose treatment (1.024% $\pm 1.767\%$, $P=0.7888$).

We next examined the proportion of eosinophils present as a percentage of CD11b+ cells and observed that neither high dose or low dose treatments were significantly different from the naïve group (0.7232% $\pm 0.375\%$, $P=0.3595$ and 0.8128 for high and low dose respectively). When comparing the Th2 and Th1 inducing parasite doses, we saw that high dose treatment (7.286%, $\pm 3.700\%$) was not different from the low dose treatment (1.037% $\pm 0.224\%$, $P=0.1239$). Collectively, this indicates that both acute and chronic *T. muris* infections do not alter granulocyte numbers at the distal infection tissue of the liver.

DCs, as previously stated, are key regulators of immune response. DCs are key regulators, linking the innate and adaptive immune system (Harris, 2017).

Monocytes /macrophages are key APCs to both Th1 and Th2 immune responses and likewise have been suspected to have a significant involvement in whipworm immune response ((De Schoolmeester *et al.*, 2009). As such, comparisons were made between the identified proportions of DC and monocyte-macrophage subsets in the liver (Fig.15).

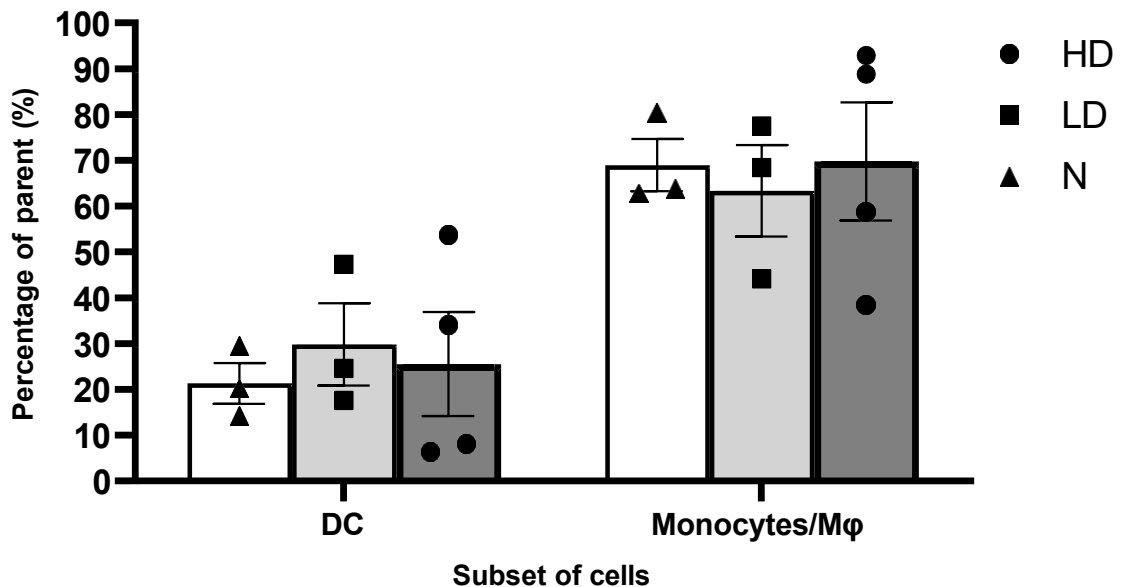


Fig.15. No significant differences were found concerning the proportions of dendritic cells and monocyte-macrophages present in the livers of mice infected with high doses of *T. muris* and low doses of *T. muris*.

Mice were infected with high (~200eggs) or low (~30 eggs) doses of *T. muris* and then culled at days 25 and 27 post-infection, where livers were removed digested in liberase before cell populations were examined via flow cytometry and presented as a percentage of CD11b+ Ly6G-MHCII+ cells.

N=3-4 mice per group are from 4 Independent experiments, presented as mean \pm SEM.

Statistical analysis was completed using ANOVA with Šidák's multiple comparison tests.

On comparison, neither a Th2 inducing high dose or Th1 inducing low dose infection had a significantly different percentage of DCs from the respective naïve group (21.30% \pm 5.674%, $P=0.9437$ and 0.8954 for high and low dose respectively). In addition,

the proportion of DCs present as a percentage of CD11b+ Ly6G- MHCII+ cells in high dose treatment (31.35%, SEM \pm 11.357%) were not different from low dose treatment (163.33% \pm 9.969%, $P=0.9957$).

We next examined the proportion of monocyte-macrophages present as a percentage of CD11b⁺ Ly6G⁻ MHCII⁺ cells and observed that neither high dose or low dose treatments were significantly different from the naïve group (68.97% ±5.674%, $P=0.9892$ and 0.9475 for high and low dose respectively). When comparing the Th2 and Th1 inducing parasite doses, we saw that high dose treatment (63.40%, SEM±12.894%) was not different from the low dose treatment (63.33% ±9.969%, $P>0.9999$).

Collectively, this indicates that both acute and chronic *T. muris* infections do not alter APC populations at the liver, a tissue distal to infection site.

Monocytes produce a waterfall during differentiation and maturation, whereby Ly6C⁺ MHCII⁻ monocytes differentiate into activated mature Ly6C⁻ MHCII⁺ macrophages, with an Ly6C⁺ MHCII⁺ intermediate phase (Desalegn and Pabst, 2019) and we therefore further subdivided our population, as the amount of activated mature macrophages present is indicative of the presence of an immune response; hence this was also investigated (Fig.16).

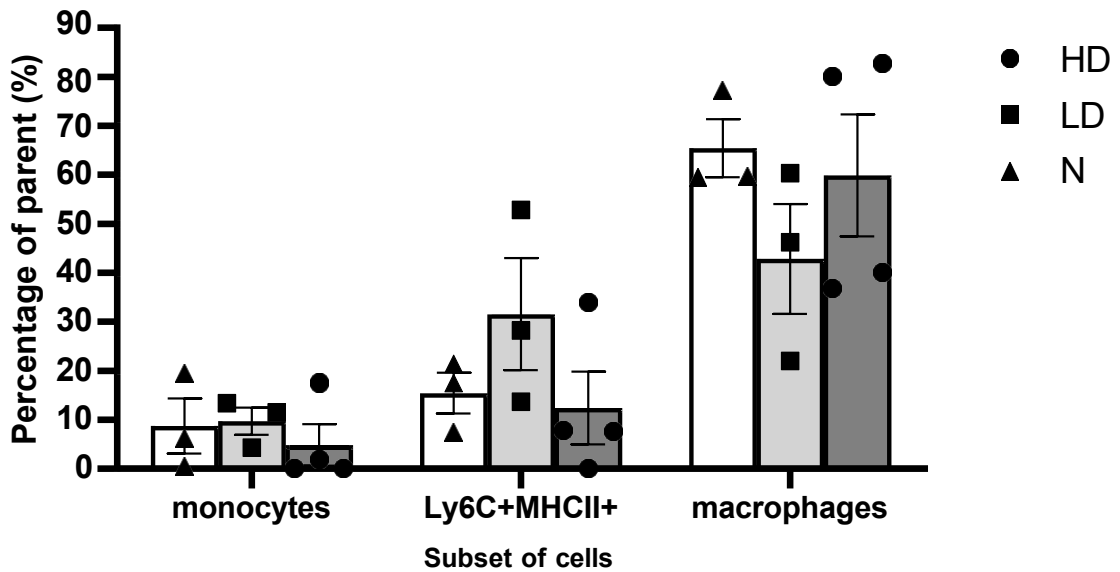


Fig.16. The monocyte waterfall found in the livers of mice infected with high doses and low doses of *T. muris* displayed no differences between treatment groups.

Mice were infected with high (~200eggs) or low (~30 eggs) doses of *T. muris* and then culled at days 25 and 27 post-infection, where livers were removed digested in liberase before cell populations were examined via flow cytometry and presented as a percentage of CD64+ monocyte-macrophage cells.

N=3-4 mice per group are from 4 Independent experiments, presented as mean \pm SEM. Statistical analysis was completed using ANOVA with Šidák's multiple comparison tests.

On comparison, neither a Th2 inducing high dose or Th1 inducing low dose infection had a significantly different percentage of monocytes from the respective naïve group (8.710% \pm 5.631%, $P=0.9614$ and 0.9788 for high and low dose respectively). Additionally, the proportion of monocytes present as a percentage of CD11b+ Ly6G- MHCII+ cells in high dose treatment (5.833%, SEM \pm 4.239%) were not different from low dose treatment (9.727 \pm 2.778, $P=0.7901$).

When examining the proportion of intermediate cells present as a percentage of CD64+ monocyte-macrophage cells and observed that neither high dose or low dose treatments were significantly different from the naïve group (4.165% \pm 5.674%, $P=0.9831$ and 0.3917 for high and low dose respectively). When comparing the Th2 and Th1 inducing parasite doses, we saw that high dose treatment (13.90%, SEM \pm 7.432%) was not different from the low dose treatment (31.57% \pm 9.969%, $P=0.6509$).

We next examined the proportion of macrophages present as a percentage of CD64+ monocyte-macrophage cells and observed that neither high dose or low dose treatments were significantly different from the naïve group (65.43% \pm 5.9336%, $P=0.4880$ and 0.1703 for high and low dose respectively). When comparing the Th2 and Th1 inducing parasite doses, we saw that high dose treatment (53.17%, SEM \pm 12.428%) was not different from the low dose treatment (42.83% \pm 11.184%, $P=0.6277$).

Collectively, this indicates that both acute and chronic *T. muris* infections do not alter the sequential monocyte differentiation at the distal tissue of the liver.

3.2.2 Analysis of Myeloid Cells in the Bladder

Myeloid cells were also examined in the bladders of mice in addition to the liver, as inflammatory subsets in the bladder may influence MUP levels due to this organ's close connections to urine.

Eosinophil and neutrophil cell subsets were identified in bladder samples (Fig.17).

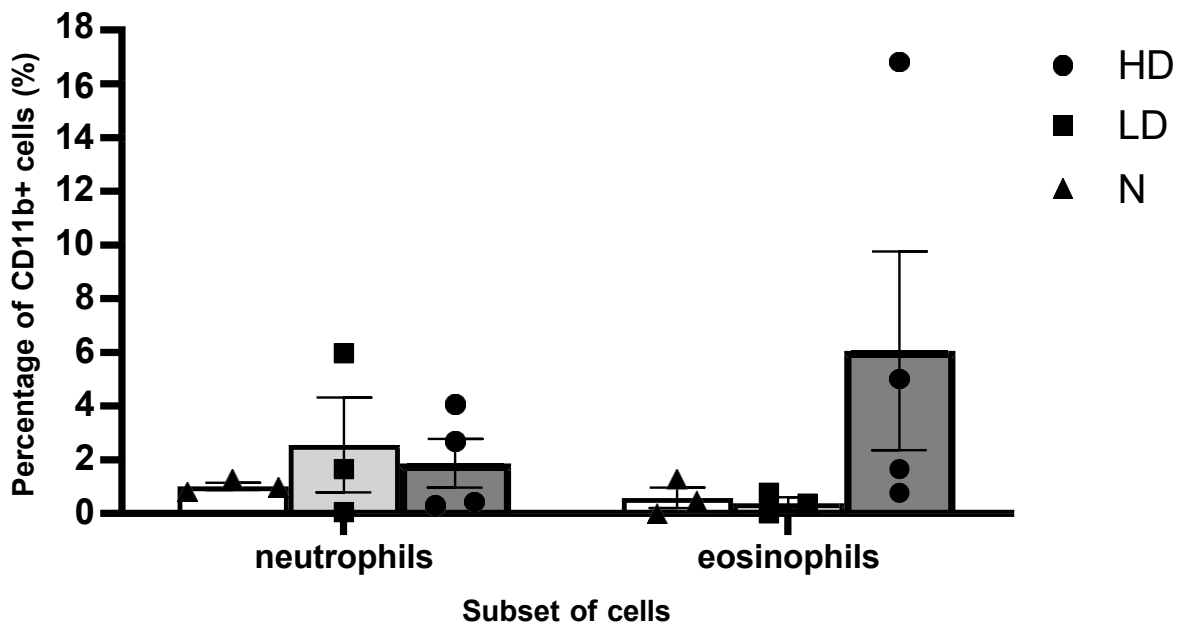


Fig.17. No significant differences were found concerning neutrophil and eosinophil subsets in the bladders of mice infected with high doses or low doses of *T. muris*.

Mice were infected with high (~200eggs) or low (~30 eggs) doses of *T. muris* and then culled at days 25 and 27 post-infection, where livers were removed digested in liberase before cell populations were examined via flow cytometry. N=3-4 mice per group are from 4 Independent experiments, presented as mean \pm SEM. Statistical analysis was completed using ANOVA with Šidák's multiple comparison tests.

On comparison, neither a Th2 inducing high dose or Th1 inducing low dose infection had a significantly different percentage of neutrophils from the respective naïve group (1.011% \pm 0.379%, $P=0.6919$ and 0.8687 for high and low dose respectively). In addition, the proportion of neutrophils present as a percentage of CD11b+ cells in high dose treatment (2.347%, SEM \pm 1.476%) were not different from low dose treatment (2.555% \pm 0.710%, $P=0.9999$).

We next examined the proportion of eosinophils present as a percentage of CD11b+ cells and observed that neither high dose or low dose treatments were significantly different from the naïve group (0.5835% \pm 0.554%, $P=0.5489$ and 0.9801 for high and low dose respectively). When comparing the Th2 and Th1 inducing parasite doses, we saw that high dose treatment (7.828%, \pm 2.304%) was not different from the low dose treatment (0.3825% \pm 0.871%, $P=0.5679$). Collectively, this indicates that both acute and chronic *T. muris* infections do not alter granulocyte numbers at the distal tissue of the bladder.

DC and monocyte-macrophage cell subsets were also examined in the bladder (Fig.18).

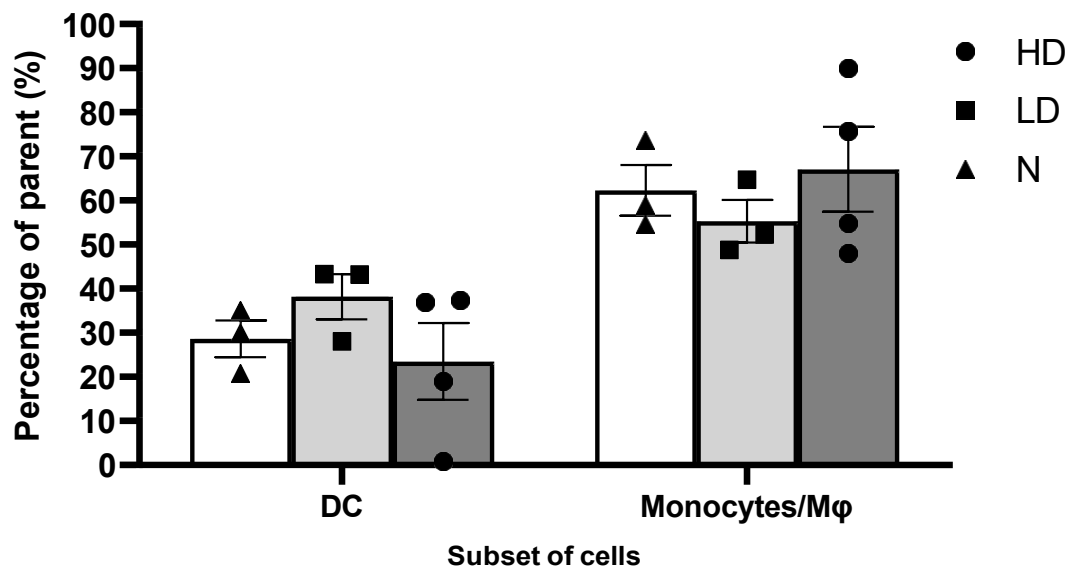


Fig.18. No significant differences were found concerning the proportions of dendritic cells and monocyte-macrophages present in the bladders of mice infected with high doses and low doses of *T. muris*.

Mice were infected with high (~200eggs) or low (~30 eggs) doses of *T. muris* and then culled at days 25 and 27 post-infection, where bladders were removed digested in liberase before cell populations were examined via flow cytometry and presented as a percentage of CD11b+ Ly6G- MHCII+ cells.

N=3-4 mice per group are from 4 Independent experiments, presented as mean \pm SEM. Statistical analysis was completed using ANOVA with Šidák's multiple comparison tests.

On comparison, neither a high dose or low dose infection had a significantly different percentage of DCs from the respective naïve group (28.60% \pm 4.159%, $P=0.9902$ and 0.6722 for high and low dose respectively). Additionally, the proportion of DCs present as a percentage of CD11b+ Ly6G- MHCII+ cells in high dose treatment (31.07%, \pm 8.7135%) were not different from low dose treatment (38.17% \pm 4.824%, $P=0.0525$).

We next examined the proportion of monocyte-macrophages present as a percentage of CD11b+ Ly6G- MHCII+ cells and observed that neither high dose

or low dose treatments were significantly different from the naïve group (62.30% \pm 5.728%, $P=0.9959$ and 0.8910 for high and low dose respectively). When comparing the Th2 and Th1 inducing parasite doses, we saw that high dose treatment (56.47%, \pm 19.616%) was not different from the low dose treatment (55.27% \pm 4.824%, $P=0.7290$).

Collectively, this indicates that both acute and chronic *T. muris* infections do not alter these cell populations at the bladder.

From this, the amount of activated mature macrophages present was also investigated in bladder samples (Fig.19).

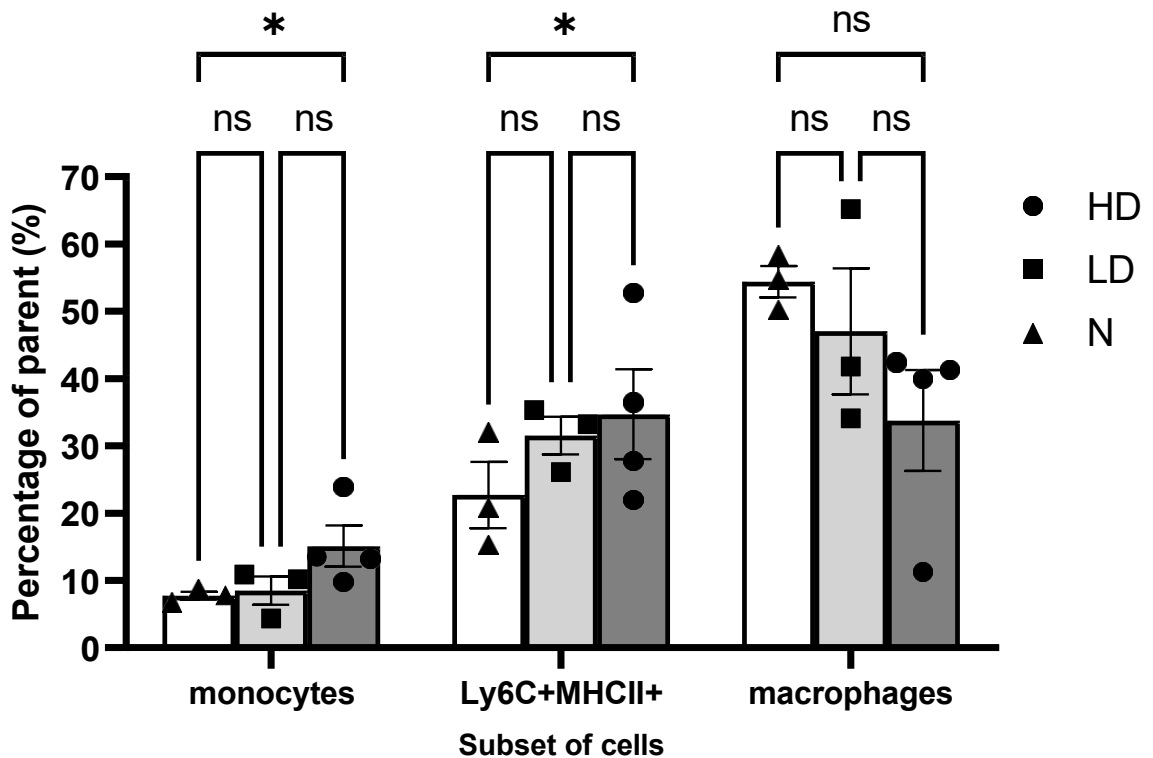


Fig.19. The monocyte waterfall found in the bladders of mice infected with high doses and low doses of *T. muris* displayed significant differences between high dose and naïve treatment groups in monocytes and CD11b+ Ly6C- MHCII+ cells.

Mice were infected with high (~200eggs) or low (~30 eggs) doses of *T. muris* and then culled at days 25 and 27 post-infection, where bladders were removed digested in liberase before cell populations were examined via flow cytometry and presented as a percentage of CD64+ monocyte-macrophage cells.

N=3-4 mice per group are from 4 Independent experiments, presented as mean \pm SEM. Statistical analysis was completed using ANOVA with Šidák's multiple comparison tests. Differences were found between high dose and naïve treatment groups concerning the percentages of monocytes (P=0.0456) and Ly6C+MHCII+ cells (P=0.0321).

On comparison, a Th2 inducing high dose (12.15%, \pm 3.057%) had a significantly different percentage of monocytes from the naïve group (7.747% \pm 4.159%, P=0.0456).

However, the Th1 inducing low dose infection (8.483% \pm 2.077%) did not have significantly different percentage of monocytes from the respective naïve group (P=0.8901).

In addition, the proportion of monocytes present as a percentage of CD11b+ Ly6G- MHCII+ cells in high dose treatment were not different from low dose treatment ($P=0.0945$).

When examining the proportion of intermediate cells present as a percentage of CD64+ monocyte-macrophage cells, high dose treatment (28.70%, $\pm 6.700\%$) was significantly different from the naïve group (22.70% $\pm 4.914\%$, $P=0.0321$).

However, low dose treatments (8.483% $\pm 2.077\%$) were not significantly different from the naïve group ($P=0.5630$). When comparing the Th2 and Th1 inducing parasite doses, we saw that high dose treatment was also not different from the low dose treatment ($P=0.9093$).

On examining the proportion of macrophages present as a percentage of CD64+ monocyte-macrophage cells and observed that neither high dose or low dose treatments were significantly different from the naïve group (54.40% $\pm 2.343\%$, $P=0.0883$ and 0.8089 for high and low dose respectively). When comparing the acute and chronic inducing parasite doses, we saw that high dose treatment (41.23%, $\pm 7.499\%$) was not different from the low dose treatment (47.03%, $\pm 9.351\%$, $P=0.8101$).

Collectively, this indicates that both acute and chronic *T. muris* infections may alter the sequential monocyte differentiation at the bladder.

Collectively, the myeloid populations examined suggest that high doses of *T. muris* seemed to only induce changes within the monocyte waterfall in the bladder, but no changes were identified in the liver.

3.2.3 Analysis of T Cells in the Liver

As mentioned previously, T cell populations, particularly CD4+ T cells, have an essential and significant role in the immune response against *T. muris*, with the depletion of CD4+ T cells in particular resulting in susceptibility (Koyama *et al.*, 1995, Koyama, 2002, Humphreys *et al.*, 2004). Unpublished data from our lab suggests T-cells could be one of the immune mechanisms that are inducing the recorded odour changes caused by trichuriasis infection. Therefore, lymphoid cells were also examined in the livers of mice with high dose and low dose infections and compared with naïve control mice bladder populations.

Both CD4+ and CD8 α + cells are significant components in whipworm-induced protective immune response, most notably CD4+ cells due to their roles in expulsion (Koyama *et al.*, 1995). As such, comparisons were made between the identified proportions of CD4+ and CD8 α + subsets within the liver, in addition to the proportions of these that are activated via the loss of expression of CD45RB (Fig.20).

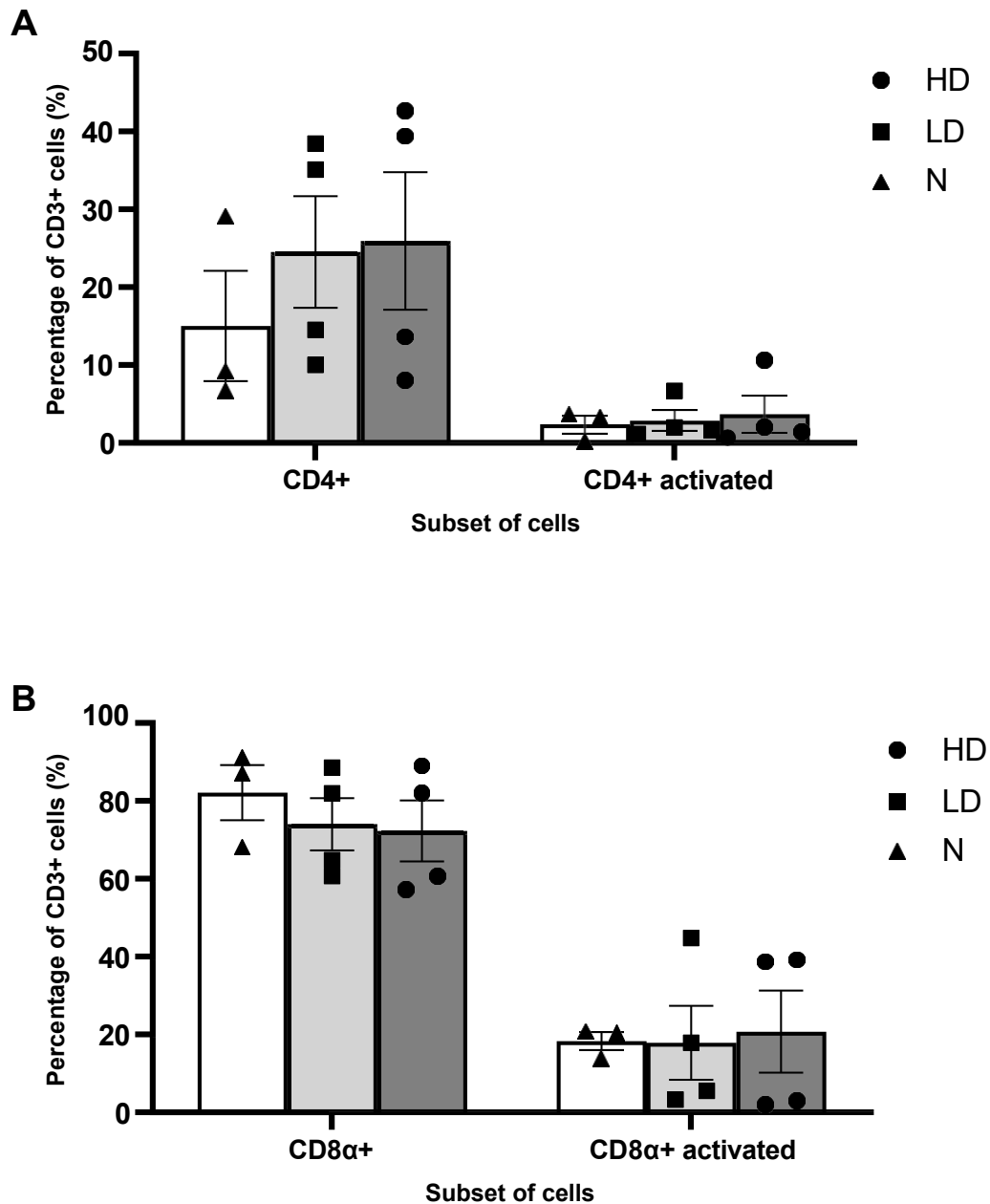


Fig.20. No significant differences were found concerning CD4+ and CD8α+ subsets in the livers of mice infected with high doses or low doses of *T. muris*. Mice were infected with high (~200eggs) or low (~30 eggs) doses of *T. muris* and then culled at days 25 and 27 post-infection, where livers were removed digested in liberase before cell populations were examined via flow cytometry. Plotted data show the percentage of CD3+ cells that are (A) CD4+ and activated CD4+; and (B) CD8α+ and activated CD8α+. N=3-4 mice per group are from 4 Independent experiments, presented as mean ± SEM. Statistical analysis was completed using ANOVA with Šidák's multiple comparison tests.

On comparison, neither a Th2 inducing high dose or Th1 inducing low dose infection had a significant impact on the percentage of CD4⁺ cells from the respective naïve group (17.26%, \pm 7.08%, $P=0.9329$ and 0.9287 for high and low dose respectively). In addition, the proportion of CD4⁺ cells present as a percentage of CD3⁺ cells in high dose treatment (25.94%, \pm 8.82%) were not different from low dose treatment (24.53%, \pm 7.89%, $P=0.7039$).

We next examined the proportion of activated CD4⁺ cells present as a percentage of CD3⁺ cells, via the loss of expression of CD45RB, and observed that neither high dose or low dose treatments were significantly different from the naïve group (2.384% \pm 1.10%, $P=0.7830$ and 0.7808 for high and low dose respectively). When comparing the Th2 and Th1 inducing parasite doses, we saw that high dose treatment (3.679% \pm 2.33%) was not different from the low dose treatment (2.359% \pm 1.26%, $P=0.7404$).

Concerning CD8 α +cytotoxic T-cells, neither a Th2 inducing high dose or Th1 inducing low dose infection had a significantly different percentage from the respective naïve group (80.02% \pm 7.09%, $P=0.9367$ and 0.9556 for high and low dose respectively). In addition, the proportion of CD8 α + cells present as a percentage of CD3⁺ cells in high dose treatment (72.27%, \pm 7.84 %) were not different from low dose treatment (74.00% \pm 7.28%, $P=0.4233$).

We next examined the proportion of activated CD8 α + cells present as a percentage of CD3⁺ cells and observed that neither high dose or low dose treatments were significantly different from the naïve group (18.29 \pm 2.28%,

P=0.8072 and 0.9458 for high and low dose respectively). When comparing the Th2 and Th1 inducing parasite doses, we saw that high dose treatment (20.379% \pm 10.52%) was not different from the low dose treatment (17.87% \pm 3.70%, $P=0.8883$).

Collectively, this indicates that both acute and chronic *T. muris* infections do not alter either CD4 helper or CD8 cytotoxic T cells at the distal tissue of the liver. The proportions of activated T-cells were further distinguished by the expression of the transcription factors T-bet and GATA3 to examine polarisation from both CD4 and CD8 α ⁺ subsets (Fig.21).

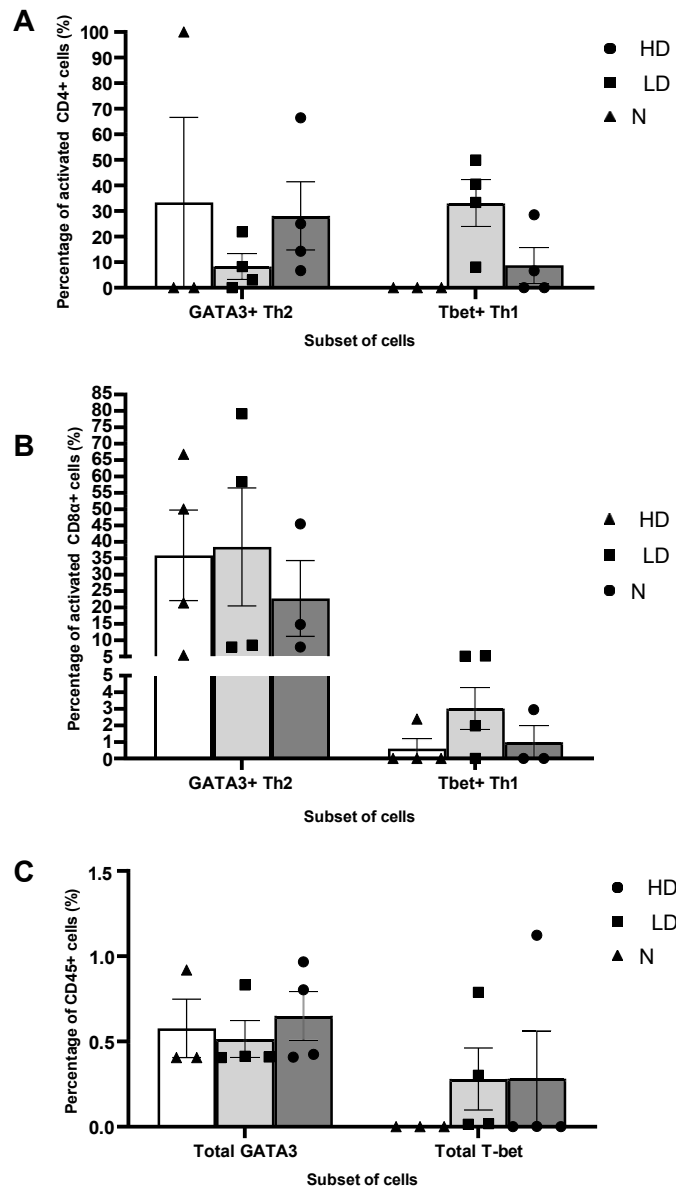


Fig.21. No significant differences were found concerning T-bet Th1 and GATA3 Th2 subsets in activated T-cells in the livers of mice infected with high doses or low doses of *T. muris*.

Mice were infected with high (~200eggs) or low (~30 eggs) doses of *T. muris* and then culled at days 25 and 27 post-infection, where livers were removed digested in liberase before cell populations were examined via flow cytometry. N=3-4 mice per group are from 4 Independent experiments, presented as mean \pm SEM. Statistical analysis was completed using ANOVA with Šidák's multiple comparison tests.

Plotted data show (A) the Th1 and Th2 cell subsets as a proportion of activated CD4+ cells; (B) the Th1 and Th2 cell subsets as a proportion of activated CD8α+ cells; and (C) the total proportion of T-bet Th1 and Gata3 Th2 cells out of all CD45+ cells.

On comparison of the activated CD4⁺ T-cells, neither a Th2 inducing high dose or Th1 inducing low dose infection had a significantly different percentage of T-bet⁺ cells out of activated CD4⁺ cells from the respective naïve group (0.00% ±0.333%, $P=0.6666$ and 0.2920 for high and low dose respectively). In addition, the proportion of T-bet⁺ cells present in high dose treatment (8.809% ±6.77%) were not different from low dose treatment (32.98% ±9.75%, $P=0.2313$).

We next examined the proportion of GATA3 cells present as a percentage of activated CD4⁺ cells and observed that neither high dose or low dose treatments were significantly different from the naïve group (33.33% ±33.33%, $P=0.9579$ and 0.8822 for high and low dose respectively). When comparing the Th2 and Th1 inducing parasite doses, we saw that GATA3 expression in activated CD4⁺ T-cells in high dose treatment (28.11%, ±13.32%) was not different from the low dose treatment (8.131%, ±0.1439%, $P=0.6908$).

Concerning activated CD8 α ⁺ cells, neither a Th2 inducing high dose or Th1 inducing low dose infection had a significantly different percentage of T-bet⁺ cells from the respective naïve group (0.9818%, ±2.28%, $P=0.8075$ and 0.2522 for high and low dose respectively). In addition, the proportion of T-bet⁺ cells present as a percentage of activated CD8 α ⁺ cells in high dose treatment (0.5965%, ±10.52%) were not different from low dose treatment (3.02%, ±3.70%, $P=0.2756$).

We next examined the proportion of GATA3 cells present as a percentage of activated CD8 α ⁺ cells and observed that neither high dose or low dose

treatments were significantly different from the naïve group (22.66% \pm 11.56%, $P=0.9747$ and 0.9034 for high and low dose respectively). When comparing the Th2 and Th1 inducing parasite doses, we saw that high dose treatment (35.83%, \pm 13.82%) was not different from the low dose treatment (38.39% \pm 18.87%, $P=0.9923$).

The total amount of T-bet positive cells present as a percentage of CD45+ cells in high dose treatment (0.2815%, \pm 0.281%) was not significantly different from low dose treatment (0.2804% \pm 0.194%, $P>0.9999$). Neither high dose or low dose treatments was significantly different from naïve group (0 \pm 0, $P=0.8063$ and 0.7833 for high and low dose respectively).

The total amount of GATA3 cells present as a percentage of CD45+ cells in high dose treatment (0.6506%, \pm 0.140%) was not different from low dose treatment (0.5150% \pm 0.117%, $P=0.5580$). Neither high dose or low dose treatments was different from naïve group (0.5770% \pm 0.171%, $P=0.5494$ and 0.8695 for high and low dose respectively).

Collectively, this indicates that both acute and chronic *T. muris* infections do not alter T-bet and GATA3 expression in cells at the distal tissue of the liver.

3.2.4 Analysis of T Cells in the Bladder

Concerning urine, the bladder could also be identified as a significant site due to its involvement in urine storage. Any signs of a whipworm-induced immune response in this site could also significantly influence MUP expression and potentially urine odour.

In addition to the liver, high dose and low dose infections were compared with naïve control mice bladders.

Comparisons were made between the identified proportions of CD4⁺ and CD8 α ⁺ subsets, and additionally, the proportions of these that were activated via CD45RB^{hi} expression loss (Fig.22).

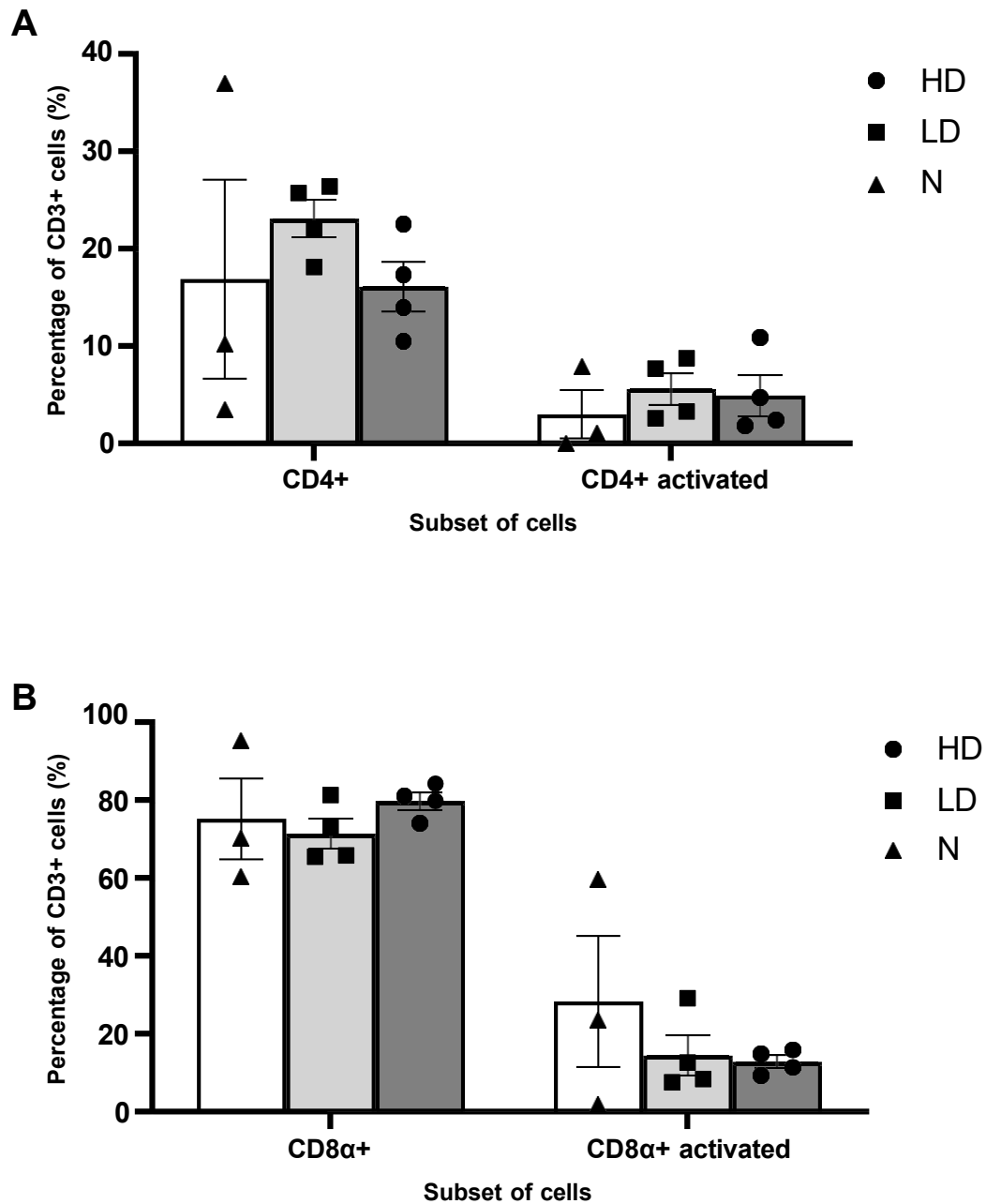


Fig.22. No significant differences were found concerning CD4+ and CD8α+ subsets in the bladders of mice infected with high doses or low doses of *T. muris*.

Mice were infected with high (~200eggs) or low (~30 eggs) doses of *T. muris* and then culled at days 25 and 27 post-infection, where bladders were removed digested in liberase before cell populations were examined via flow cytometry. Plotted data show the percentage of CD3+ cells that are (A) CD4+ and activated CD4+; and (B) CD8α+ and activated CD8α+. N=3-4 mice per group are from 4 Independent experiments, presented as mean ± SEM. Statistical analysis was completed using ANOVA with Šidák's multiple comparison tests.

On comparison, neither a Th2 inducing high dose or Th1 inducing low dose infection had a significantly different percentage of CD4+ cells from the respective naïve group (16.88%, $\pm 10.2\%$, $P > 0.9999$ and 0.7167 for high and low dose respectively). In addition, the proportion of CD4+ cells present as a percentage of CD3+ cells in high dose treatment (16.09%, $\pm 2.55\%$) were not different from low dose treatment (23.07%, $\pm 1.90\%$, $P = 0.2391$).

We next examined the proportion of activated CD4+ cells present as a percentage of CD3+ cells and observed that neither high dose or low dose treatments were significantly different from the naïve group (2.98% $\pm 2.48\%$, $P = 0.7711$ and 0.4659 for high and low dose respectively). When comparing the Th2 and Th1 inducing parasite doses, we saw that high dose treatment (4.927%, $\pm 2.07\%$) was not different from the low dose treatment (5.57%, $\pm 1.54\%$, $P = 0.8213$).

Concerning CD8 α + cells, neither a Th2 inducing high dose or Th1 inducing low dose infection had a different percentage from the respective naïve group (75.17%, $\pm 10.38\%$, $P = 0.9357$ and 0.8430 for high and low dose respectively). In addition, the proportion of CD8 α + cells present as a percentage of CD3+ cells in high dose treatment (79.77%, SEM $\pm 2.14\%$) were not significantly different from low dose treatment (71.38% $\pm 3.73\%$, $P = 0.2540$).

We next examined the proportion of activated CD8 α + cells present as a percentage of CD3+ cells and observed that neither high dose or low dose

treatments were significantly different from the naïve group (28.31%, \pm 16.85%, $P=0.6236$ and 0.7980 for high and low dose respectively). When comparing the Th2 and Th1 inducing parasite doses, we saw that high dose treatment (12.82%, \pm 1.53%) was not different from the low dose treatment (14.41% \pm 5.02%, $P=0.9641$).

Collectively, this indicates that both acute and chronic *T. muris* infections do not alter these T cells at the distal tissue of the bladder.

The proportions of activated Th2/Th1 cells were also identified from both CD4 and CD8 α ⁺ subsets (Fig.23).

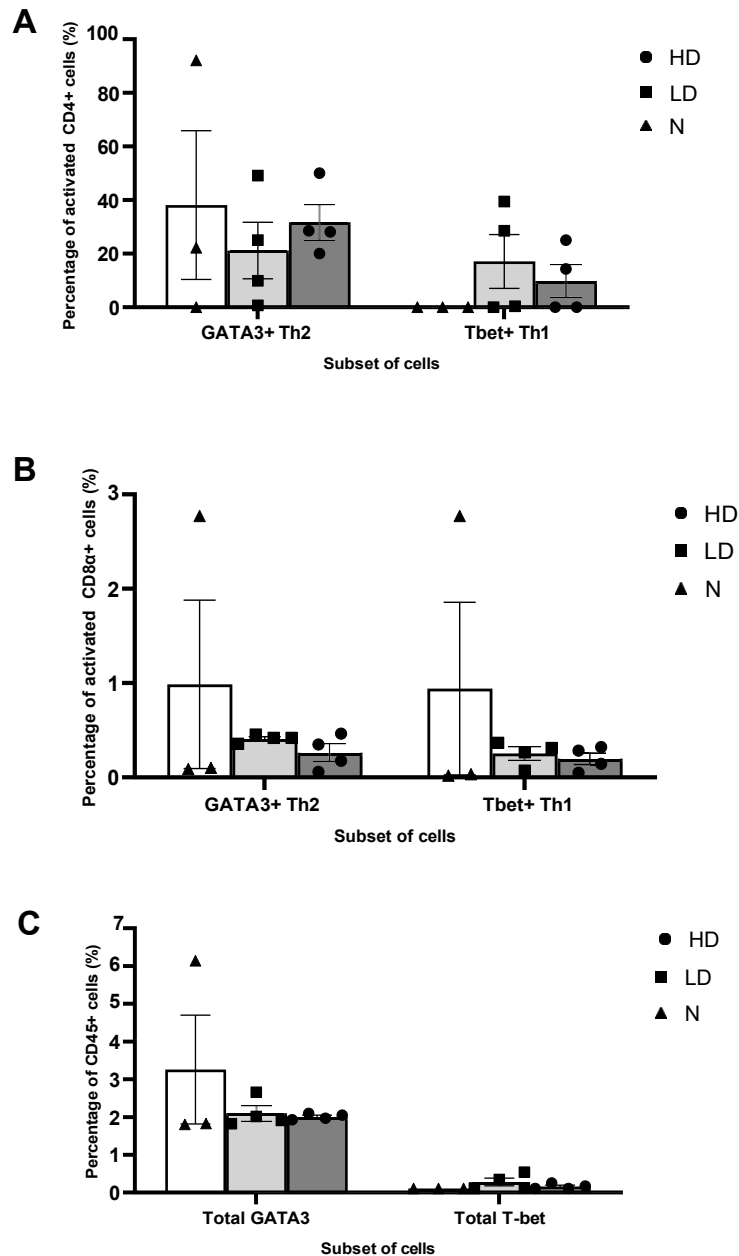


Fig.23. No significant differences were found concerning Th1 and Th2 subsets in the bladders of mice infected with high doses or low doses of *T. muris*.

Mice were infected with high (~200eggs) or low (~30 eggs) doses of *T. muris* and then culled at days 25 and 27 post-infection, where bladders were removed digested in liberase before cell populations were examined via flow cytometry. N=3-4 mice per group are from 4 Independent experiments, presented as mean \pm SEM. Statistical analysis was completed using ANOVA with Šidák's multiple comparison tests.

Plotted data show (A) the Th1 and Th2 cell subsets as a proportion of activated CD4+ cells; (B) the Th1 and Th2 cell subsets as a proportion of activated CD8 α + cells; and (C) the total proportion of Th1 and Th2 cells out of all CD45+ cells.

On comparison, neither a Th2 inducing high dose or Th1 inducing low dose infection had a significantly different percentage of T-bet⁺ cells out of activated CD4⁺ cells from the respective naïve group (0%, ±0%, $P=0.8075$ and 0.8003 for high and low dose respectively). In addition, the proportion of T-bet⁺ cells present as a percentage of activated CD4⁺ cells in high dose treatment (9.821%, ±6.484%) were not different from low dose treatment (17.09%, ±10.01%, $P=0.4364$).

We next examined the proportion of GATA3 cells present as a percentage of activated CD4⁺ cells and observed that neither high dose or low dose treatments were different from the naïve group (38.11%, ±27.75%, $P=0.9702$ and 0.9876 for high and low dose respectively). When comparing the Th2 and Th1 inducing parasite doses, we saw that high dose treatment (31.67%, ±6.418%) was not significantly different from the low dose treatment (21.16 ±10.57%, $P=0.9024$).

Concerning activated CD8 α ⁺ cells, neither a Th2 inducing high dose or Th1 inducing low dose infection had a significantly different percentage of T-bet⁺ cells from the respective naïve group (0.9414%, ±915%, $P=0.8191$ and 0.9354 for high and low dose respectively). In addition, the proportion of T-bet⁺ cells present as a percentage of activated CD8 α ⁺ cells in high dose treatment (0.1991%, ±0.0630%) were not different from low dose treatment (0.2535%, ±3.70%, $P=0.5602$).

We next examined the proportion of GATA3 cells present as a percentage of activated CD8 α ⁺ cells and observed that neither high dose or low dose

treatments were different from the naïve group (0.9869%, $\pm 0.892\%$, $P=0.8386$ and 0.9160 for high and low dose respectively). When comparing the Th2 and Th1 inducing parasite doses, we saw that high dose treatment (0.2617%, $\pm 0.090\%$) was not significantly different from the low dose treatment (0.4122%, $\pm 0.020\%$, $P=0.9656$).

When compared, the total amount of T-bet positive cells presents as a percentage of CD45+ cells in high dose treatment (0.1608, SEM ± 0.038) was not significantly different from low dose treatment (0.2787 ± 0.189 , $P=0.3378$). Neither high dose or low dose treatments was significantly different from naïve group (0.1094 ± 0 , $P=0.6452$ and 0.6219 for high and low dose respectively).

The total amount of GATA-3 cells presents as a percentage of CD45+ cells in high dose treatment (2.011, SEM ± 0.038) was also not different from low dose treatment (2.102 ± 0.189 , $P=0.9057$). Neither high dose or low dose treatments were different from naïve group (3.257 ± 1.44 , $P=0.6890$ and 0.8002 for high and low dose respectively).

Collectively, this indicates that both acute and chronic *T. muris* infections do not alter Th1 and 2 cells at the distal tissue of the bladder.

Concerning all the examined lymphoid cells, *T. muris* seemed to cause no immune changes in the liver and bladder.

3.3 Preliminary Testing of Mouse Urine Suggested That Low Dose *T. muris* Infection was Not Detectable by VOC Analysis

Changes in MUP expression suggest that there may be *T. muris*-induced changes in the VOC profile of mouse urine, however, the immune populations in relevant organs suggest limited infection-induced changes beyond monocyte waterfall alterations. To conclude if infection can produce distinctive infection-induced VOC profiles, VOC analysis has previously been conducted on *T. muris*-infected mouse hair. This displayed distinct differences when compared with naïve populations. To examine if this was the case with urine, principal component analysis was conducted on the VOC profiles detected by the VOC analyser, using all 24 extracted divergencies/peak heights and areas. These sensors recorded the response patterns for each sample as a quantitative odour fingerprint.

Based on these sensor data, PCA suggested that there is no significant visible differences between low dose and naïve control group odour profiles when samples from day 35 post-infection was examined. As seen in Fig.24, the two treatment groups were randomly clustered with no stark distinction between either treatment group.

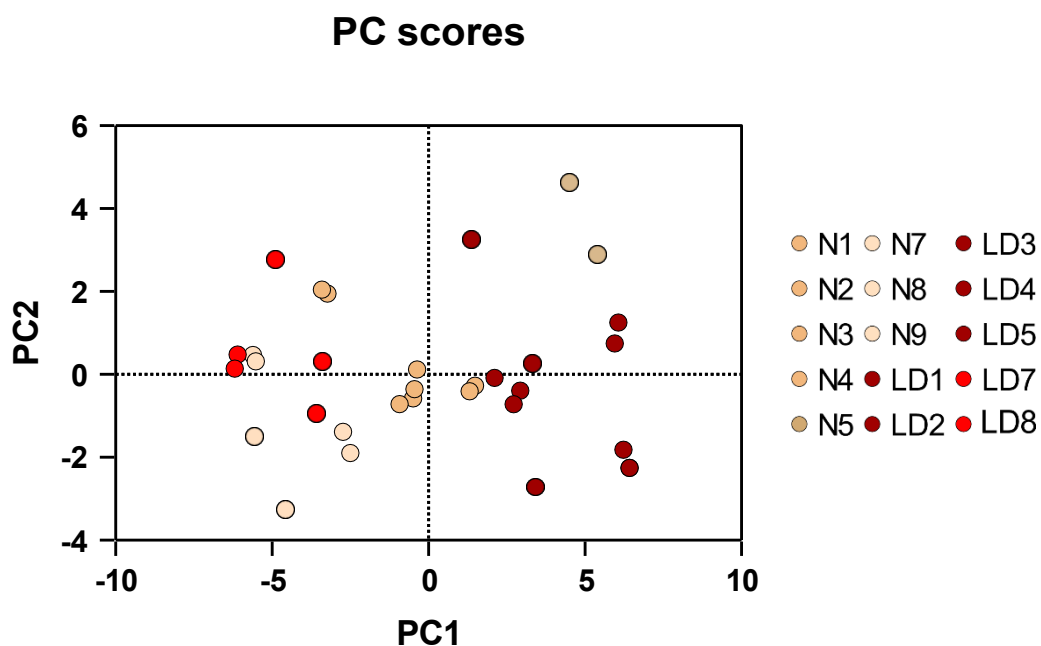


Fig.24. Preliminary examination of the urine of mice with low dose *T. muris* infection displayed little change in VOC profile.

The urine from C57BL/6 mice infected with ~30 *T. muris* eggs was taken after 35 days post-infection. Mouse urine VOC profiles were then analysed using a portable VOC analyser (Model 720, Roboscientific Ltd). Data (n=9 naive, 8 low dose) were analysed twice each and all 24 extracted divergencies/peak heights and areas collected from sensors were analysed and presented using principal component analysis (PCA) using similar colours represent cage groups. Further analysis on this data was conducted using machine learning models for model training and classification analysis.

Machine learning models were applied for model training and classification analysis. Based on these sensor data, three common machine learning methods were applied combined with PCA, including Logistic Regression, Multi-Layer Perceptron (MLP), and Random Forest (Fig.25).

When models were able to consistently classify the samples accurately, this indicated that samples were distinguishable. Results were evaluated using overall accuracy for straightforward interpretation.

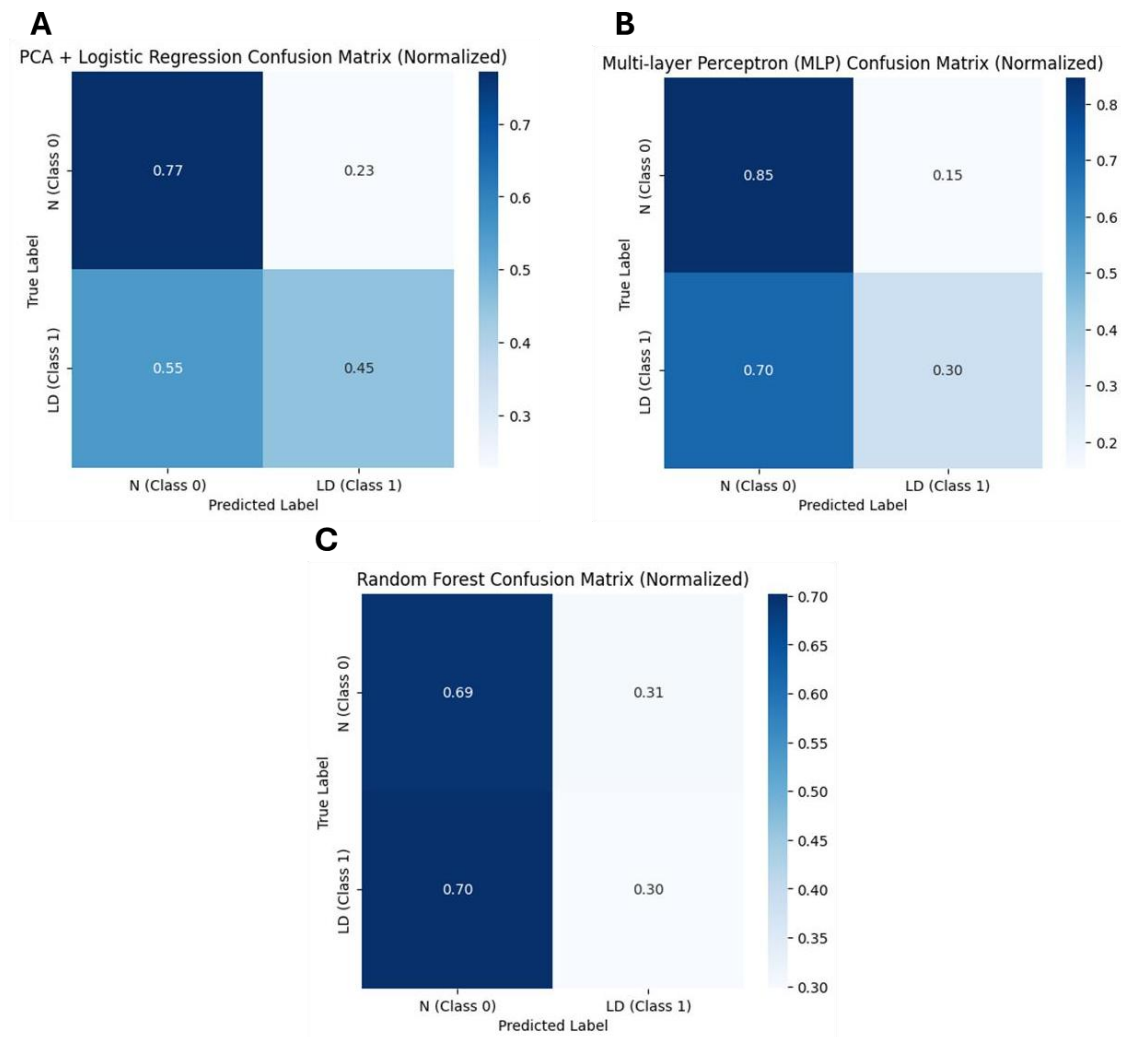


Fig.25. Machine learning analysis of low dose *T. muris*-infected mouse urine indicates that there are some differences between naïve and infected VOC profiles.

The urine from C57BL/6 mice infected with ~30 *T. muris* eggs was taken after 35 days post-infection. Mouse urine VOC profiles (n=9 naïve, 8 low dose) were then analysed twice per sample using a portable VOC analyser (Model 720, Roboscientific Ltd). Data was subject to 3 machine learning models: (A) a principal component analysis and Logistic Regression model, (B) a multi-layer perceptron model, and (C) a Random Forest model, displayed as normalised confusion matrices.

'N (class 0)' denotes naïve VOC profiles and LD (class 1) denotes low dose infected urine profiles. True positive identification of low dose urine VOC profiles is present on the bottom right of each matrix.

From the 9 samples analysed, three methods achieved high recognition accuracy rates for naïve samples, with Logistic Regression accurately identifying 77% and Random Forest accurately identifying 69%, particularly in the MLP model (with up to 85% accuracy).

However, model recognition accuracy was relatively low for low dose samples (ranging across models from 30-45%). This was also lower than random recognition (which would be 50% overall accuracy). All models struggled with sensitivity, misidentifying low dose samples as naïve (55-70%).

Overall, whilst the MLP model had the highest accuracy identifying naïve samples, Logistic Regression had the highest accurate recognition of low dose samples. Random Forest performed the worst overall, with the lowest accuracy concerning both low dose and naïve samples out of the models tested.

Whilst both groups were not completely identical in terms of sensor characteristics, there did seem to be a certain degree of separability. Low dose samples were challenging to identify, suggesting that infection-induced odour changes were present but unclear, unstable, or subtle. This prompted further analysis including more samples.

3.4 More extensive testing over the course of infection suggests that the VOC profiles present in mouse urine do change with infection

To further study infection-induced differences in urine, VOC analysis was conducted comparing urine from mice with high and low dose infections on days 7, 14, 25 post-infections against naïve urine (Fig.26).

Based on these sensor data, PCA indicated a clear visual difference between uninfected samples and infected counterparts, implying clear infection-induced VOC change. When judging the period of time infected, both low (red, B) and high dose (blue, C) samples seem to produce unclear clusters with overlaps, implying indistinct differences between days 7, 14, and 25 post-infections. High and low dose treatment groups overall seem to be hard to distinguish from PCA alone, spread across the x axis (A) and displaying overlap between the different treatment groups and no clear distinction between them. When compared with the infected groups (blue and red) however, the naïve group (yellow) samples were distinctly clustered together with no overlap to the infected groups, suggesting a clear, marked difference between infected and uninfected. From these graphs overall, whilst displaying poor distinction between days post-infection and overlaps between infected treatment groups, PCA suggests a clear distinction between infected and uninfected groups.

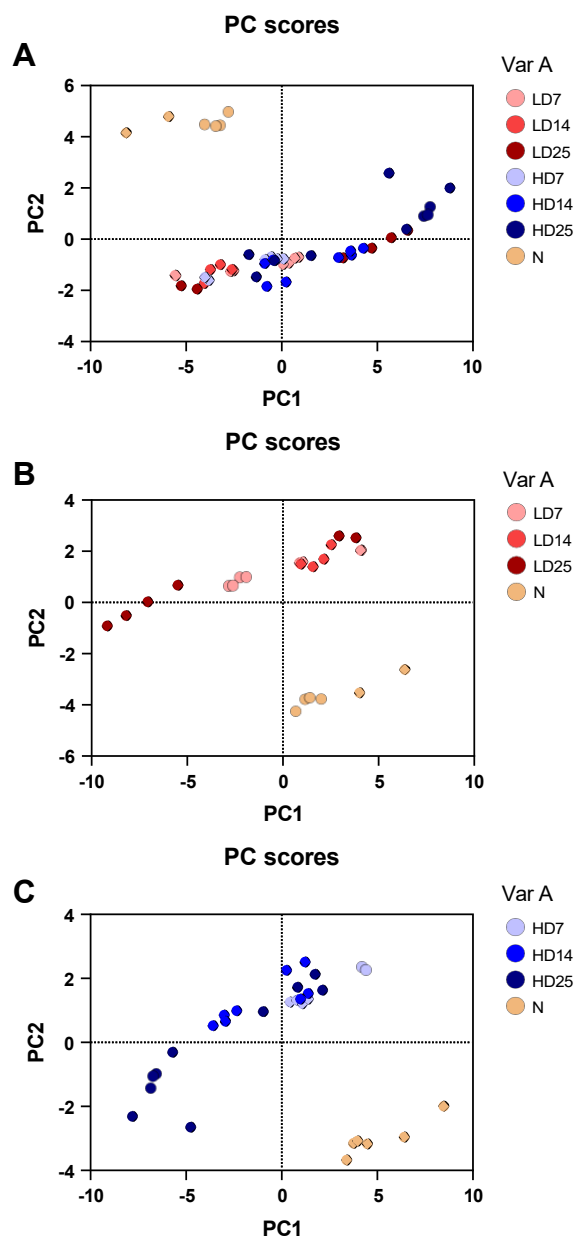


Fig.26. Further examination of *T. muris* infected mouse urine suggests clear infection-induced changes in VOC profiles.

The urine from C57BL/6 mice infected with either ~200 (HD) or ~30 (LD) *T. muris* eggs was collected on days 7, 14, and 25 post-infection, Mouse urine VOC profiles were then analysed using a portable VOC analyser (Model 720, Roboscientific Ltd). This analysis in total used 4 low dose samples from day 7 post-infection (LD7), 2 from day 14 (LD14), and 3 from day 25 (LD25). Regarding high dose infections, 3 day 7 post-infection (HD7), 4 day 14 (HD14), and 5 day 25 (HD25) samples were used. (A) all data (n=3 naive, 9 low dose, 12 high dose) were analysed twice each and presented using principal component analysis. (B) Low dose infected urine was compared with naïve samples, as was high dose infected urine (C).

Based on these data, a range of common machine learning models both alone and combined with PCA were applied for model training and classification analysis, including Random Forest, Logistic Regression, MLP, and radial basis function support vector machine. Machine learning analysis were conducted using a variety of algorithms which were trained on the same dataset, leading to more accurate and robust conclusions. Classification analysis consisted of day-dose classification (distinguishing between different days post-infection); 3-class dose classification (naïve, high dose, or low dose); and binary classification (infection vs non-infection). When models were able to consistently classify the samples accurately, this indicated that samples were distinguishable. Results were evaluated using overall accuracy for straightforward interpretation. In addition to overall accuracy, Macro F1 was calculated to evaluate the balanced performance of the model as a harmonic mean of precision and recall averaged across equally weighted groups. This score can help determine if the model is robust and performs well in balancing the predictions from both classes, so that no class is underrepresented.

3.4.1 Day-Dose Classification

Overall, all models tested performed consistently weakly when distinguishing between infection at different time periods (Table.6). Even the best performing model, Random Forest, had relatively low scores of 50% overall accuracy, with a Macro F1 of 41.67% indicating relatively low performance. Across all machine learning models tested, there was a low average accuracy of 37.5% (SEM±1.582%) and low average Macro F1 of 32.27% (±1.354%).

Table.6. Test set metrics for the classification of urine samples on days 7, 14, 25 and 35 of infection.

Model	Accuracy	Macro F1
RF	0.500000	0.416667
PCA10+LogReg	0.437500	0.402778
PCA10+RF	0.437500	0.385185
PCA30+RF	0.375000	0.325794
MLP	0.375000	0.320635
PCA20+RF	0.375000	0.319444
LogReg	0.375000	0.305556
PCA30+LogReg	0.375000	0.305556
PCA20+LogReg	0.375000	0.305556
PCA10+RBF SVM	0.312500	0.288889
RBF SVM	0.312500	0.273016
PCA20+RBF SVM	0.312500	0.273016
PCA30+RBF SVM	0.312500	0.273016

Models tested include RF (random forest), MLP (multilayer perceptron), LogReg (logistic regression), and RBF SVM (radial basis function support vector machine). These models were also combined with PCA (principal component analysis) using different PCA subspaces (10 components, 20 components and 30 components).

All models performed consistently weakly with low accuracy and Macro F1 scores (models are in order of best to worst performing).

This indicates that the differences between odour profiles at different periods of infection are insufficiently significant for the sensors to detect.

3.4.2 3-Class Dose Classification

Concerning the classification of different treatment groups, performance across all models was sufficient (Table.7), with an average accuracy of 67.79% ($\pm 2.536\%$) and an average Macro F1 of 69.77% ($\pm 2.913\%$). This suggests that the differences in the odour profiles of high dose, low dose and uninfected treatments were relatively distinct from one another.

Table.7. Test set metrics for the classification of high dose, low dose and uninfected urine samples.

Model	Accuracy	Macro F1
RF	0.937500	0.944056
MLP	0.750000	0.756614
RBF SVM	0.687500	0.656085
PCA20+ RBF SVM	0.687500	0.656085
PCA10+ RBF SVM	0.687500	0.656085
PCA30+RBF SVM	0.687500	0.656085
PCA20+RF	0.687500	0.622222
PCA10+RF	0.625000	0.590476
LogReg	0.625000	0.585714
PCA10+LogReg	0.625000	0.585714
PCA20+LogReg	0.625000	0.585714
PCA30+LogReg	0.625000	0.585714
PCA30+RF	0.562500	0.533333

Models tested include RF (random forest), MLP (multilayer perceptron), LogReg (logistic regression), and RBF SVM (radial basis function support vector machine). These models were also combined with PCA (principal component analysis) using different PCA subspaces (10 components, 20 components and 30 components).

All models had relatively high accuracy and Macro F1 scores (models are in order of best to worst performing).

Random Forest was the highest performing model, achieving quite high accuracy and high Macro F1 scores (Fig.27).

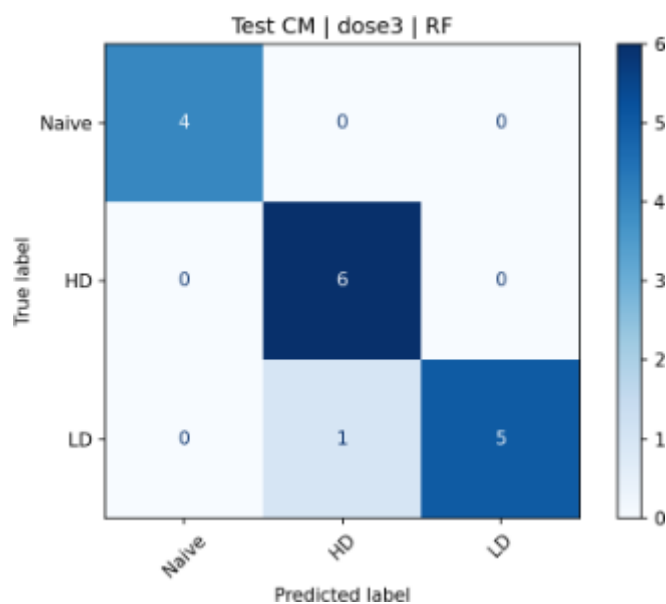


Fig.27. Random Forest analysis could identify differences between *T. muris*-infected high dose, *T. muris*-infected low dose, and uninfected mouse urine with reasonable accuracy.

The urine from C57BL/6 mice infected with either ~200 (HD) or ~30 (LD) *T. muris* eggs was collected on days 7, 14, and 25 post-infection, Mouse urine VOC profiles were then analysed twice per sample using a portable VOC analyser (Model 720, Roboscientific Ltd).

From the data (n=4 naive, 6 low dose, 6 high dose), this confusion matrix shows that the best performing machine learning model, Random Forest, identified correctly 15 samples from the VOC analysis: 4 uninfected samples, 6 high dose samples and 5 low dose samples (true positives, the top left, middle and bottom right respectively). One low dose sample was misclassified as high dose (middle bottom square).

Samples were classified with this model with an overall accuracy of 93.75%, and a Macro F1 score of 94.41%, indicating that this model performed well across all three classes. From the 15 samples used for this analysis, only one low dose sample was misclassified as high dose, with sensitivity and specificity calculated at 100% and 90% respectively for the high dose treatment group, and 83.33% and 100% respectively for low dose treatment group, averaging at overall 95% sensitivity and 91.67% specificity for this model.

This clearly indicates that between treatment groups VOC profiles were somewhat distinct, and that the models were rather robust.

3.4.3 Binary Classification

Concerning infection vs non-infection classification, it was determined that odour clearly differs between naïve and infected samples.

Overall, this test suggests that the sensors could detect infection-related odour changes, with a consistent average accuracy across all models tested of 72.16% ($\pm 1.677\%$) and an average Macro F1 of 67.65% ($\pm 2.293\%$) (Table.8).

Table.8. Test set metrics for the binary classification of infected vs uninfected urine samples.

Model	Accuracy	Macro F1
RF	0.875000	0.854545
MLP	0.812500	0.768116
LogReg	0.687500	0.653680
RBF SVM	0.687500	0.653680
PCA10+ LogReg	0.687500	0.653680
PCA10+RBF SVM	0.687500	0.653680
PCA20+LogReg	0.687500	0.653680
PCA20+RBF SVM	0.687500	0.653680
PCA30+LogReg	0.687500	0.653680
PCA30+RBF SVM	0.687500	0.653680
PCA10+RF	0.750000	0.589744
PCA20+RF	0.687500	0.542857
PCA30+RF	0.687500	0.542857

Models tested include RF (random forest), MLP (multilayer perceptron), LogReg (logistic regression), and RBF SVM (radial basis function support vector machine). These models were also combined with PCA (principal component analysis) using different PCA subspaces (10 components, 20 components and 30 components).

All models had relatively high accuracy and Macro F1 scores (models are in order of best to worst performing).

The predictions of the highest performing model, Random Forest, had an overall accuracy of 87.5% and a macro F1 of 0.8545 (Fig.28).

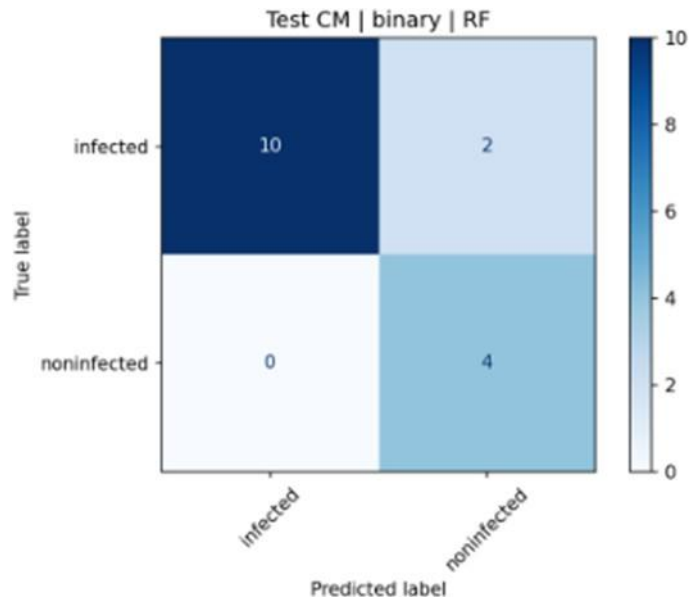


Fig.28. Random Forest machine learning analysis could distinguish between *T. muris* infected vs uninfected urine samples with high accuracy.

The urine from C57BL/6 mice infected with *T. muris* eggs was collected on days 7, 14, and 25 post-infection, Mouse urine VOC profiles were then analysed twice per sample using a portable VOC analyser (Model 720, Roboscientific Ltd).

From the data ((n=4 naive, 12 infected), this confusion matrix displays that from Random Forest analysis; 10 samples were correctly identified as infected (true positive, top left), 4 were correctly identified as uninfected (true negative, bottom right) 2 infected samples were incorrectly identified as uninfected (top left) and none of the uninfected samples were incorrectly identified as infected (bottom left).

From the 16 samples analysed for this test, the sensitivity and specificity were calculated 83.33% and 100% respectively. This suggests that the odour signals contained detectable information and that the data generated by the sensors could capture distinctive features associated with each sample category and

reflect genuine differences between the odours of infected and uninfected treatment groups.

Summarising the VOC analysis of urine samples, whilst distinction is hard to determine between days post-infection, it is somewhat clear to identify differences between high dose, low dose and naïve groups, and classification is even clearer between infected and uninfected groups using this VOC analyser and these sensors, especially when considering the best performing models. Urine odour is clearly different when discerning between infected and uninfected states.

3.5 Infected Urine Exhibited No Significant Signs of Differential Sandfly Attraction

Sandflies were previously used as biological detectors to determine preferential vector attraction (Staniek *et al.*, 2019). As previously mentioned, prior unpublished research from our lab has indicated that sandflies often exhibit a significant preference for infected odours and have been shown to clearly distinguish between *T. muris* infected mouse hair following immune response. As sandfly bioassays tend to be user sensitive, a blind control test was conducted (Fig. 29). This control successfully identified that responses to the positive control occurred at a significantly greater proportion compared to responses to the negative control (binomial test with 0.5 probability, $P=0.0012$).

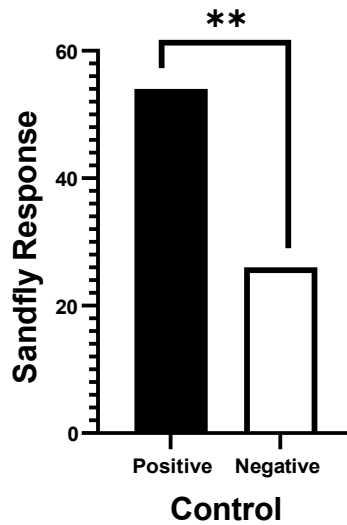


Fig. 29. Blind Control Bioassay successfully indicated attraction towards the positive control.

This control experiment was conducted blind by subjecting virgin female Campo Grande *L. longipalpis* sandflies to a Y-tube olfactometer (~27.45 °C, RH= 42.5%) with male pheromone hexane extract in one arm as a positive control and hexane in the other as a negative control. Data (n=80) was presented using mean ±SEM. All the sandflies tested responded to either the positive or negative control.

The differences between responses were determined significant by binomial testing, dictating that the proportion of flies choosing the positive control over the negative control significantly differed and that this result was not coincidental ($P > 0.0012$, **).

3.5.1 Sandfly Response to the Urine of Mice Infected with Low Doses of *T. muris* Showed No Significant Attraction

We first examined the ability of sandflies to distinguish urine odour from naïve and low dose infection across the time course of infection. The results of binomial testing were not significant for low dose and naïve urine at days 7, 14, 21, 28 and 42 post-infections ($P > 0.2$ for all days tested post-infection). This indicates that sandfly attraction to low dose samples did not occur at a greater proportion compared to naïve dose responses on any experiment day (Fig. 30).

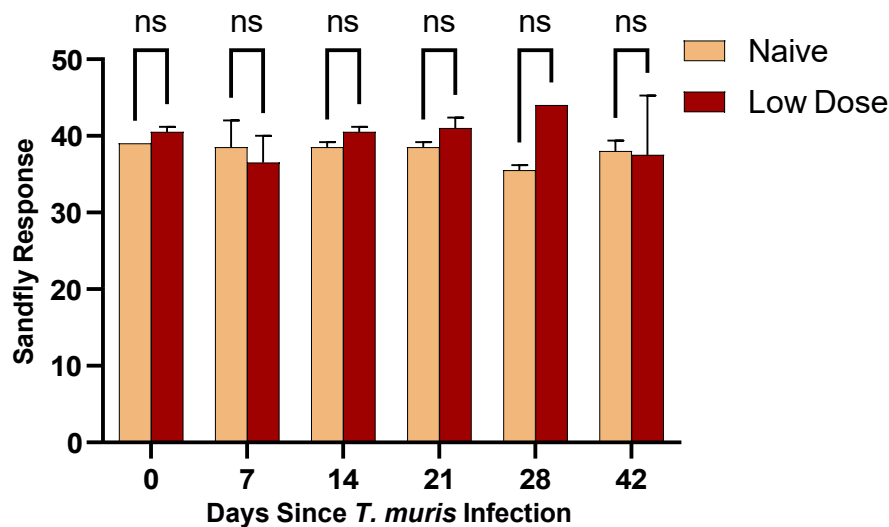


Fig.30. *L. longipalpis* did not exhibit preferential attraction to the urine of mice infected with low dose *T. muris* over the course of infection.

C57BL/6 mice were infected with ~30 *T. muris* eggs and urine was collected 0, 7, 14, 21, 28, and 42 days after infection. Data from 2 samples were taken from 2 independent experiments per time point, in which female Campo Grande *L. longipalpis* sandflies (n=80) underwent Y-tube olfactometer choice experiments to examine if preferential attraction was present when subject to low dose infected urine against naïve urine.

Data was presented as mean ±SEM and was found to be normally distributed (Shapiro-Wilk test, $p>0.05$).

The pairwise comparisons were conducted using 2-way ANOVA with Bonferroni multiple comparison tests.

On average (\pm SEM), sandflies that responded were not significantly more attracted to low dose urine (40.00, \pm 1.095) than naïve control urine (38.00, \pm 0.516) (paired T-test $p=0.2323$).

When compared using the percentage of sandflies responding, this was also the case (low dose infected urine $50.00\pm 1.369\%$ vs naïve control urine $47.50\pm 0.6455\%$, paired T-test $p=0.2323$). On average 2.000 (\pm 0.8756) sandflies did not respond. Collectively, these data indicate that sandflies do not have a preference for naïve versus low dose infected urine across the time course of infection.

3.5.2 Sandfly Response to the Urine of Mice Infected with High Doses of *T. muris* Showed No Significant Attraction

We next examined the ability of sandflies to distinguish urine odour from naïve and high dose infection across the time course of infection. The results of binomial testing were not significant for high dose and naïve urine ($P > 0.2$ for all days tested post-infection). This indicates that low dose response did not occur at a greater proportion compared to high dose responses on any experiment day (Fig.31).

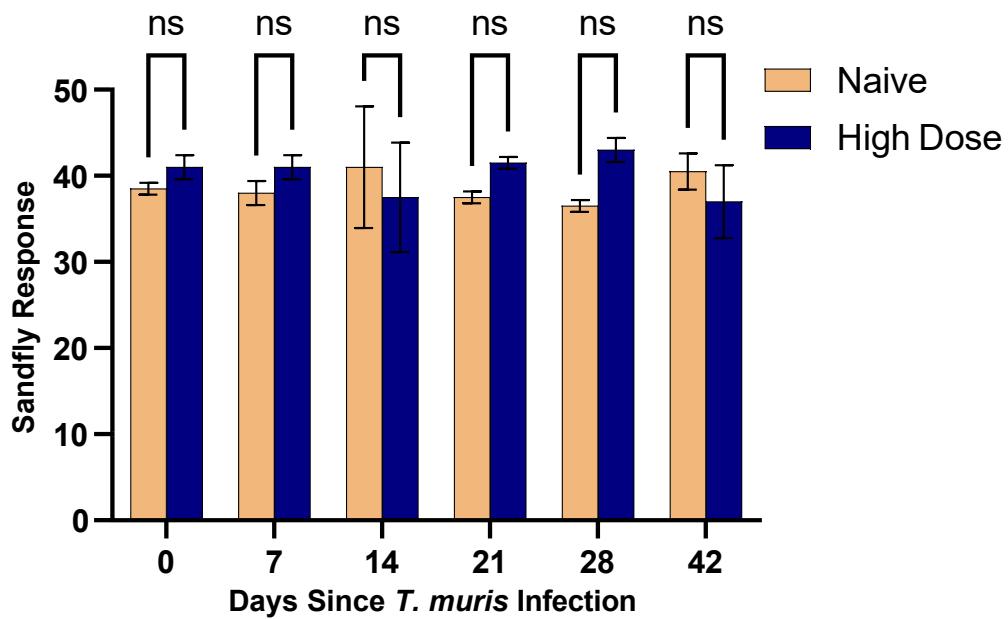


Fig.31. *L. longipalpis* did not exhibit preferential attraction when subjected to the urine of mice infected with high dose *T. muris* over the course of infection.

C57BL/6 mice were infected with ~200 *T. muris* eggs and urine was collected 0, 7, 14, 21, 28, and 42 days after infection. Data from 2 samples was taken from 2 independent experiments per time point, in which female Campo Grande *L. longipalpis* sandflies (n=80) underwent Y-tube olfactometer choice experiments to examine if preferential attraction was present when subject to low dose infected urine against naïve urine.

Data was presented as mean ±SEM and was found to be normally distributed (Shapiro-Wilk test, $p > 0.05$).

The pairwise comparisons were conducted using 2-way ANOVA with Bonferroni multiple comparison tests.

On average (\pm SEM), sandflies that responded were not significantly more attracted to high dose urine (40.17, \pm 0.972) than naïve control urine (38.67, \pm 0.715) (paired T-test $p = 0.4124$).

When compared using the percentage of sandflies responding, this was also the case (high dose infected urine $48.77 \pm 1.588\%$ vs naïve control urine $48.33 \pm 0.8937\%$, paired T-test $p = 0.8561$). On average $1.167 (\pm 0.307)$ sandflies did not respond. Collectively, these data indicate that sandflies do not have a

preference neither naïve nor high dose infected urine across the time course of infection.

3.5.3 Sandfly Response Showed No Significant Preference for Either Low Dose or High Dose *T. muris* Infection That Could be Separated from Chance

We then examined the ability of sandflies to distinguish low dose treatment group urine odour from high dose treatment group urine odour across the time course of infection.

The results of binomial testing were not significant for low dose and high dose urine ($P > 0.2$ for all days tested post-infection). This indicates that low dose response did not occur at a greater proportion compared to high dose responses on any experimental time point (Fig.32).

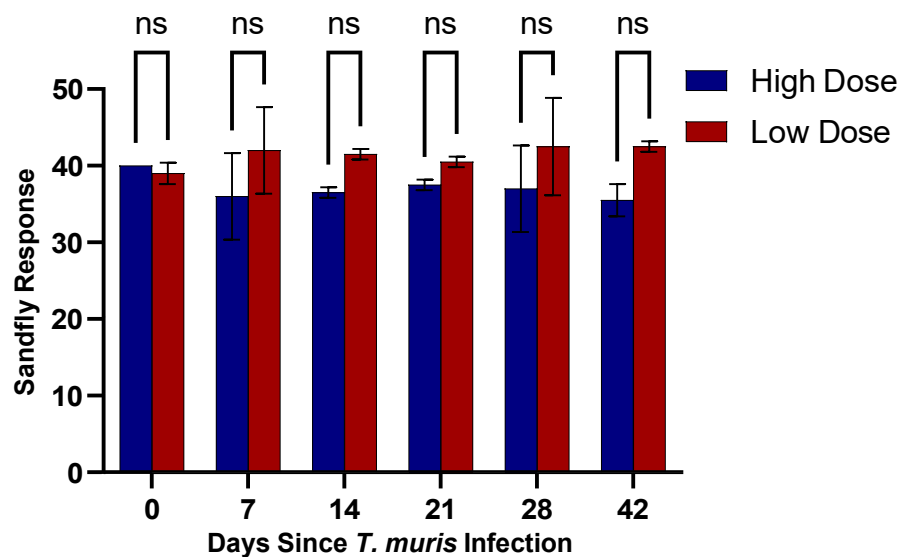


Fig.32. *L. longipalpis* did not exhibit preferential attraction when subject to the urine of mice infected with high dose *T. muris* and the urine of mice infected with low dose *T. muris* over the course of infection.

C57BL/6 mice were infected with ~30 or ~200 *T. muris* eggs and urine was collected 0, 7, 14, 21, 28, and 42 days after infection. Data from 2 samples was taken from 2 independent experiments per time point, in which female Campo Grande *L. longipalpis* sandflies (n=80) underwent Y-tube olfactometer choice experiments to examine if preferential attraction was present when subject to low dose infected urine against high dose infected urine.

Data was presented as mean \pm SEM and was found to be normally distributed (Shapiro-Wilk test, $p > 0.05$).

The pairwise comparisons were conducted using 2-way ANOVA with Bonferroni multiple comparison tests.

On average (\pm SEM), sandflies that responded were significantly more attracted to low dose urine (41.33, \pm 0.558) than high dose urine (37.08, \pm 0.651) (paired T-test $p = 0.026$).

When compared using the percentage of sandflies responding, this was also the case (low dose infected urine $51.67 \pm 0.697\%$ vs high dose infected urine $46.35 \pm 0.814\%$, paired T-test $p = 0.0156$). On average, 1.333 (\pm 0.247) sandflies did not respond.

When accounting for binomial testing, these data indicate that sandflies may have preferred low dose versus high dose infected urine across the time course of infection, but this could not be separated from random chance.

3.6 Th1/Th2 Cytokines Do Not Induce Any Differential Vector Attraction in Isolation That Could be Separated from Chance

Previous unpublished data from our lab has suggested that sandflies can differentiate between *T. muris*-induced Th1 and Th2 immune response via hair samples. Despite sandflies not exhibiting as clear of a preference towards infected urine, there was a potential indication of Th1 attraction over Th2, although this preference could not be separated from random chance.

Examining this using Th1/Th2-associated cytokines directly could reveal a mechanistic link, as it would indicate cytokine presence as a significant driver of infection-induced odour change.

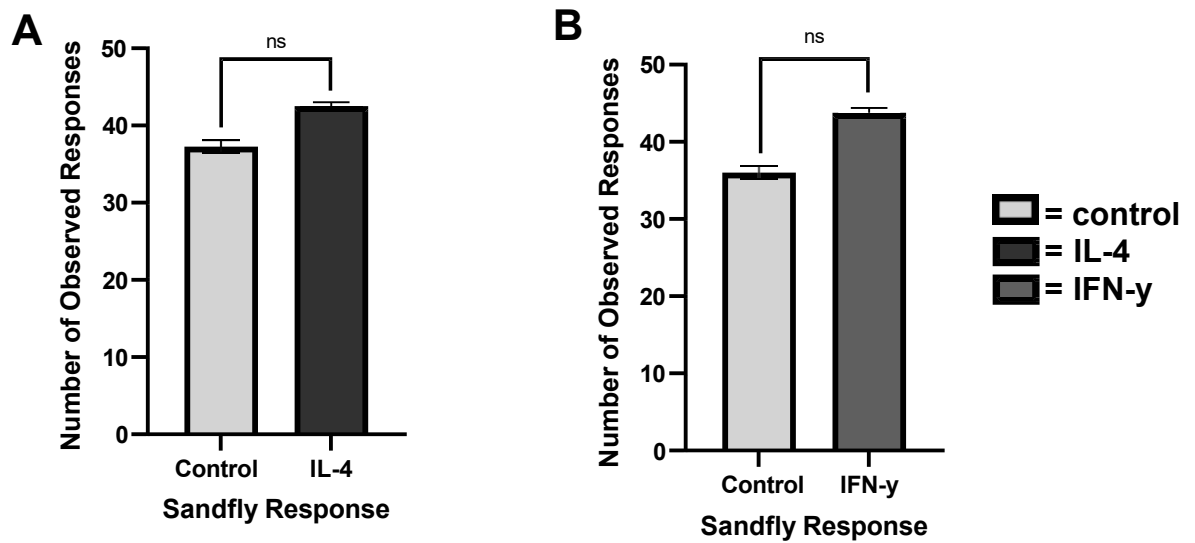


Fig.33. The average observed responses of female *L. longipalpis* sandflies when subjected to Th1-associated IFN- γ and Th2-associated IL-4 cytokines against the relevant diluent in a Y-tube olfactometer indicate no preferential attraction.

Y-tube olfactometer choice experiments were conducted using (A) the Th2-associated cytokine IL-4 and (B) the Th1-associated cytokine IFN- γ , against the relevant diluents.

For each graph, the data (N=320) are from 4 independent experiments per cytokine, in which female Campo Grande *L. longipalpis* sandflies (n=80) underwent Y-tube olfactometer choice experiments to examine preferential attraction, presented as mean \pm SEM. For both cytokines, on average 0.25 (\pm 0.25) sandflies didn't respond to the bioassays.

Data was found to be normally distributed (Shapiro-Wilk test, $p > 0.05$).

Binomial tests dictated that any differences present were not significant ($P > 0.05$).

On average (\pm SEM), sandflies that responded were significantly more attracted to IL-4 (42.5 ± 0.5) than control diluent (37.25 ± 0.75) (Mann-Whitney test, $p = 0.0286$).

When compared using the average percentage of sandflies that responded, IL-4 ($53.3\% \pm 0.799\%$) also had significantly more responses than the control diluent ($46.7 \pm 0.799\%$) (Mann-Whitney test $p = 0.0286$). On average, 0.25 sandflies did not respond (± 0.25).

However, binomial tests were conducted to determine whether the proportions of sandfly responses preferring IL-4 were significantly different from 50%.

The results of this were not significant ($P=0.368$). This indicates that responses preferring IL-4 did not occur at a greater proportion compared to responses favouring the control diluent in a way that could not be explained by chance (Fig.33).

Significant differences were also found when the mean (\pm SEM) of IFN- γ and control responses were compared with mean non-responsive sandflies (0.25 ± 0.250 , paired T-test, for both $p<0.0001$).

On average (\pm SEM), sandflies that responded were significantly more attracted to IFN- γ ($43.75, \pm 0.629$) than control diluent ($36.00, \pm 0.817$) (paired T-test $p=0.0125$).

When compared using the average percentage of sandflies that responded, IFN- γ ($54.87\%\pm 0.914\%$) had significantly more responses than the control diluent ($45.13\%\pm 0.914\%$) (paired T-test $p=0.013$). On average, 0.25 sandflies did not respond (± 0.25).

However, binomial tests were conducted to determine whether the proportions of sandfly responses preferring IFN- γ were significantly different from 50%.

The results of this were not significant ($P=0.434$). This indicates that responses preferring IFN- γ did not occur at a greater proportion compared to responses favouring the control diluent in a way that could not be explained by chance (Fig.33).

Summarising the results of all these bioassays, any preferential attraction found were determined as insignificant because of binomial testing, thus concluding that despite some significant differences, neither immune-related cytokines nor infected urine were not more attractive to sandflies in a way that could not be explained by chance.

3.7 VOC Profile of Mouse Faeces Exhibits Detectable *T. muris*-Induced Changes

As mentioned previously, faeces could also be a potential target for detecting trichuriasis-specific changes in VOC profiles as it may be likely that there are other immune interactions present that incite strong sandfly attraction and aid in altering VOC profiles, such as those with the microbiome, as this is present in the hair and skin examined previously (Houlden, *et al.*, 2015).

Following this, preliminary examination of the VOC profiles found in faeces was conducted, which is rich in microorganisms.

This preliminary examination was conducted using faeces from mice infected with high and low dose infections on days 14 and 25 post-infections, compared against naïve faeces. Initial PCA indicated notable differences between treatment groups (Fig.34) when visualised, PCA displays a clearly seen distinction between naïve and infected treatment groups, providing a promising outlook for VOC profile distinction via further analysis.

When judging the differences between days post-infection, high dose (blue) samples seem to display distinctive clusters with no overlaps (C). Low dose samples (red) also seem to display no overlaps (B), although the differences

between day 14 (light red) and day 25 (dark red) seem to be a bit less clear, with two day 14 data points located the bottom left of the graph more closely associated with the day 21 data points than the other day 14 data points.

High and low dose treatment groups overall seem to be hard to distinguish from PCA alone, spread along the x axis (A) and displaying many overlaps with samples of the other infected group.

When compared with the infected groups (blue and red) however, naïve group (yellow) samples were distinctly clustered together with no overlap with the infected treatment groups, suggesting that the sensors could make out a clear, marked difference in odour.

From these graphs overall, whilst overlaps are visible between infected treatment groups, some days post-infection seem to be somewhat separable (or at least more distinct than urine in Fig.26), and PCA suggests a clear distinction between infected and uninfected groups.

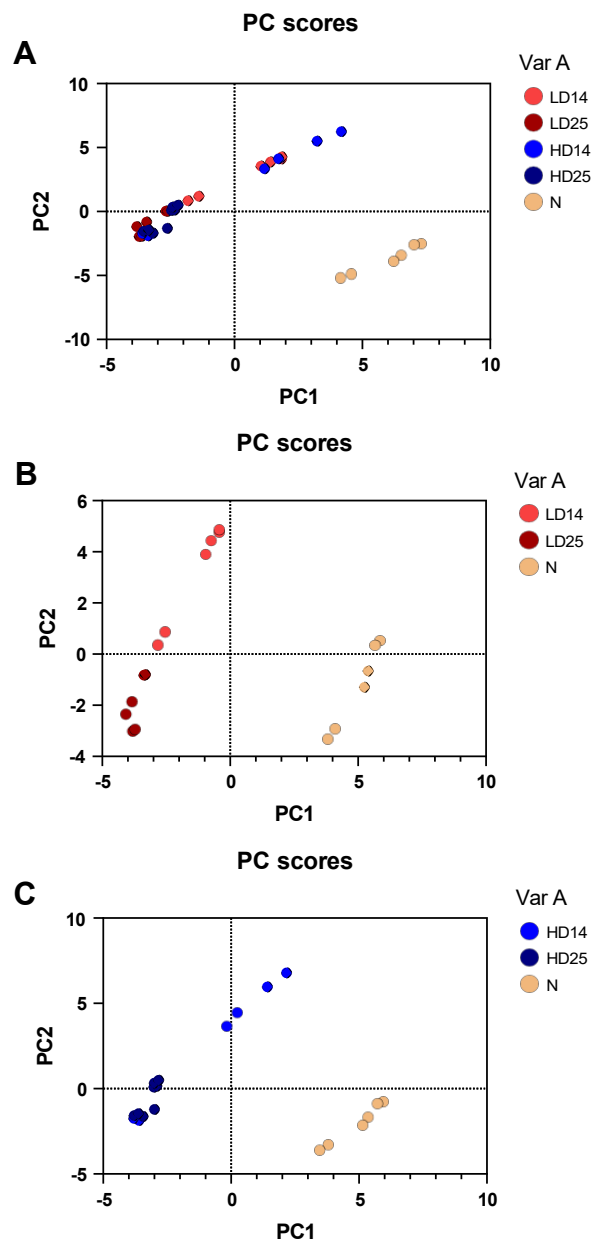


Fig.34. Preliminary examination of *T. muris* infected mouse faeces suggests clear infection-induced changes in VOC profiles.

The faeces from C57BL/6 mice infected with either ~200 (HD) or ~30 (LD) *T. muris* eggs was collected on days 14 and 25 post-infection, Mouse faecal VOC profiles were then analysed using a portable VOC analyser (Model 720, Roboscientific Ltd). This analysis in total used 3 low dose samples from day 14 post-infection (LD14), and 3 from day 25 (LD25). Regarding high dose infections, 3 day 14 post-infection (HD14) and 4 day 25 (HD25) samples were used. (A) all data (n=3 naïve, 6 low dose, 7 high dose) were analysed twice each and presented using principal component analysis. (B) Low dose infected faeces were compared with naïve samples, as was high dose infected faeces (C).

Like with the VOC analysis of urine, a range of common machine learning models both alone and combined with PCA were applied for model training and classification analysis, including Random Forest, Logistic Regression, MLP, and radial basis function support vector machine. Classification analysis consisted of day-dose classification (distinguishing between different days post-infection); 3-class dose classification (naïve, high dose, or low dose); and binary classification (infection vs non-infection). When models were able to consistently classify the samples accurately, this indicated that samples were distinguishable. Results were evaluated using overall accuracy for straightforward interpretation.

In addition to overall accuracy, Macro F1 was calculated to evaluate the balanced performance of the model as a harmonic mean of precision and recall averaged across equally weighted groups. This score can help determine if the model is robust and performs well in balancing the predictions from both classes, so that no class is underrepresented.

3.7.1 Day-Dose Classification

The models tested performed consistently weakly when distinguishing between infection at different time periods (Table.9), with an average overall accuracy of 25% (SEM $\pm 0\%$) and Macro F1 score of 13.45% (SEM $\pm 0.51\%$). Even the best performing model, Random Forest, had relatively low scores of 50% overall accuracy, with a Macro F1 of 41.67%.

Table.9. Test set metrics for the classification of faeces samples on days 7, 14, 25 and 35 of infection.

Model	Accuracy	Macro F1
MLP	0.250000	0.166667
PCA10+MLP	0.250000	0.142857
PCA10+RF	0.250000	0.133333
RF	0.250000	0.133333
LogReg	0.250000	0.125000
RBF SVM	0.250000	0.125000
LPCA10+RBF SVM	0.250000	0.125000
PCA10+LogReg	0.250000	0.125000

Models tested include RF (Random Forest), MLP (multilayer perceptron), LogReg (Logistic Regression), and RBF SVM (radial basis function support vector machine). These models were also combined with PCA (principal component analysis) using 10 components. All models performed consistently weakly with low accuracy and Macro F1 scores (models are in order of best to worst performing).

This indicates that, like urine, the differences between odour profiles at different periods post-infection are do not vary enough for accurate classification.

All models' performance failed when classifying uninfected, high dose and low dose faecal samples as day 14 and day 25, with an accuracy of 25% across all models. Even when PCA was applied to reduce dimensionality, performance did not improve. This indicates that no dominant signals were captured, and that the models did not learn enough meaningful patterns from the data input and instead could be performing through random guessing, because either the sensors could not capture or the samples did not contain sufficient information to distinguish between the classes.

3.7.2 3-Class Dose Classification

Concerning 3-class dose classification, the performance of other models performed with an overall average accuracy of 62.5% ($\pm 6.25\%$) and an average Macro F1 of 61.10% ($\pm 7.64\%$). This suggests that moderate distinctions could be made between classes (Table. 10).

Table.10. Test set metrics for the classification of high dose, low dose and uninfected faecal samples.

Model	Accuracy	Macro F1
LogReg	0.750000	0.777778
RBF SVM	0.750000	0.777778
PCA10+ RBF SVM	0.750000	0.777778
PCA10+ LogReg	0.750000	0.777778
PCA10+RF	0.625000	0.555556
PCA10+MLP	0.625000	0.555556
RF	0.500000	0.500000
MLP	0.250000	0.166667

Models tested include RF (random forest), MLP (multilayer perceptron), LogReg (logistic regression), and RBF SVM (radial basis function support vector machine). These models were also combined with PCA using 10 components.

All models had relatively high accuracy and Macro F1 scores (models are in order of best to worst performing).

Logistic Regression performed the best out of the models tested (Fig. 35).

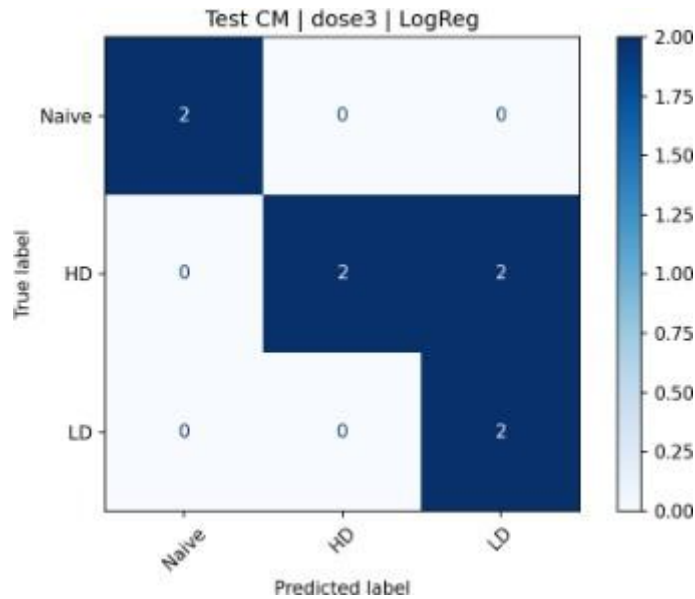


Fig.35. Logistic Regression machine learning analysis could distinguish between *T. muris* infected vs uninfected faecal samples with moderate accuracy.

The faeces from C57BL/6 mice infected with either ~200 or ~30 *T. muris* eggs was collected on days 14 and 25 post-infection, Mouse urine VOC profiles were then analysed twice per sample using a portable VOC analyser (Model 720, Roboscientific Ltd).

From the data (n= 2 naïve, 4 high dose, 2 low dose) this confusion matrix shows that the Logistic Regression model correctly identified 6 out of 8 samples: 2 uninfected samples, 2 high dose samples and 2 low dose samples (top left, middle and lower right respectively). Two high dose samples were misclassified as low dose (middle right square).

Samples were classified with Logistic Regression with an overall accuracy of 75%, indicating that this model performed moderately well across all three classes, correctly predicting 3/4 of the samples. Two high doses were misclassified as low dose out of a total of 8 samples examined. However, when compared to urine, it indicates that odour differences between treatment groups are less distinct in faeces.

Concerning Macro F1, this model scored 77.78% and indicated some imbalanced performance across classes particularly concerning high dose against low dose.

Faecal samples exhibited higher precision with naïve and high dose samples compared to low dose samples, with lower recall for high dose samples. From this model, sensitivity and specificity could be calculated at 50% and 100% respectively for the high dose treatment group, and 100% and 66.67% respectively for the low dose treatment group, averaging at 75% sensitivity and 83.34% specificity. This suggests that models could distinguish between the treatment groups with somewhat moderate accuracy, but not as well as urine samples.

3.7.3 Binary Dose Classification

Concerning infection vs non-infection classification, it was determined that odour clearly differs between naïve and infected samples.

All models performed with on average 100% accuracy (± 0.0) and an average Macro F1 score 94.29% ($\pm 5.714\%$) (table.11), suggesting that these models are robust and performs well so that no class is underrepresented.

Table.11. Test set metrics for the binary classification of infected vs uninfected faecal samples.

Model	Accuracy	Macro F1
LogReg	1.000000	1.000000
RBF SVM	1.000000	1.000000
RF	1.000000	1.000000
MLP	1.000000	1.000000
PCA10+LogReg	1.000000	1.000000
PCA10+RBF SVM	1.000000	1.000000
PCA10+RF	1.000000	1.000000
PCA10+MLP	1.000000	0.542857

Models tested include RF (random forest), MLP (multilayer perceptron), LogReg (logistic regression), and RBF SVM (radial basis function support vector machine). These models were also combined with PCA (principal component analysis) using 10 components. All models had 100% accuracy and Macro F1 scores, suggesting that they were perfectly balanced across all classes (models are in order of best to worst performing).

This indicates that the odour signals present in faecal samples are distinct enough between infected and uninfected groups that models can perfectly separate them. From this test, the sensitivity and specificity were both calculated to be 100%.

This suggests that the odour signals contained clearly detectable information and that the data generated by the sensors could easily capture characteristic features associated with each sample category and reflect genuine differences between the odours of infected and uninfected treatment groups. This also suggests that the determined differences were clearer than those found during the classification of urine odour.

Summarising the VOC analysis of faecal samples, whilst distinction is hard to determine between days post-infection, it is somewhat possible to identify

differences between high dose, low dose and naïve groups, and classification between infected and uninfected groups using this VOC analyser and these sensors were 100% accurate using the data from this examination. Odour appears to be emphatically different when discerning between infected and uninfected states.

Chapter 4: Discussion

This study is one of the first to examine VOC profiles of urine for *T. muris*-induced infection changes, which could help contribute to opening alternative VOC-based diagnostic avenues and investigating the immune system's potential involvement with these changes, helping reveal the pathophysiological mechanisms of trichuriasis (Shirasu and Touhara, 2011).

Using alternative sources of entrained odour other than hair would also benefit mechanism clarification and present a less invasive source, which could easily be used diagnostically.

As urine is used by mice to communicate important information and signals through specific, detectable scent changes (Ferkin *et al.*, 1997), this could support whipworm-specific VOC changes, and exhibit preference in biological detectors like sandflies. We found that urine exhibited several detectable *T. muris*-induced changes, namely identifiable changes in MUP transcript expression and the presence of distinctive, distinguishable VOC profiles between the infected and uninfected groups.

Whilst acute high dose infection-induced changes in monocytes were determined in the bladder, no other immune population changes were found in

the bladder, and no significant immune population changes were found in the liver via flow cytometry. Additionally, when submitted to sandfly attraction choice experiments, binomial tests determined that sandflies had no preferences to infected urine that could not be distinguished from random chance, despite exhibiting clear preferences for *T. muris*-infected mouse hair in past unpublished experiments.

Preliminary experiments conducted using the VOC profiles of faeces suggest that they have potential to be a method of infection detection with a clear distinction between infected and uninfected groups, however accuracy was lower than urine when distinguishing between acute and chronic infection, and as such would benefit from further examination.

4.1 Infection Induced Differences in Hepatic MUP Expression

To confirm the hypothesis that the VOCs of *T. muris*-infected mice could be potentially different and distinguishable from uninfected mice due to changes in urine VOCs, comparisons of MUP-related gene expression from the site of production (the liver of mice (Flower *et al.*, 2000)) were made between infected mice and uninfected mice using RT-qPCR, to help define the presence of VOCs in the urine (Roberts *et al.*, 2018) and determine if these change with disease state.

Determining if these changes are present could indicate distinguishable odour changes in urine with infection (Edink *et al.*, 2010). Therefore, MUPS were a good subject for sandfly attraction comparisons and hypothetically would reflect any attraction preferences found in mouse hair odour.

RT-qPCR results provide additional evidence of MUP gene expression changes following infection. There were significant changes present in individual MUPs. MUPs 1, 20, and 21 were found to significantly increase following low dose-induced chronic infection, with MUP 18 expression showing significant reduction.

Based on sequence similarity and position, the 21 functional genes for mouse MUPs has been divided into the ancestral peripheral class A MUPs (MUP 3, 4, 5, 6, 20, and 21), and central class B MUPs (which includes MUP 15, 18, 1, 16), which are nearly identical highly homologous likely recent duplications (Logan *et al.*, 2008, Mudge *et al.*, 2008). High similarity makes this region hard to research in detail.

Because so much variation exists in expression across MUP loci, the results from studies measuring a specific MUPs' expression would not likely generalize to other loci (Penn *et al.*, 2022), and so should not be extrapolated, especially if the targeted method is specific.

Targeted methods like qPCR are not too specific, as they do not entirely discriminate between the high homology found in MUPs. The primers used in this study were validated by the National Centre for Biotechnology BLAST program, however Holloway *et al.*, (2006) found that qPCR primers selected for MUP 1,2,6,8 were unable to be distinguished, despite being validated by the BLAST program, due to up to 97% percent nucleotide identities. These inaccuracies likely apply to some of the MUPs identified in this study.

More precision has been found using RNA sequencing for comparing MUPs (Connerney *et al.*, 2017), however this was not required as this experiment was

not focused solely on MUP expression, and qPCR sufficiently exhibited significant changes in MUP expression with infection status.

Contrary to the recorded increases in MUP expression in these results, in male mice infection tends to downregulate MUP expression. Poor health seems to feminise male MUP expression and eradicate sex differences (Penn *et al.*, 2022).

Results found by Oldstone (2021) suggest that infection alters the expression of MUP 20, which is inherently attractive to females - substantially reducing expression during acute infection. Infection suppressed the expression of the male central MUP signature, which following clearance was regained and even expressed enhanced output by ~30 days post-infection. Infection can cause reduced embryo survival and lifelong offspring infection, and so a proposed explanation of this is that an evolutionary mechanism drives females to avoid direct infection from male. In females, infection likely seems to induce similar effects as well, as seen with other parasitic helminth diseases like schistosomiasis (Isseroff *et al.*, 1986) and ascariasis (Deslyper *et al.*, 2019).

The effect of infection on the MUP expression of female mice is not well studied, due to significant reduced sexually dimorphic MUP expression, and infection could still interact differently with expression than in males.

This experiment was conducted on the livers of female mice, despite MUP expression having a sexually dimorphic male bias, due to practical availability. Males excrete and synthesize easily over 2-8 times more MUPs than female counterparts (Penn *et al.*, 2022). MUPs 7, 11, 20, and 21 have been recorded

as highly expressed in male mice, with female mice expressing negligible amounts by comparison. Males display much more variation in expression across loci, with some having high expression (7, 20, 9, 17, 3, 10) and others displaying low expression (6, 15, 2, 5, 13). Despite low expression, females display variation across loci too, with MUPs 17, 9, 3, and 10 having higher expression than most male MUPs. Specifically, MUP 20 exhibits male-bias sexual dimorphism - a male chemical signal that influences female brains, behaviour and physiology (Penn *et al.*, 2022), mainly expressed in males to increase female attraction and induces rapid associative learning to cause attraction to that individuals' odour alone.

Whilst thought to only be expressed in males, MUP 20 can be upregulated at certain times, such as during oestrus or around ovulation (Luzynski *et al.*, 2021), (Černá, 2017). Female MUP expression is studied sparsely in comparison to male MUP expression, due to these differences in presentation. However, these results do demonstrate that *T. muris* does induce expression changes in female mice. Due to the sexually dimorphic nature of this expression, it is likely that these differences would be much greater/visible in male mice if this was tested with trichuriasis in the future.

Additionally, mice produce MUPs that are not present in humans, making this difficult to apply to human diseases (Suzuki *et al.*, 2021). In this study, MUPs were used just to identify that the products of urine change when exposed to trichuriasis-induced immune challenge. However, this would require separate testing using human urine if this was required to be studied in more detail for

this topic, as MUPs are known to significantly contribute to the odour of mouse urine.

Specific features such as infective species, types of mice, or how they are maintained in captivity could implicate differences in MUP expression (Penn *et al.*, 2022).

MUP expression differs between lab and wild mice populations (Logan *et al.*, 2008). Wild mice tend to exhibit unique MUP expression patterns, whereas lab mice tend to exhibit identical repertoires, suspected due to inbreeding.

Wild mice have been reported to more commonly experience chronic infection and have high exposure to infection (Mair *et al.*, 2024).

Mair *et al.*, (2024) determined that levels of cytokine production in response to chronic, low-level infection, with antigen-specific cytokine response reflected in effector/memory CD4+ T cell phenotype. Th1/Th2 balance was only associated with worm burden in older mice. Whilst like lab mice concerning the relationship between *T. muris* resistance and CD4+ T helper cell response, quantitative differences were present between lab and wild mice.

Such factors could affect results if they were compared with natural systems, however MUPs likely still change with infection, just on a more variable, individual basis. The mice used in this study were all maintained under the same conditions and guidelines, so any variation this would give to MUP expression would be extremely limited.

The molecular mechanisms dictating the dynamic expression of MUPs are determined by many factors, particularly in males, such as social status, endocrine and growth hormone secretion (Penn *et al.*, 2022). Oldstone *et al.*,

(2021) suggested that there are likely multiple factors contributing towards MUP expression, such as metabolic function, the overall energetic demand of MUP synthesis, hormonal changes, with some effects that are isoform specific.

Real *et al.*, (2024) found results indicating that MUP production represents a considerable energy investment. Gut microbiota and MUPs could also have an interlinked relationship. Deletion of the *Mup* gene cluster significantly reduced diversity in microbial families and functions in the guts of sexually mature male mice.

Significant infection-induced changes in microbiota composition have been recognised between days 14-28 post-infection (Houlden *et al.*, 2015), and have been shown to cause a substantial, significant impact on intestinal microbiota, digestive function, and long-term immune regulation. This period was prior to our analysis. This could be caused by the increasing activity of immune response during this time.

Concerning immune response, changes in MUP expression could be unique to the infective species. Some changes in MUP seem to be disease-specific and can change with strain. Different diseases host different interactions with different populations of cells, particularly immune cells, which are projected to play a part in these changes. This experiment was only done using mice with low dose infections, and so it is implied that high dose infections would also provide changes in MUP expression. It could be worth confirming this and perhaps comparing the differences in MUP expression between these two treatment groups.

MUP changes have been recorded in other parasitic helminth diseases. Isseroff *et al.*, (1986) determined that chronic schistosome infection reduced MUP mRNA levels, caused by an infection-induced testosterone reduction. MUP levels could be restored with testosterone administration. Upon investigation of the liver proteome, Deslyper *et al.*, (2019) identified a downregulation of MUPs with ascariasis infection, suggesting that a conserved response to parasite infection may be present in the liver.

Immune response has been linked to changes in MUP expression, such as in LCMV, where MUPs were shown to be induced during viral infection.

Ware *et al.*, (2019) found that LCMV variant 2.2 presented with significantly greater amounts of MUPs, peaking at day 30 post-infection, compared to the minimal/equivalent MUP expression recorded in V54-infected (which generates a weak virus-specific CD8 and CD4 T cell response compared to v2.2) and naïve controls.

CD8⁺ T cells played an essential role as deletion of CD8⁺ T cells aborted MUP production in v2.2-infected mice. Furthermore, persistent v2.2 infection was not associated with enhanced MUP levels. However, when such mice had a restoration of functional virus-specific cytotoxic T lymphocytes (CTL), infection was curtailed and significant elevation of MUP occurred. This indicates that immune cells could likely underlie the changes observed in this project, particularly T cells. Additionally, examining the differences in odour and MUP expression changes between whipworm strains could be a useful avenue for future comparison, as it could help untangle the causes of these changes.

Overall, MUP expression was shown to change with infection, likely moderated by immune challenge.

This indicated that urine is changed by infection and could be a potential detection target, prompting further testing into changes present in VOC and immune profiles.

4.2 Monocyte Changes Present in the Bladder of Mice with Acute *T. muris* Infection

The liver is, as previously outlined, a site of MUP production, which change with infection and as such could influence odour changes (Flower *et al.*, 2000). It is therefore prudent to determine what features of immune response are present in the liver and bladder of infected mice, compared with naïve controls, as this could reveal immunological reasons behind infection induced expression changes.

The bladder is the site of urine storage prior to urination and so could have an influence on urine odour. Hence, enzymatic digestion was performed on the liver and bladder of both high and low dose-infected mice, followed by flow cytometric analysis, to compare the immune populations present within these organs.

We examined adaptive immune cells in terms of CD4 and CD8 T-cells and observed no significant changes in these populations in terms of percentage or transcription factor expression of T-bet and GATA-3 (Th1 and Th2 driving factors respectively) within the bladder or liver. T cells are vital components of the cell-mediated adaptive immune response to whipworm, particularly for

expulsion (Lee *et al.*, 1983). Protective immune responses against *T. muris* seem to be mainly regulated by CD4⁺ helper T cells, (Koyama *et al.*, 1995, Humphreys *et al.*, 2004, Koyama, 2002), with past studies suggesting that *T. muris* protective immunity development is likely almost exclusively dependent on CD4⁺ T lymphocytes and the related cytokines, and that this may influence infection-induced VOC changes. Likewise, CD8⁺ cells may also play a role in response to *T. muris* (Ware *et al.*, 2019). However, this experiment indicated that treatment caused no systemic impact on CD4⁺ and CD8 α ⁺ T cell populations concerning the liver or bladder.

Low dose infection induces a chronic infection and a predominantly Th1 response (Else *et al.*, 1994, Artis, 2006, Hadidi *et al.*, 2012), whereas high dose infections induce an acute infection and a predominantly Th2 response. Key Th1 and Th2-associated cytokines are often present in other areas of the body and reflect the local immune response to *T. muris* (Taylor *et al.*, 2000). Notably, high dose-induced Th2-associated cytokines that respond to *T. muris* are often overwhelmingly sourced from ILC2s and CD4⁺ Th2 cells (Yousefi *et al.*, 2021). Despite this, there was no significant difference between the Th1 and Th2 expression of CD4⁺ and CD8 α ⁺ cells in either the liver or bladder.

Whipworm can induce strong local immune response in the intestinal mucosa to induce expulsion (Schachter *et al.*, 2020). However, despite living entirely in the gut of the host, embedded primarily in the cecum and ascending colon (CDC, 2024), chronic whipworm can also produce a systemic immune response, which has been shown to impact other organs as well (Hayes and Gencis, 2021). Examples of these impacts include: exacerbating neurological conditions and

stroke outcomes in the brain by increasing pro-inflammatory Th1-associated cytokine mediators like CCL5 and altering Treg response (Dénes *et al.*, 2010); suppressing Th2-induced inflammation in other locations such as the lungs by upregulating Th1-associated cytokines such as IFN- γ and IL-10 (myeloid cells) (Chenery *et al.*, 2016) and inhibiting anti-tumour immunity by blocking Treg response and myeloid-derived suppressor cells (Hayes *et al.*, 2017, Stevenson *et al.*, 2022). In systemic responses outlined by prior research, the dominant immune response tends to suppress the alternative, for example, Th1 activation during cases of chronic whipworm downregulating allergic Th2 immune responses (Smits *et al.*, 2010, Dige *et al.*, 2016). An example of this inflammation and immune suppression was noted by Hayes and Grencis (2021) during which trichuriasis inhibited and suppressed responses to chemical skin sensitizers.

These recorded instances suggest that there may be systemic impacts of trichuriasis in myeloid and lymphoid subsets in these organs as well. In particular, the involvement of T cells and T cell regulation is prominent in these studies. In previous unpublished correlation analysis of odour changes within this project concerning immune cells, cytokines and worm burden showed that odour changes were relevant to gut T cells, DCs and myeloid cells. Worm burden and Th1-related cytokines (CD4+, and CD3+IFN γ +) correlated positively with VOCs, whereas dendritic cells and Th2-related cytokines (CD8+, and CD3+IL-5+) correlated negatively, in addition to Ware *et al.*, (2019) determining that CD8+ cells may exhibit an important role in MUP expression, as the deletion of CD8+ T cells aborted MUP production in normally resistant mice.

Our data suggests little to no impact of systemic whipworm infection on the liver or the bladder, at least at the parameters selected to be measured by flow cytometry.

On the contrary, Le *et al.*, (2020) found that the effect of chronic whipworm infection exacerbated *Schistosoma mansoni* egg-induced hepatopathology, potentially due to the resulting higher COX2 expression down-regulating immune responses in the liver. This would suppress T cell function and inhibit systemic Th2 response, suggesting that whipworm infection can affect the liver. Likewise, it is suspected that systemic immune alterations caused by trichuriasis are also indicated to impact bladder pathology with co-infection (Maizels, 2016). Past research therefore dictates that trichuriasis should have at least some impact on the immune functions of these organs, though perhaps it is too minor to be significant and requires more subjects to be observed clearly. Perhaps the impact of this infection could be studied at a later period post-infection (particularly in chronic low dose infections), as it is indicated that systemic immune response may be more prevalent then, and at the level of specific cytokine release from T-cells.

Many questions persist regarding *T. muris* infection and immune response. It is likely that natural hosts normally experience mixed Th1/Th2 responses, as fully polarized response development is restricted by STH-induced immunosuppression (Colombo and Grecis, 2020). Systemic responses showing the classical polarised activation seen in laboratory conditions may be local to the site of infection or present in some organs and the blood but maybe

not so clearly present the liver or bladder at this time period, and so examining mixed populations of mice may better model potential human changes.

Myeloid cells are primarily components of the innate immune system, and there is evidence to suggest that whipworm would impact these cell populations. It has been shown in previous studies that amounts of neutrophils, eosinophils, macrophages, and lymphocytes were all significantly greater in the intestinal submucosa of *T. muris*-infected mice than in the control animals (Schachter *et al.*, 2020).

Eosinophils, a common hallmark of infection, particularly for Th2-induced expulsion, exhibited no changes with treatment group in both the liver and the bladder.

Elevated numbers of eosinophils in the colon and MLNs during *T. muris* infection were found to be present in Th2-dominant resistant mice (Dixon *et al.*, 2006, Svensson *et al.*, 2011). Whilst this is likely dispensable for protective immunity (Svensson *et al.*, 2011), eosinophils are still recruited to the site of infection upon expulsion. According to the results of this experiment, it appears that this recruitment does not impact the liver or bladder.

In both the liver and the bladder there was no change in neutrophils with treatment group either. Neutrophils are more involved in initial innate immune response and are recruited to the intestinal mucosa in chronic infections during ineffective Th1 response (Klementowicz *et al.*, 2012).

No significant increase in either of these cell subsets for either infected treatment indicates that there is an insignificant response to whipworm present

in these organs, and that the recruitment of either cell subset to the site of infection is not particularly impactful on the immune profiles of these organs.

Monocyte-macrophages and DC subsets were examined and compared. As mentioned prior, susceptibility/resistance to trichuriasis infection may be linked to differences in DC phenotype (Harris, 2017), and changes in these subsets may correlate with odour changes in unpublished research.

Monocytes and macrophages are important components of innate immunity.

Monocytes are bone marrow derived leukocytes that differentiate into macrophages and dendritic cells (Chiu and Bharat *et al.*, 2017). Macrophages are mature, activated and often terminally differentiated cells.

In both the liver and bladder, there were no changes present between treatment groups in either cell subsets, again indicating a lacking systemic response to whipworm in these organs. This contrasts the systemic effects of trichuriasis observed by Chenery *et al.*, (2016), who determined changes in myeloid populations occurred in the lung independent of overt pathology, when mice had low dose *T. muris*. Most notably a significant expansion of CD11b⁺ CD11c⁺ myeloid cells and with a significant increase of IL-10 production.

Macrophages are an important antigen presenting cell (APC) for both Th1 and Th2 responses (De Schoolmeester *et al.*, 2009). Quantifying the process of circulating Ly6C⁺ MHCII⁻ monocytes differentiating into specialised fixed location Ly6C⁻ MHCII⁺ macrophages in specific organs would be beneficial for revealing immune response. During inflammation or infection, a marked increase in intermediate Ly6C⁺ MHCII⁺ cells may be present, in addition to the

recruitment of monocytes to the site of infection/inflammation (Desalegn and Pabst, 2019). In the liver, there were no changes present between treatment groups for any subsets.

However, interestingly the bladder displayed significant differences between the Th2-associated high dose group and naïve controls in both monocytes and intermediate cells. This trend likely also effected macrophages in the high dose treatment group, which was reduced in the high dose group compared to other groups, but failed to reach significance.

These cell populations seem to be altered by *T. muris* infection in the bladder, indicative of inflammation or signs of systemic immune response. It would be expected for the liver to exhibit signs of immune response over the bladder, as the liver is a site of complex immunological activity, poised to detect invading pathogens invading or damaging the gut (Kubes and Jenne, 2018). It would therefore be expected for the liver to more rapidly detect infection and induce a response.

Perhaps, some immune response could be present in the bladder and not the liver due to the local *T. muris*-induced mucosal response in the gut inducing some inflammation in distal mucosal sites, such as mentioned by Chenery *et al.*, (2016), where immunological cross talk between mucosal tissues was suspected to cause *T. muris*-induced changes in the lungs. As the bladder possesses a defined mucosal layer, but the liver lacks a prominent mucosal layer and instead has preferentially localised mucosal-associated cells (Bolte and Rehmann, 2019), this could potentially explain these unexpected results.

Additionally, it would be expected that a systemic response would be recorded in a chronic Th1-dominant infection over an acute Th2-dominant infection. This is because a local Th2- dominant response is normally sufficient for expulsion with no systemic involvement, whereas a Th1-dominant response induces chronic infection and longer-term inflammation responses with more far-reaching effects (Hayes and Grencis, 2021). This experiment was conducted on days 25-27 post-infection, which is just after the approximate peak immune response at ~ day 21, whereby Th2 responses lead expulsion and Th1 responses become chronic, so if a significant immune response was occurring in these organs, there would likely still be some evidence of it, especially concerning high dose-induced acute infection (Little *et al.*, 2005). In low dose infection the peak of inflammation can present later in the infection course (Donaldson *et al.*, 2020), so perhaps this is why this response is only present in the high dose Th2-dominant group.

To determine if any immunological changes occur in these organs during the infection course, a longitudinal study could be done using samples from a range of time periods, however this may not be necessary, with how little change seems to be present. It may also be useful to determine in more detail if macrophages are polarised Th1-like (M1) or Th2-like (M2), to examine more clearly what is occurring immunologically in this scenario.

Encompassing both the lymphoid and myeloid experiments, results might suggest that if trichuriasis infection was modulating immune response in these organs, it would be very slight. High dose-infection induced changes in the

monocyte subsets of the bladder were observed, however no other significant changes were determined in the bladder, and in the liver, there is no significant evidence at all of any infection-induced changes.

If few immunological changes are present in organs that contribute to urine release and production, then immune populations may not be the main driving force of trichuriasis-induced MUP changes. There does not seem to be much available evidence indicating that monocyte populations have any direct link with MUP expression.

It is likely that MUP expression is influenced by several factors in combination with each other. For example, endocrine mechanisms can influence expression, such as testosterone as previously mentioned (Isseroff *et al.*, 1986). The secretion of growth hormone (GH) also modulates MUP expression, and in males can be downregulated for many reasons, such as via neurotransmitters in the brain, circadian rhythm, aging, microbiota depletion, and ageing (Penn *et al.*, 2022).

It is suggested by Penn *et al.*, (2022) that mice in poor condition, such as infection, are less able to afford the energetic cost of MUP expression and the fitness costs of scent markings, so production is consequently downregulated. It was also concluded by Weger *et al.*, (2019) using an RNA-seq study on germ-free mice that the microbiome is a major component of MUP expression. Other factors affected by infection, such as these examples, could influence the production of MUP instead, or have a greater involvement during whipworm infection than immune cells in these organs do.

Concerning odour changes, this could suggest that immune response could have a lesser or more distant influence than previously considered.

Perhaps other relevant areas could be examined, such as the kidneys, which may affect urine odour through filtration, homeostasis, waste excretion and hormone production (Novella-Rausell *et al.*, 2023) and may also be systemically impacted by infection.

To summarize the results of these experiments, no significant *T. muris*-induced changes were observed in the liver, whereas in the bladder, changes in monocyte subsets were present in the high dose treatment group.

4.3 Clear Differences Between the VOC Profiles of Infected Urine and Naïve Urine

A portable eNose is a useful tool and could be used for infection-induced VOC perception, allowing for fast and accurate disease detection. Using the Roboscientific VOC analyser, odour changes were detected between infected and uninfected dogs (Staniek *et al.*, 2019), and likewise such differences have also been detected from hair VOC in *T. muris* infected mouse models, thought to be driven by adaptive immune response.

VOC analysis was therefore conducted on mouse urine using a portable eNose, which quantified a unique odour fingerprint for each sample using data collected from 24 sensors. PCA was used to display the data collected from the VOC analyser sensors, as it is among the most effective for determining sources of VOCs (Lan *et al.*, 2014, Guo, 2011), by reducing large sets of interrelated variables into a few factors that can be used to identify variance sources (Chen *et al.*, 2020).

Regarding the comparison of naïve urine with the urine of mice with low dose infections at day 35 post-infection, the inconclusive results indicated that whilst not visually different when analysed using PCA, the two groups did have some degree of separability when subject to machine learning model analysis, as naïve samples could often be classified correctly, but low dose samples was subject to less accurate classification.

This could be because some specific differences could be masked by more prevalent shared components, making low dose samples harder to identify compared with naïve samples.

Equally, the infection-induced changes to low dose urine metabolites/volatile compounds may make them more complex and volatile, causing inconsistent sensor readings and making it difficult to extract a unified basis for judgement, thus affecting the model's accuracy of identification. In this case, using more or different sensors may be necessary to determine any differences, as the use and properties of some sensors can sometimes limit VOC detection (Guillot, 2016).

Further analysis including more samples suggested a much clearer discernment than those analysed using day 35 alone, suggesting that the main reason for previous inconclusive results was likely small sample size, which didn't allow for sufficient information to be collected for successful classification analysis.

This secondary analysis suggested that there are identifiable differences present between naïve mouse urine and infected mouse urine, although it is more difficult to determine differences between time periods post-infection.

Even the highest scoring model only had 50% accuracy score when classifying different days post-infection, indicating a low success.

VOCs from samples can degrade over time in storage, reducing identifiable differences in odour, however our samples were collected and used within 3 months so this should not be an issue.

The differences present in these samples' VOCs were not clear enough to differentiate between different periods post-infection during day-dose classification.

VOC profiles paint complex pictures, built from potentially thousands of compounds, involving the emission of hydrocarbons, ketones, aldehydes and alcohols (Mazzatenta et al., 2021).

PCA analysis reduces dimensionality without supervision, potentially leading to the loss of information and discarded features that could have aided in classification. However, PCA was suitable for this study as sensor data contained many interrelated variables, and so this analysis was able to determine a baseline visualisation for the differences between datapoints by increasing interpretability and minimising information loss (Jolliffe and Cadima, 2016). Additionally, machine learning analysis was undertaken both with and without the aid of PCA, to reduce this loss of information. The data was put through multiple machine learning models per analysis category to determine which model had the best fit (Alnuaimi and Albaldawi, 2024). More models could be utilised compared with the first experiment due to increased sample size.

The use of multiple models also accounted for each model's individual limitations. Complex models such as radial basis function support vector machines may struggle to perform due to insufficient data, while simpler models like logistic regressions may not have the accuracy to capture any patterns present. The models that scored highest accuracy and macro F1 scores could be determined the best fit for the data, as they have the most accurate classification and the least imbalance across classes.

The data set could also still be too small or poorly balanced, causing small Macro F1 scores and unbalanced data. This in particular would be an issue concerning multi-class classification, like day-dose classification, where classes contain fewer samples with overlapping or ambiguous class boundaries (Fernandes and Carvalho, 2019). Perhaps this could be rectified using an even larger data set, with equal amounts of samples per class to reduce bias. More and Rana (2017) state that small sample size and lacking density is a crucial problem for classification, especially when working with data sets that are multidimensional and imbalanced. Additionally, spacing out time periods could perhaps provide more identifiable differences for the machine learning models to use in analysis and increase the precision of identification.

When classifying uninfected, high dose and low dose infection, odour was determined to be different between treatment types (naïve, high dose, low dose), especially in urine. 3-dose classification had on average a high sensitivity of 95% and a high specificity of 91.67%, which together with an accuracy of 93.75%, could be considered clearly distinguishable.

Likewise, VOC analysis implicated that odour is clearly different between infected and uninfected states. Binary classification of infected vs uninfected, a useful metric for the diagnostic potential of portable VOC analysis, displayed 100% specificity and 83.33% sensitivity.

The Kato Katz gold standard has an 84.8% sensitivity and 97.5% specificity, as determined by Nikolay *et al.*, (2014) through meta-analysis. Obviously, calculating sensitivity and specificity accurately to the standard of diagnostics requires significantly more testing and significantly larger sample sizes (Bujang and Adnan, *et al.*, 2016) and would of course have to occur using Trichuris-infected human urine, but from the results of this experiment the VOC analysis of urine shows promise at being useful for screening or diagnostics, if this was consistent with further testing, especially when considering speed and ease of application in real-world scenarios.

Additionally, Nikolay *et al.*, (2014) found that with lower intensity infections, sensitivity dropped by at least ~20% when using Kato-Katz, however both high and low dose infections could be detected with similar sensitivity and specificity, and furthermore, despite being indistinguishable between a range of days post-infection, infected treatment groups were clearly distinguishable from uninfected counterparts in binary and 3-dose classification.

Also, *T. muris*, egg-laying adult forms are not present until day ~32 post infection (Klementowicz *et al.*, 2012). Detection of *T. muris* through stool sample would have to occur after this period, when eggs appear in the faeces.

However, VOC analysis seemed to recognise infection at even earlier time points in this experiment, prior to eggs in stool, which may be beneficial for early confirmation and screening. Even day 7, day 14 and day 25 infections seemed

distinguishable from naïve samples by odour, as clearly visualised using PCA. Perhaps it would be beneficial to determine how early post-infection whipworm could be clearly detected by odour analysis, as early diagnosis is often beneficial for maximising patient outcomes.

As an additional note, it could also be worth submitting different strains of *T. muris* (E, J, and S) for VOC analysis, as the different immune responses they can elicit could aid in separating parasite load from immune response, which could aid in understanding.

4.4 Infected Urine Odour Does Not Induce Differential Sandfly Attraction

As *T. muris* low dose infected urine seemed to exhibit detectable changes, urine samples were examined under sandfly attraction olfactometer bioassays, to assess preference to altered infective states using sandflies as biological VOC detectors. Sandfly preference was compared to chronic and acute infection (and therefore to Th1 and Th2 response respectively), to examine for any differences or preferences. Sandfly preference assessments were carried out throughout infection evolution to establish a stronger understanding of the correlations between infection/immune response and attraction progression.

Despite VOC analysis concluding that there were significant odour differences present between infected and uninfected samples, and significant differences between responses recorded between chronic and acute treatment groups, there was no sign of significant attraction towards the infected urine of either

treatment group at any point post-infection that could not be put down to chance.

Concerning progression, usually for acute infection, immune response peaks at days 21-28 post-infection, higher than chronic infection, with worm expulsion occurring on days 18-21 (Yousefi *et al.*, 2021). Elimination of the infection is achieved by ~day 32 when faced with resistant Th2 immune response.

For chronic infection, worm survival is facilitated through a dominant Th1 immune response (Cliffe and Grencis, 2004). This allows for immune response to remain elevated at day 42 post-infection, where at that point the strength of immune response to acute infection would be reduced post-expulsion. Immune response maintains a chronic low-level activation in response to the persisting infection (Klementowicz *et al.*, 2012). One would expect attraction and preferences to favour greater strengths of immune response, highlighting the use of longitudinal study for determining any links or correlations between immune responses and odour.

This type of experiment is prone to user error, however any experimental errors that may have occurred when conducting these bioassays are unlikely to be responsible for this result, as confirmed by the success of the blind control. It is unlikely that the VOC profiles of the urine samples used degraded prior to the experiment, as urine can be stored without massively significant VOC degradation for seemingly unlimited duration at -80°C, providing that there are minimal freeze-thaw cycles (Holbrook *et al.*, 2023, Petrucci *et al.*, 2024). There

was also no notable sign of any of the more recently taken samples exhibiting more attraction than older samples.

Regarding the bioassays conducted, a Y-tube olfactometer was used. This equipment is commonly used to measure insect olfaction and is useful for testing relative attractiveness (Varley and Edwards, 1953). Sandflies were subjected to the olfactometer one at a time, to reduce the behavioural impact of a group in an enclosed environment. Any environmental conditions (temperature gradients, humidity etc.) were controlled to reduce impact and rotating the olfactometer after every 20 sandflies reduced potential directional bias. The time these bioassays were conducted was standardised over the course of the project to reduce any variability time of day might cause due to circadian rhythm (Roberts *et al.*, 2023, Meireles-Filho and Kyriacou, 2013, Meireles-Filho *et al.*, 2006, Rivas *et al.*, 2008),).

The average amount of non-responding sandflies across all bioassays conducted was $1.217(\pm SD 1.988)$, which could be considered low, and was lower than what was reported by Staniek *et al.*, (2021). The blind control was successful, and so this would suggest that the experimental design used in this study was sufficient for sandfly response, and any attraction that was present would have been captured regardless of any unoptimized conditions.

To further reduce the possibility for discrepancies, the same mice used through the infection course could have been used to collect naïve samples for comparison, however this is unlikely to have much impact on genetically similar lab mice reared under the same experimental conditions.

For future research, like with MUP expression, the urine of male mice could be tested instead of female mice, since male mice urine have been proven to have more factors in urine contributing to scent (Penn *et al.*, 2022). As previously mentioned, male mice urine is also evolutionarily selected for more communication than female mice urine, as it is also more involved in communicating social status, territory and mating. These could facilitate attraction more readily than female mice urine, which have less signalling molecules present.

Further proposed study into VOC changes adds on from the Hamilton group, namely in the use of *L. infantum*-infected dog hair by Staniek and Hamilton *et al.*, (2021), and their contribution towards the growing examples of disease state altering host odour. Studies into *L. infantum* have indicated that VOC profiles could be distinguished between (O'Shea *et al.*, 2002) and identified through eNose analysis (Staniek *et al.*, 2019). These differences drive vector attraction towards potential hosts and the infection-induced physiological changes brought on by *L. infantum* infection altered VOCs in ways that increased transmission success (Chelbi *et al.*, 2021). It was determined by the Hamilton group that sandflies held an attraction towards *P. berghei*-infected mouse hair compared to naïve controls (a parasite that cannot be transmitted by sandflies), and that the beneficial phenotype expression produced by leishmaniasis was likely a by-product of immune activation: an example of non-adaptive manipulation and not evidence of 'true' direct manipulation (Poulin, 2010).

Therefore, it was assumed that the distinctive VOC profiles identified in *T. muris* urine would be distinguishable to sandflies too. Especially as differences were found between infected and uninfected VOC profiles via VOC analysis, and attraction was found towards *T. muris*-infected mouse hair samples. However, this was not the case in this experiment. This could be due to the specific nature of immune response.

L. infantum interacts with the host immune response by replicating and residing within cells of the monocyte-macrophage lineage (Mazire *et al.*, 2022). Th1-type cellular immune responses are significant for protection against leishmaniasis parasites, whereas Th2-type cells can allow disease progression (Shahi *et al.*, 2013). As sandfly attraction was suspected to be influenced by and corresponding to strength of immune response, there may be differences between sandfly preference to whipworm upon comparison to leishmaniasis based on the differences between immune response to each parasite.

However, research following the Hamilton group has discovered a sandfly attraction to whipworm using entrained hair VOC has also been shown to correlate with the strength of immune response.

Using sandfly Y-tube olfactometer choice experiments that compared to naïve controls, low dose *T. muris*-infected mice hair was preferred on days 21, 28 and 42, correlating with strength of immune response and high worm burden. High dose also displayed these preferences, whereby high dose mice had stronger Th1 immune responses and higher worm burdens, although it was not present on day 42, post worm clearance. Comparing high and low dose, high dose mice

hair was preferred on days 21 and 28, with a day 42 preference for low dose, indicating that worm burden increases and correlates with sandfly attraction. Th1 type immune response has been found to be expressed more in high dose groups than low dose groups on days 21 and 28. On day 28, high dose Th1 type immune response peaked, negatively correlated with CD8+ expression in skin-draining lymph nodes. On day 42, high dose groups showed significant Th2 response, with IL-5+CD11b+ cells and IL-5+CD3+ cells significantly increased in the back and ears. Attraction exhibited towards skin and hair could be due to the immune changes occurring at these sites, as determined by this unpublished research. Other evidence for trichuriasis exhibiting a distal response on the skin include the evidence that this infection can modulate chemical skin sensitizers in mice (Hayes and Grencis, 2021).

These results indicate that immune response does cause sufficient immune-induced odour changes, just that those in urine are not attractive to sandflies. The results of this project have already shown evidence that the odour profile of mouse urine changes over the course of whipworm infection through differential MUP expression and VOC analysis, suggesting that there would be differences for sandflies to pick up on. The mechanisms behind these differences are entangled between the involvement of whipworm itself and immune response. However, maybe the changes in scent are difficult for sandflies to detect (i.e., are inconsistent and hard to determine).

It is also possible that attraction to mouse urine is not something that sandflies evolutionarily select for. There is previous evidence suggesting that dog hair odour is more impactful on sandfly response than rodent hair odour when both

have *L. infantum* (Nevatte *et al.*, 2017). In the *L. infantum* study, dog odour causes stimulated responses in ~90% of male *L. longipalpis* whereas Nevatte *et al.*, (2017), who used similar methods, but hamsters were not exposed via blood-feeding, had only ~50% of male sandflies responding to hamster odour. Mice are not a common natural host choice for blood-feeding when compared to dogs or humans, and so the urine of mice may be too far removed to develop an evolutionary selection pressure that pushes for attraction.

Studies have suggested that the urine of some mammals, namely cattle and sheep, is attractive (Yousefi *et al.*, 2020, Olaide, *et al.*, 2019). However, there is sparse evidence involving smaller rodents. Sandflies have been noted to be attracted to hamster urine, in combination with heat, CO₂, and male *Lutzomyia longipalpis* pheromone by Nigam and Ward, (1991), however when deprived of heat and pheromone these factors were rendered unattractive to sandflies. This could explain the lack of response that bioassay experiments exhibited.

The lack of attraction to urine could also be more to do with immune-induced interactions with local microbiome influencing attraction, rather than solely the immune system. This would indicate that the attraction within studies where attraction was witnessed towards hair or skin (Staniek and Hamilton *et al.*, 2021) particularly in the instance where whipworm-infected mouse hair was attractive, could be due to vital interactions involved with immune response and the site's microbiome, not the immune system in isolation. Compared to the skin, urine may have insufficient immune response and microorganisms to interact and facilitate these odour change-inducing interactions, and so despite the presence of distinct infection-induced odour profiles and changes in MUP

expression, sandfly responses exhibit no preference to urine but do towards skin.

4.5 Th1/Th2 Cytokines Alone Do Not Induce Differential Sandfly Attraction

Several studies illustrate that inflammation affects body odour. However, few explanations are available concerning the mechanisms which translate detection of a pathogen into a unique body odour. The previous findings have indicated there is information found within body odours about the presence of specific cytokines, distinguishable through both C57BL/6J trained mice biosensors and gas chromatography (Millet *et al.*, 2018).

Cytokines in general are highly involved with the immune response combating trichuriasis (Cliffe and Grencis, 2004, Grencis, 2001, Bancroft *et al.*, 1998).

Cytokines IL-12 and IL-4 (drivers of Th1 and Th2 responses respectively) have been used to initiate immune response in C57 mice, and sandflies preferred IL-12 injected mice in sandfly attraction tests (Worthington lab, unpublished data).

It was therefore considered prudent to investigate whether these preferences were solely due to the presence of immune cells or the interactions between them and the body/microbiota.

Whilst determined statistically insignificant through binomial testing, the results of these bioassays do indicate consistent differences present between attraction in addition to between cytokines and control substances, more notably concerning IFN γ against its' respective diluent control. Higher sandfly attraction has been observed towards Th1 when compared with Th2 induced odour changes in previous research. Whilst displaying a greater preference for

cytokines than was visible in the conducted urine bioassays, the preference was still insignificant, especially when compared with the positive response of the blind control and other bioassays conducted in other studies (E.g., Staniek *et al.*, 2021).

These data demonstrate that sandflies aren't attracted to the cytokines alone due to the various other biological components involved in identifying a blood meal source- cytokines alone may be too far removed/specific for sandflies evolution to favour attraction to it. Sandflies are instead attracted to inflammatory response induced by these cytokines, or these cytokines acting in conjunction to other biological components and microbiota, not just the diluent. These results suggest that cytokines may contribute to pathogen-induced odour changes but are not main driver of odour in isolation despite inducing the interactions that would cause these changes.

This could suggest that interactions with the microbiome play a greater role in sandfly attraction and detectable odour changes than previously considered. Despite healthy urine being considered sterile in the past, this was due to limited microorganism detection which did not detect the slow-growing anaerobic microorganisms and bacteria with complex nutritional needs that was later detected through next-generation sequencing technologies (Perez-Carrasco, *et al.*, 2021). However, urinary microbiota still has a low biomass ($\sim <10^4$ colony forming units/mL total bacteria) and low diversity relative to other microbial sites (skin, mouth, gastrointestinal etc.), and with close proximity to other bacterial niches, it is difficult to examine without some form of

contamination present (Microbiome Human Project, 2012, Grice *et al.*, 2009).

The urinary microbiome is more easily comparable to low abundance sites like the eye (Pearce, *et al.*, 2014).

Sandflies have been shown previously to be attracted to skin and hair odour post-infection, both of which include microbiome interactions that would be less prevalent/absent in urine. Sandflies were not attracted to urine alone nor the immune challenge-induced cytokines that would influence any changes in VOC profile that infection would cause. It is therefore sensible to assume that whilst immune cells themselves may cause some change in odour, interactions with microbiota induce more significant, detectable changes.

4.6 VOC Profile Differences Present in Faeces

Faeces can be a good area to target for VOC detection, as whilst often overlooked in favour of urine as a communication device, VOC-rich faeces are also suspected to divulge information to other mice regarding social environment (Goodrich *et al.*, 1990). This could be utilized evolutionarily to communicate health and status. Goodrich *et al.*, (1990) found that the VOCs emanating from faeces were quantitatively and qualitatively different to urine and concluded that at least some of the VOCs studied appeared to transfer information regarding territory.

Additionally, as mentioned previously, faeces are interconnected with abundant microbiota and microbial interactions within the gut (Nishijima *et al.*, 2025), which as suggested by the other experiments in this study, could be significant contributors towards infection-induced changes in VOC profiles for the purposes of detection.

To summarise the result of this experiment, whilst day-dose classification was indistinguishable, moderate distinction could be made between treatment groups, and infected samples could clearly be determined from uninfected samples.

Faecal samples would have the intrinsic influence of gut microbiota, known to be altered by digestive tract-dwelling trichuriasis infection and immune response. Faeces and the gut microbiome likely have an interlinked relationship (Weger *et al.*, 2019). Such interactions could have been driving the differences detected in whipworm-infected hair samples in prior unpublished research.

The direct and indirect effects caused by the presence of whipworm itself and trichuriasis-induced immune activation may get entangled by the metabolic differences found between infected and control animals (Houlden *et al.*, 2015), however. Houlden *et al.*, (2015) documents significant changes in microbiota between 14-28 post-infection, namely involving an abundance of *Bacteroidetes* (such as *Parabacteroides* and *Prevotella*) and a reduction in diversity. Greater distinction could perhaps be made if samples were analysed before and after days 14-28 post-infection, when Houlden *et al.*, (2015) had indicated changes in microbiome composition, especially to determine whether these changes are distinct. This is supported by Holm *et al.*, (2015), who determined that chronic *T. muris* induced a drop in diversity, with a marked increase of the *Lactobacillus* genus, parallel to affecting the adaptive immune system. These changes were transient and required the presence of the parasite but caused metabolic changes and seemingly long-lasting immunological consequences. Such

metabolic changes could have perhaps influence MUP expression, as previously suggested (Oldstone *et al.*, 2021).

According to the results of this experiment, faeces may be less useful than urine for more fine-tuned determinations of infection progression, such as determining how long the infection has occurred and whether the infection is chronic or acute.

Neither urine nor faeces could be used to identify time period differences in infections, although faeces seems to be distinctly worse.

It is important to note that the sample size for faeces was significantly smaller than the sample size of urine analysis, and so a more throughout and accurate comparison could be made with a similar number of samples. Urine analysis included samples from days 35 and 7 post-infection, whereas faecal analysis was limited to samples days 14 and 25 post-infection, producing a small, unbalanced data set. Any issues that would arise from small imbalanced sample sizes would be amplified in this study compared with the urine analysis, as even less samples were used and the models were given less information to use for classification. Whilst promising that distinct differences can be picked out from this data, this may affect the machine learning model training, leading to less significant and reliable classification (More and Rana, 2017). Smaller sample sizes are subject to increased influence of outliers and often lack robustness. It may be worth conducting further VOC analysis on faeces with larger sample sizes, as this may increase the accuracy of machine learning identification and therefore alter these conclusions.

When determining between infected and uninfected samples, accuracy was higher when using faecal VOC profiles than urine VOC profiles, with machine learned analysis distinguishing between faecal samples accurately every time. This could be due to a greater number of microbiome interactions, and that odour changes are caused by host immune response and/or *T. muris* interacting with the microbiome. Faecal VOCs have been considered to reflect gut microbiota composition, including their metabolic activity and any concurrent host interactions (Berkhout *et al.*, 2018).

McFarlane *et al.*, (2019) even determined that changes in urinary VOC profiles due to colorectal cancer correlated with significant differences in stool-derived microbiota.

Intestinal helminths have been shown to interact with microbial organisms within infected mice, establishing metabolic and immunologic consequences.

It has been determined that the microbiome undergoes *T. muris*-induced alterations throughout infection, dependent on dose (White *et al.*, 2016).

T. muris worms inhabit the most microbe-dense sections of the GI tract and likely rely on cues from gut microbiota in addition to the host for infection to initiate, inducing a distinct intestinal microbiota within the host that promotes parasite fitness (White *et al.*, 2018). The presence of whipworm dictates distinct host-derived intestinal microbiota, promoting long term survival of the STH (White, *et al.*, 2016). Notably, *E. coli* or *Staphylococcus aureus* enable successful larvae, as determined in gut explants by Hayes *et al.*, (2010) and Koyama (2013).

This topic would benefit from further study to examine which specific components differ in faeces and why. This could include whether preferential sandfly attraction exists in response to the faeces of an infected individual and establishing the extent of immune involvement in infection-induced VOC profile changes. The skin microbiome has been shown to influence attraction in hematophagous arthropods via the metabolome released by skin bacteria (Verhurst *et al.*, 2018), and these could have contributed to the attraction stated prior. Hence it is entirely likely that these microbiota or subsequent host interactions could influence attraction in faeces.

Concerning VOC analysis, Boots *et al.*, (2014) determined that four different pulmonary bacteria (*Escherichia coli*, *Klebsiella pneumoniae*, *Staphylococcus aureus* and *Pseudomonas aeruginosa*) could be cultured and when analysed, presented with distinct differences in VOC profiles. Potentially, the *T. muris*-induced presence of some bacteria could be identified from faecal samples, and this could be useful for diagnostics or research.

If present, this may also establish the mechanism that drives this attraction.

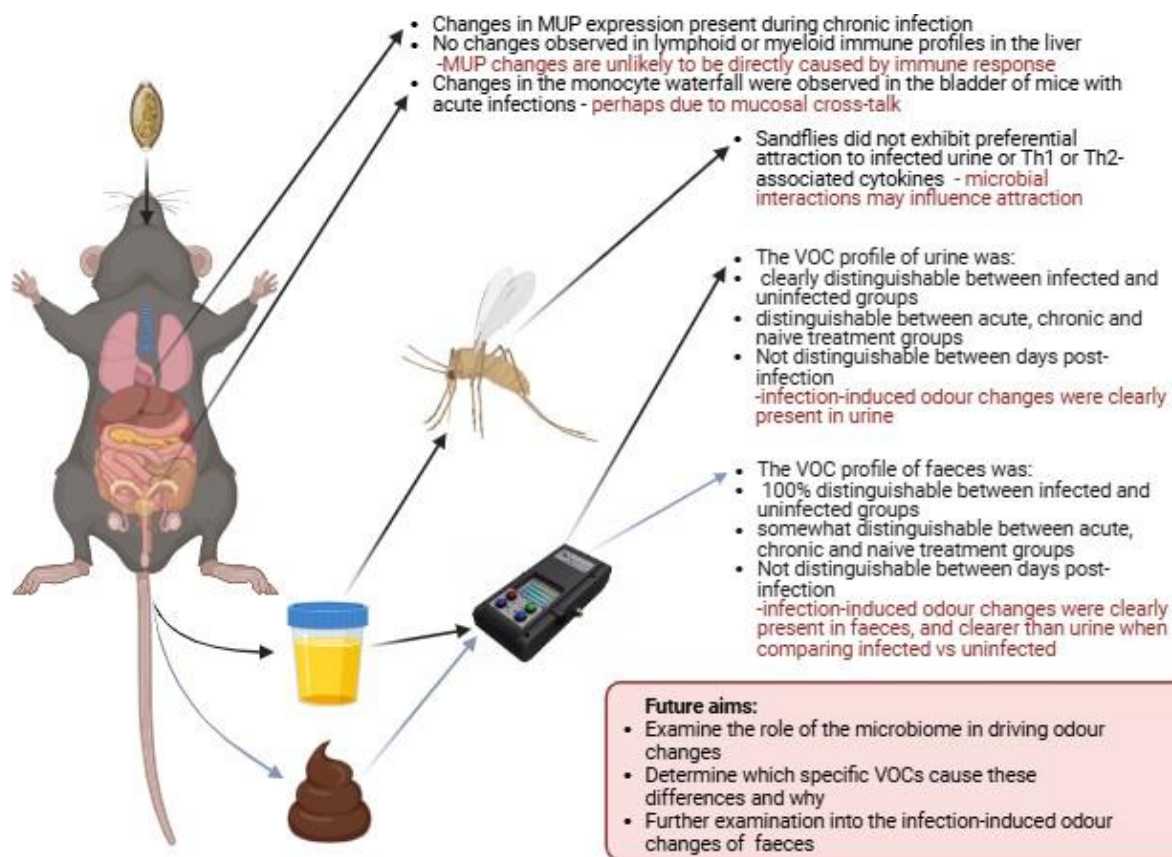
When the microbiome of the intestinal mucosa was compared with faeces, faeces has much vaster gene-richness and a greater number of genera (Yin *et al.*, 2024). The involvement of microbiota could be examined by utilizing antibiotics to isolate different colonies and performing bioassays and VOC analysis on samples with these arrangements, to get a better idea of the relationship microbiota has with odour.

Additionally, comparing the faeces of infected mice to infected germ-free (GF) mice could be a good comparison to make, for determining the extent of the

involvement of microbiota in odour changes. It would be worth noting however, that microbiota and the immune system are intrinsically linked, and so GF mice would show reduced immune response compared to naïve mice anyway, namely reduced Th1 cells (Choden and Cohen, 2022). White *et al.*, (2018) also determined that successful trichuriasis infection require microbiota, and in the absence of all microorganisms genetically susceptible germ-free mice are rendered resistant.

4.7 Conclusions

If the underlying mechanisms of the production of specific odours could be identified, more efficient therapeutic targeting could be utilised. An understanding of disease-specific VOC emissions and uncovering the molecular mechanisms behind disease-induced odour changes could progress the investigation and understanding of the pathophysiological mechanisms of specific diseases (Shirasu and Touhara, 2011). This would aid in the development of diagnostic tools and the successful treatment of whipworms in human populations, especially in areas where whipworm is both most prevalent and diagnostic methods are the most inaccessible.



Created in BioRender.com

Fig.36. A summary of the conclusions of this research.

Created in <https://BioRender.com>

Urine has been shown to be a suitable target source for detection using eNose analysis (Fig.36). Infection-induced changes in the VOC profiles of urine did seem to be distinguishable when comparing infected with uninfected samples, and to a lesser extent when comparing between high dose, low dose and uninfected samples. However, the length of time post-infection could not be identified using urine, and additionally *T. muris* infection in urine could not be detected using sandflies as biological detectors, despite prior research utilizing the VOCs from skin and hair displaying more distinctive *T. muris* infection-induced changes. This indicates that the changes in odour could be entwined

with the involvement of the body's microbiome. This supported by preliminary faecal VOC analysis, whereby infected samples could be perfectly distinguished from uninfected samples using an eNose. Further, more through study involving more samples and bioassays involving faecal samples could help clarify said involvement. Also, the use of antibiotics to isolate the contributions of specific microbiome communities would be of benefit.

Determining the mechanisms behind specific infection-induced odour changes would be taking steps towards the faster and easier diagnosis of whipworm, contributing to quicker treatment, better patient outcomes, and reduced transmission, in addition to validating such methods in the public and scientific community.

References

- Abadi, M., Barham, P., Chen, J., Chen, Z., Davis, A., Dean, J., & Zheng, X. (2016) TensorFlow: A system for large-scale machine learning. Proceedings of the 12th USENIX Symposium on Operating Systems Design and Implementation, pp. 265–283.
- Aksenov, A. A., Gojova, A., Zhao, W., Morgan, J. T., Sankaran, S., Sandrock, C. E., Davis, C. E. (2012) Characterization of Volatile Organic Compounds in Human Leukocyte Antigen Heterologous Expression Systems: a Cell's "Chemical Odor Fingerprint". *Chem Bio Chem*, 13(7), 1053-1059.
- Alnuaimi, A. F. A. H., Albaldawi, T. H. K. (2024) An overview of machine learning classification techniques. *BIO Web Conf.* 97(00133), 24.
- Alvar, J., Vélez, I. D., Bern, C., Herrero, M., Desjeux, P., Cano, J., Jannin, J., Boer, M. D. (2012) Leishmaniasis Worldwide and Global Estimates of Its Incidence, *PLoS ONE*, 7(5), e35671.
- Artis, D., Humphreys, N. E., Bancroft, A. J., Rothwell, N. J., Potten, C. S., Grencis, R. K. (1999) Tumor Necrosis Factor α Is a Critical Component of Interleukin 13–Mediated Protective T Helper Cell Type 2 Responses during Helminth Infection, *J Exp Med*, 190(7), 953-962.
- Artis, D., Wang, M. L., Keilbaugh, S. A., He, W., Brenes, M., Swain, G. P., Knight, P. A., Donaldson, D. D., Lazar, M. A., Miller, H. R. P., Schad, G. A., Scott, P., Wu, G. D. (2004) RELM β /FIZZ2 is a goblet cell-specific immune-effector molecule in the gastrointestinal tract. *Proc Natl Acad Sci U S A*, 101(37), 13596-13600.
- Artis, D. (2006) New weapons in the war on worms: Identification of putative mechanisms of immune-mediated expulsion of gastrointestinal nematodes, *Int J Parasitol*, 36(6), 723-733.

Artis D., Spits. H. (2015) The biology of innate lymphoid cells. *Nature.*, 517, 293–301.

Azeredo-Coutinho, R. B., Pimentel, M. I., Zanini, G. M., Madeira, M. F., Cataldo, J. I., Schubach, A. O., Quintella, L. P., De Mello, C. X., Mendonça, S. C. (2016) Intestinal helminth coinfection is associated with mucosal lesions and poor response to therapy in American tegumentary leishmaniasis. *Acta Trop*, 154, 24-9.

Bancroft, A. J., Else, K. J., Grecis, R. K. (1994) Low-level infection with *Trichuris muris* significantly affects the polarization of the CD4 response, *Eur J Immunol*, 24(12), 113-8.

Bancroft, A. J., McKenzie, A. N., Grecis, R. K. (1998) A critical role for IL-13 in resistance to intestinal nematode infection, *J Immunol* 160(7), 3453-61.

Bancroft, A. J., Artis, D., Donaldson, D. D., Sypek, J. P., Grecis, R. K. (2000) Gastrointestinal nematode expulsion in IL-4 knockout mice is IL-13 dependent, *Eur J Immunol*, 30(7), 2083-2091.

Bancroft, A. J., Else, K. J., Humphreys, N. E., Grecis, R. K. (2001) The effect of challenge and trickle *Trichuris muris* infections on the polarisation of the immune response, *Int J Parasitol.*, 31(14), 1627-37.

Bancroft, A. J., Humphreys, N. E., Worthington, J. J., Yoshida, H., Grecis, R. K. (2004) WSX-1: A Key Role in Induction of Chronic Intestinal Nematode Infection, *J Immunol*, 172(12), 7635-7641.

Bancroft, A., Levy, C. W., Jowitt, T. A., Hayes, K. S., Thompson, S., Mckenzie, E. A., Ball, M. D., Dubaissi, E., France, A. P., Bellina, B., Sharpe, C., Mironov, A., Brown, S. L., Cook, P. C., MacDonald, A. S., Thornton, D. J., Grecis, R. K.

(2019) The major secreted protein of the whipworm parasite tethers to matrix and inhibits interleukin-13 function. *Nat Commun*, 10, 2344.

Bancroft, A., Grencis, R. K. (2021) Immunoregulatory molecules secreted by *Trichuris muris*. *Parasitol*, 148(14), 1757-1763.

Bates, P. A. (2007) Transmission of *Leishmania* metacyclic promastigotes by phlebotomine sandflies, *Int J Parasitol.*, 37(10-3), 1097-1106.

Bell, L. V., Else, K. J. (2011) Regulation of colonic epithelial cell turnover by IDO contributes to the innate susceptibility of SCID mice to *Trichuris muris* infection, *Parasite Immunol*, 33(4), 244-249.

Bellaby, T., Robinson, K., Wakelin, D. (1996) Induction of differential T-helper-cell responses in mice infected with variants of the parasitic nematode *Trichuris muris*, *Infect immun*, 64(3), 791-795.

Berdoy, M., Webster, J. P., Macdonald, D. W. (2000) Fatal attraction in rats infected with *Toxoplasma gondii*, *Proc Royal Soc B*, 267(1452), 1591-1594.

Berkhout, D. J. C., Niemarkt, H. J., de Boer, N. K. H., Benning, M. A., de Meij, T. G. J. (2018) The potential of gut microbiota and fecal volatile organic compounds analysis as early diagnostic biomarker for necrotizing enterocolitis and sepsis in preterm infants. *Expert Rev Gastroenterol Hepatol*.12(5), 457-470.

Betts, C. J., Else, K. J. (1999) Mast cells, eosinophils and antibody-mediated cellular cytotoxicity are not critical in resistance to *Trichuris muris*, *Parasite Immunol*, 21(1), 45-52.

Betts, J., deSchoolmeester, M. L., Else, K. J. (2000) *Trichuris muris*: CD4+ T cell-mediated protection in reconstituted SCID mice, *Parasitol* 121(6), 631-7.

- Beynon, R. J., Hurst, J. L. (2004) Urinary proteins and the modulation of chemical scents in mice and rats, *Peptides*, 25(9), 1553-1563.
- Blackwell, N. M., Else, K. J. (2001) B Cells and Antibodies Are Required for Resistance to the Parasitic Gastrointestinal Nematode *Trichuris muris*, *Infect Immun*, 69(6), 3860-3868.
- Blackwell, N. M., Else, K. J. (2002) A comparison of local and peripheral parasite-specific antibody production in different strains of mice infected with *Trichuris muris*, *Parasite Immunol*, 24(4), 203-211.
- Blackwell, A. D. (2016) Helminth infection during pregnancy: insights from evolutionary ecology. *Int. J. Womens Health.*, 8, 651-661.
- Bolte, F. J., Rehmann, B. (2019) Mucosal-associated invariant T cells in chronic inflammatory liver disease. *Semin Liver Dis.* 31(1), 60-65.
- Bomers, M. K., van Agtmael, M. A., Luik, H., van Veen, M. C., Vandenbroucke-Grauls C. M., Smulders, Y. M. (2012) Using a dogs superior olfactory sensitivity to identify *Clostridium difficile* in stools and patients: proof of principle study, *BMJ*, 345.
- Bomers, M. K., van Agtmael, M. A., Luik, H., Vandenbroucke-Grauls, C. M., Smulders, Y. M. (2014) A detection dog to identify patients with *Clostridium difficile* infection during a hospital outbreak, *J Infect* 69, 456-461.
- Boots, A. W., Smolinska, A., van Berkel, J. J. B. N., Fijten, R. R. R., Stobberingh, E. E., Boumans, M. L. L., Moonen, E. J., Wouters, E. F. M., Dallinga, J. W., Van Schooten, F. J. (2014) Identification of microorganisms based on headspace analysis of volatile organic compounds by gas chromatography-mass spectrometry. *J Breath Res.* 8, 027106.

- Bos, L. D. J., Sterk, P. J., Schultz, M. J. (2013) Volatile Metabolites of Pathogens: A Systematic Review, *PLoS Pathogens*, 9(5), e1003311.
- Bowcutt, R., Bell, L. V., Little, M., Wilson, J., Booth, C., Murray, P. J., Else, K. J., Cruickshank, S. M. (2011) Arginase-1-expressing macrophages are dispensable for resistance to infection with the gastrointestinal helminth *Trichuris muris*. *Parasite Immunol.* 33(7), 411-20.
- Braks, M. A. H., Meijerink, J., Takken, W. (2001) The response of the malaria mosquito, *Anopheles gambiae*, to two components of human sweat, ammonia and l-lactic acid, in an olfactometer, *Physiol Entomol*, 26(2), 142-148.
- Bray, D. P., Hamilton, J.G. (2007) Host odor synergizes attraction of virgin female *Lutzomyia longipalpis* (Diptera: Psychodidae), *J Med Entomol.* , 44(5), 779-87.
- Bujang, M. A., Adnan, T. H. (2016) Requirements for minimum sample size for sensitivity and specificity analysis. *J Clin Diagn Res.* 10(10), 01-06.
- Cambau, E., Poljak, M. (2020) Sniffing animals as a diagnostic tool in infectious diseases, *Clin Microbiol Infect*, 26(4), 431-435.
- Cator, L. J., Lynch, P. A., Read, A. F., Thomas, M. B. (2012) Do malaria parasites manipulate mosquitoes?, *Trends Parasitol*, 28(11), 466-470.
- Cator, L. J., George, J., Blanford, S., Murdock, C. C., Baker, T. C., Read, A. F., Thomas, M. B. (2013) Manipulation without the parasite: altered feeding behaviour of mosquitoes is not dependent on infection with malaria parasites, *Proc royal Soc B*, 280(1763), 20130711.
- Carvalho, A. M., Guimarães, L. H., Costa, R., Saldanha, M. G., Prates, I., Carvalho, L. P., Arruda, S., Carvalho, E. M. (2021) Impaired Th1 Response Is

Associated With Therapeutic Failure in Patients With Cutaneous Leishmaniasis Caused by *Leishmania braziliensis*. *J Infect Dis*, 223, 527-535.

Centers for Disease Control and Prevention (2020) *Malaria Lifecycle Centers for Disease Control and Prevention* [Online]. U.S.A gov: Department of Health and Human Services. Available at:

<https://www.cdc.gov/malaria/about/biology/index.html#tabs-1-5> [Accessed: 7th June 2023].

Centers for Disease Control and Prevention (2020) *Parasites- Leishmaniasis, Biology* [Online]. USA.gov: U.S Department of Health and Human services.

Available at: <https://www.cdc.gov/parasites/leishmaniasis/biology.html> [Accessed: 12th June 2023].

Centers for Disease Control and Prevention (2024) *Trichuriasis* [Online].

USA.gov: U.S Department of Health and Human services. Available at:

<https://www.cdc.gov/dpdx/trichuriasis/index.html>. [Accessed: 16th October 2024].

Černá, M., Kuntova, B., Talacko, P., Stopkova, R., Stopka, P. (2017) Differential regulation of vaginal lipocalins (OBP, MUP) during the estrous cycle of the house mouse. *Sci Rep*, 7(11674).

Cevallos, W., Calvopiña, M., Nipáz, V., Vicente-Santiago, B., López-Albán, J., Fernández-Soto, P., Guevara, Á., Muro, A. (2017) Enzyme-linked immunosorbent assay for diagnosis of *Amphimerus* spp. liver fluke infection in Humans, *Mem Inst Oswaldo Cruz*, 112(5), 364-369.

Cecílio, P., Cordeiro-Da-Silva, A., Oliveira, F. (2022) sandflies: Basic information on the vectors of leishmaniasis and their interactions with *Leishmania* parasites, *Commun Biol*, 5(1).

Chen, S., Zieve, L., Mahadevan, V. (1970) Mercaptans and dimethyl sulfide in the breath of patients with cirrhosis of the liver. Effect of feeding methionine. *J Lab Clin Med*, 75(4), 628-35.

Chen, G-F., Lai, C-H., Chen, W-H. (2020) Principal component analysis and mapping to characterize the emission of volatile organic compounds in a typical petrochemical industrial park. *Aerosol Air Qual Res.* 20, 465-476.

Chen Z., L. J., Li J., Kim G., Stewart A., Urban J.F., Jr., Huang Y., Chen S., Wu L.-G., Chesler A., Trinchieri, G., Li, W., Wu, C. (2021) Interleukin-33 Promotes Serotonin Release from Enterochromaffin Cells for Intestinal Homeostasis. , *Immunity*, 54, 151–163.

Chenery, A. L., Antignano, F., Burrows, K., Scheer, S., Perona-Wright, G., Zaph, C. (2016) Low-Dose Intestinal *Trichuris muris* Infection Alters the Lung Immune Microenvironment and Can Suppress Allergic Airway Inflammation, *Infect Immunol*, 84.

Choden, T., Cohen, N. A. (2022) The gut microbiome and the immune system. *Explor Med*, 3, 219-233.

Chiu, S., Bharat, A. (2017) Role of monocytes and macrophages in regulating immune response following lung transplantation. *Curr Opin Organ Transplant.* 21(3), 239-245.

Cliffe, L. J., Grecis, R. K. (2004) The *Trichuris muris* system: a paradigm of resistance and susceptibility to intestinal nematode infection, *Adv Parasitol* 57, 255-307.

Cliffe, L. J., Humphreys, N. E., Lane, T. E., Potten, C. S., Booth, C., Grecis, R. K. (2005) Accelerated Intestinal Epithelial Cell Turnover: A New Mechanism of Parasite Expulsion, *Science*, 308(5727), 1463-1465.

Cliffe, L. J., Potten, C. S., Booth, C. E., Grencis, R. K. (2007) An Increase in Epithelial Cell Apoptosis Is Associated with Chronic Intestinal Nematode Infection, *Infect Immun*, 75(4), 1556-1564.

Colombo, S. A. P., Grencis, R. K. (2020) Immunity to Soil-Transmitted Helminths: Evidence from the Field and Laboratory Models. *Front Immunol*, 11.10.3389/fimmu.2020.01286

Connerney, J., Lau-Corona, D., Rampersaud, A., Waxman, D. J. (2017) Activation of female liver chromatin accessibility and STAT5-dependant gene transcription by plasma growth hormone pulses. *Endocrinol*, 158(5), 1386-1405.

Cornu J.-N., Cancel-Tassin G., Ondet V., Girardet C., Cussenot, O. (2010) Olfactory detection of prostate cancer by dogs sniffing urine: A step forward in early diagnosis, *Eur. Urol*, 59, 197-201.

Coronel Teixeira. R., Rodríguez, M., Jiménez De Romero, N., Bruins, M., Gómez, R., Yntema, J. B., Chaparro Abente, G., Gerritsen, J. W., Wiegerinck, W., Pérez Bejerano, D., Magis-Escurra, C. (2017) The potential of a portable, point-of-care electronic nose to diagnose tuberculosis, *J Infect*, 75(5), 441-447.

Cortes A., P. L., Scotti R., Jenkins T.P., Cantacessi C. (2019) Helminth-microbiota cross-talk—A journey through the vertebrate digestive system, *Mol. Biochem. Parasitol.*, 233, 111222.

Cozzarolo, C.-S., Pigeault, R., Isaïa, J., Wassef, J., Baur, M., Glazot, O., Christe, P. (2022) Experiment in semi-natural conditions did not confirm the influence of malaria infection on bird attractiveness to mosquitoes, *Parasit Vectors*, 15(1).

Cruickshank, S. M., Deschoolmeester, M. L., Svensson, M., Howell, G., Bazakou, A., Logunova, L., Little, M. C., English, N., Mack, M., Grencis, R. K.,

Else, K. J., Carding, S. R. (2009) Rapid Dendritic Cell Mobilization to the Large Intestinal Epithelium Is Associated with Resistance to *Trichuris muris* Infection, *J Immunol*, 182(5), 3055-3062.

D'Elia, R., Else, K. J. (2009) In vitro antigen presenting cell-derived IL-10 and IL-6 correlate with *Trichuris muris* isolate-specific survival, *Parasite Immunol*, 31(3), 123-131.

Dénes, A., Humphreys, N., Lane, T. E., Grecis, R., Rothwell, N. (2010) Chronic systemic infection exacerbates ischemic brain damage via a CCL5 (regulated on activation, normal T-cell expressed and secreted)-mediated proinflammatory response in mice. *J Neurosci*, 30, 10086–10095.

Desalegen, G., Pabst, O. (2019) Inflammation triggers immediate rather than progressive changes in monocyte differentiation in the small intestine. *Nature*, 10(3229).

Deslyper, G., Holland, C. V., Colgan, T. J., Carolan, J. C. (2019) The liver proteome in a mouse model for *Ascaris suum* resistance and susceptibility: evidence for an altered innate immune response, *Parasit. Vectors*, 12(1).

Dardalhon, V., A. A., Kwon, H., Galileos, G., Gao W., Sobel, R.A., Mitsdoerffer, M., Strom, T.B., Elyaman, W., Ho, I.-C. (2008) IL-4 inhibits TGF- β -induced Foxp3⁺ T cells and, together with TGF- β , generates IL-9⁺ IL-10⁺ Foxp3⁻ effector T cells, *Nat. Immunol*, 9, 1347–1355.

Darlan D. M., Winna, M., Simorangkir, H. A. H., Rozi, M. F., Arrasyid, N. K., Panggabean, M. (2019) Soil-transmitted helminth and its associated risk factors among school-aged children, *IOP Conf. Ser.: Earth Environ. Sci*, 305, 012066.

Darlan D.M., Rozi, M. F., Yulfi, H. (2021) Overview of Immunological Responses and Immunomodulation Properties of *Trichuris* sp.: Prospects for Better Understanding Human Trichuriasis, *Life*, 11, 188.

Dawkins, R. (1982). *The Extended Phenotype*. United Kingdom: Oxford University Press Inc.

De Angeli Dutra, D., Poulin, R., Ferreira, F. C. (2022) Evolutionary consequences of vector-borne transmission: how using vectors shapes host, vector and pathogen evolution, *Parasitology*, 149(13), 1667-1678..

De Schoolmeester M.L., M. P. L., Gordon S., Else K.J. (2009) The mannose receptor binds *Trichuris muris* excretory/secretory proteins but is not essential for protective immunity, *Immunology*, 126, 246–255.

Dénes, Á., Humphreys, N., Lane, T. E., Grecis, R., Rothwell, N. (2010) Chronic Systemic Infection Exacerbates Ischemic Brain Damage via a CCL5 (Regulated on Activation, Normal T-Cell Expressed and Secreted)-Mediated Proinflammatory Response in Mice, *J Neurosci*, 30(30), 10086-10095.

Deng, C., Zhang, X., Li, N. (2004) Investigation of volatile biomarkers in lung cancer blood using solid-phase microextraction and capillary gas chromatography-mass spectrometry, *J. Chromatogr. B Analyt. Technol. Biomed. Life Sci*, 808, 269-277.

Desruisseaux, M. S., Guinello, M., Smith, D. N., Lee, SH. C., Tsuji, M., Weiss, L. M., Spray, D. C., Tanowitz, H. B. (2009) Cognitive dysfunction in mice infected with *Plasmodium berghei* strain ANKA. *J Infect Dis*, 11, 1621-1627.

Devaraj, H., Pook, C., Swift, S., Aw, K. C., McDaid, A. J. (2018) Profiling of headspace volatiles from *Escherichia coli* cultures using silicone-based sorptive media and thermal desorption GC–MS, *J Sep Sci*, 41(22), 4133-4141.

Dharmani P., S. V., Kisson-Singh V., Chadee K. (2009) Role of intestinal mucins in innate host defense mechanisms against pathogens, *J. Innate Immun.* , 1, 123-125.

Dige, A., Rasmussen, T. K., Nejsum, P., Hagemann-Madsen, R., Williams, A. R., Agnholt, J., Dahlerup, J. F., Hvas, C. L. (2016) Mucosal and systemic immune modulation by *Trichuris trichiura* in a self-infected individual. *Parasit. Immunol.* 39(1), 12394.

Dima, A. C., Balaban, D. V., Dima, A. (2021) Diagnostic Application of Volatile Organic Compounds as Potential Biomarkers for Detecting Digestive Neoplasia: A Systematic Review, *Diagnostics.*, 11(12), 2317

Dixon, H., Blanchard, C., Deschoolmeester, M. L., Yuill, N. C., Christie, J. W., Rothenberg, M. E., Else, K. J. (2006) The role of Th2 cytokines, chemokines and parasite products in eosinophil recruitment to the gastrointestinal mucosa during helminth infection, *Eur J Immunol*, 36(7), 1753-1763.

Doherty, J.-F. (2020) When fiction becomes fact: exaggerating host manipulation by parasites, *Proc Royal Soc B*, 287(1936), 20201081.

Donaldson, D., Bradford, B., Else, K. J., Mabbott, N. (2020) Accelerated onset of CNS prion disease in mice co-infected with a gastrointestinal helminth pathogen during the preclinical phase. *Sci Rep*, 10, 4554.

Dormont, L., Mulatier, M., Carrasco, D., Cohuet, A. (2021) Mosquito Attractants. *J Chem Ecol*, 47, 351-393.

Duffy, E., Morrin, A. (2019) Endogenous and microbial volatile organic compounds in cutaneous health and disease, *Trends Analyt Chem*, 111, 163-172.

Duque-Correa MA, K. N., McCarthy C, Forman S, Goulding D, Sankaranarayanan G, Jenkins Tp., Reid, AJ., Cmabridge, EL., Reviriego, CB., The Sanger Mouse Genetics project, the 3i consortium, Muller, W., Cantacessi, C., Dougan, G, Grecis, RK., Berriman, M. (2019) Exclusive dependence of IL-10R α signalling on intestinal microbiota homeostasis and control of whipworm infection, *PLOS Pathogens*, 15(1).

Edelaar, P., Drent, J., De Goeij, P. (2003) A double test of the parasite manipulation hypothesis in a burrowing bivalve, *Oecologia*, 134(1), 66-71.

Edink, E., Jansen, C., Leurs, R., de Esch, I. J. P. (2010) The heat is on: thermodynamic analysis in fragment-based drug discovery, *Drug Discov Today Technol*, 7(3), 189-201.

Else, K., Wakelin, D. (1988) The effects of H-2 and non-H-2 genes on the expulsion of the nematode *Trichuris muris* from inbred and congenic mice, *Parasitol*, 96(3), 543-550.

Else, K. J., Wakelin, D., Wassom, D. L., Hauda, K. M. (1990) The influence of genes mapping within the major histocompatibility complex on resistance to *Trichuris muris* infections in mice, *Parasitology*, 101(1), 61-67.

Else, K. J., Hültner, L., Grecis, R. K. (1992) Modulation of cytokine production and response phenotypes in murine trichuriasis, *Parasite Immunol*, 14(4), 441-9.

Else, K. J., Finkelman, F. D., Maliszewski, C. R., Grecis, R. K. (1994) Cytokine-mediated regulation of chronic intestinal helminth infection, *J Exp Med*, 179(1), 347-351.

Else, K. J., Grecis, R. K. (1996) 'Antibody-independent effector mechanisms in resistance to the intestinal nematode parasite *Trichuris muris*', *Infect Immunol*, 64(8), 2950-2954.

Else, K. J., Keiser, J., Holland, C. V., Grencis, R. K., Sattelle, D. B., Fujiwara, R. T., Bueno, L. L., Asaolu, S. O., Sowemimo, O. A., Cooper, P. J. (2020) Whipworm and roundworm infections, *Nat Rev Dis Primers*, 6(1).

Emami, S. N., Lindberg, B. G., Hua, S., Hill, S. R., Mozuraitis, R., Lehmann, P., Birgersson, G., Borg-Karlson, A. K., Ignell, R., Faye, I. (2017) A key malaria metabolite modulates vector blood seeking, feeding, and susceptibility to infection, *Science*, 355(6329), 1076-1080

Faulkner, H., Renauld, J. C., Van Snick, J., Grencis, R. K. (1998) Interleukin-9 Enhances Resistance to the Intestinal Nematode *Trichuris muris*, *Infect Immunol*, 66(8), 3832-3840.

Ferkin, M. H., Sorokin, E. S., Johnston, R. E., Lee, C. J. (1997) Attractiveness of scents varies with protein content of the diet in meadow voles, *Anim. Behav*, 53, 133-141.

Fernandes, E. R. Q., de Carvalho, A. C. P. L. F. (2019) Evolutionary inversion of class distribution in overlapping areas for multi-class imbalanced learning. *Inf Sci*. 494, 141-154.

Flower, D. R., North, A. C., Sansom, C. E. (2000) The lipocalin protein family: structural and sequence overview, *Biochem. Biophys. Acta* 1482, 9-24.

Forman R.A., de Schoolmeester M.L., Hurst R.J.M., Wright S.H., Pemberton A.D., Else, K. J. (2012) The goblet cell is the cellular source of the anti-microbial angiogenin 4 in the large intestine post *Trichuris muris* infection, *PLoS ONE*, 7, e42248.

Foth, B. J., Tsai, I. J., Reid, A. J., Bancroft, A. J., Nichol, S., Tracey, A., Holroyd, N., Cotton, J. A., Stanley, E. J., Zarowiecki, M., Liu, J. Z., Huckvale, T., Cooper, P. J., Grencis, R. K., Berriman, M. (2014) Whipworm genome and dual-species

transcriptome analyses provide molecular insights into an intimate host-parasite interaction, *Nat Genet*, 46(7), 693-700.

Garner, C. E., Smith, S., de Lacy Costello, B., White, P., Spencer, R., Probert, C. S., Ratcliffe, N. M. (2007) Volatile organic compounds from feces and their potential for diagnosis of gastrointestinal disease, *FASEB J*, 21, 1675-1688.

Garner, C. E., Smith, S., Bardhan, P. K., Ratcliffe, N. M., Probert, C. S. A. (2009) pilot study of faecal volatile organic compounds in faeces from cholera patients in Bangladesh to determine their utility in disease diagnosis, *Trans R Soc Trop Med Hyg.*, 103, 1171-1173.

Géron, A. (2019) Hands-On Machine Learning with Scikit-Learn, Keras, and TensorFlow: Concepts, Tools, and Techniques to Build Intelligent Systems. 2nd ed. O'Reilly Media.

Giacomin, P. R., Kraeuter, A. K., Albornoz, E. A., Jin, S., Bengtsson, M., Gordon, R., Woodruff, T. M., Urich, T., Sarnyai, Z., Magalhaes, R. J. S. (2018) Chronic helminth infection perturbs the gut-brain axis, promotes neuropathology and alters behaviour. *J Infect Dis*, 218(9), 1511-1516.

Gilbert, J. A., Blaser, M. J., Caporaso, J. G., Jansson, J. K., Lynch, S. V., Knight, R. (2018) Current understanding of the human microbiome, *Nat Med*, 24, 392-400.

Glover, M., Colombo, S. A. P., Thornton, D. J., Grecis, R. K. (2019) Trickle infection and immunity to *Trichuris muris*, *PLOS Pathogens*, 15(11), e1007926.

Goldberg, E., M., Blendis, L. M., Sandler, S. A. (1981) gas chromatographic–mass spectrometric study of profiles of volatile metabolites in hepatic encephalopathy, *J. Chromatogr.*, 226, 291-299.

Grau-Pujol B, G. J., Escola V, Marti-Soler H, Cambra-Pelleja M, Demontis M, Brienen, E. A. T., Jamine, J. C., Mucisse, O., Cossa, A., Sacoer, C., Cano, J., Lieshout, L. V., Martinez-valladares, M., Munoz, J. (2022) Single-Nucleotide Polymorphisms in the Beta-Tubulin Gene and Its Relationship with Treatment Response to Albendazole in Human Soil-Transmitted Helminths in Southern Mozambique, *Am J Trop Med Hyg.*, 107(3), 649-57.

Grencis, R. K., Entwistle, G. M. (1997) Production of an interferon-gamma homologue by an intestinal nematode: functionally significant or interesting artefact?, *Parasitology*, 115(7), 101-105.

Grencis R.K., Humphreys N.E., Bancroft, A. J. (2014) Immunity to gastrointestinal nematodes: Mechanisms and myths, *Immunol Rev*, 260(183-205).

Grice, E. A., Kong, H. H., Conlan, S., Deming, C. B., Davis, J., Young, A. C., Bouffard, G. G., Blakesley, R. W., Murray, P. R., Green, E. D., Turner, M. L., Segre, J. A. (2009) Topographical and temporal diversity of the human skin microbiome. *Science*, 324, 1190-1192.

Guilot, J-M. (2016) E-noses: actual limitations and perspectives for environmental odour analysis. *Chem Eng Trans*. 54.

Guo, H. (2011) source apportionment of volatile organic compounds in Hong Kong homes. *Build Environ*. 46(11), 2280-2286.

Hadidi, S., Antignano, F., Hughes, M. R., Wang, S. K. H., Snyder, K., Sammis, G. M., Kerr, W. G., McNagny, K. M. and Zaph, C. (2012) Myeloid cell-specific expression of Ship1 regulates IL-12 production and immunity to helminth infection, *Mucosal Immunology*, 5(5), 535-543.

Hamann K. J., Barker R. L., Loegering D. A., Gleich, G. J.. (1987) Comparative toxicity of purified human eosinophil granule proteins for newborn larvae of *Trichinella spiralis*, *J Parasitol*, 73, 523-529.

Hammerschmidt, S. I., Ahrendt, M., Bode, U., Wahl, B., Kremmer, E., Förster, R., Pabst, O. (2008) Stromal mesenteric lymph node cells are essential for the generation of gut-homing T cells in vivo, *J Exp Med*, 205 (11), 2483-2490.

Harris, N. L. (2017) Recent advances in type-2-cell-mediated immunity: Insights from helminth infection, *Immunity*, 47, 1024–1036.

Hasnain, S. Z., Wang, H., Ghia, J. E., Haq, N., Deng, Y., Velcich, A., Grecis, R. K., Thornton, D. J., Khan, W. I. (2010) Mucin Gene Deficiency in Mice Impairs Host Resistance to an Enteric Parasitic Infection, *Gastroenterology*, 138(5), 1763-1771.e5.

¹Hasnain, S. Z., Thornton, D. J., Grecis, R. K. (2011) Changes in the mucosal barrier during acute and chronic *Trichuris muris* infection, *Parasite Immunol*, 33(1), 45-55.

²Hasnain, S. Z., Evans, C. M., Roy, M., Gallagher, A. L., Kindrachuk, K. N., Barron, L., Dickey, B. F., Wilson, M. S., Wynn, T. A., Grecis, R. K., Thornton, D. J. (2011) Muc5ac: a critical component mediating the rejection of enteric nematodes, *J Exp Med*, 208(5), 893-900.

Hayes, K. S., Bancroft, A. J., Grecis, R. K. (2007) The role of TNF- α in *Trichuris muris* infection II: global enhancement of ongoing Th1 or Th2 responses, *Parasite Immunol*, 29(11), 583-594.

Hayes, K. S., Bancroft, A. J., Goldrick, M., Portsmouth, C., Roberts, I. S., Grecis, R. K. (2010) Exploitation of the intestinal microflora by the parasitic nematode *Trichuris muris*. *Science*, 328(5984), 1391-4.

Hayes, K. S., Cliffe, L. J., Bancroft, A. J., Forman, S. P., Thompson, S., Booth, C., Grencis, R. K. (2017) Chronic *Trichuris muris* infection causes neoplastic change in the intestine and exacerbates tumour formation in APC min/+ mice. *PLOS Neg Trop Dis.* 11, e005708.

Hayes, K. S., Grencis, R. K. (2021) *Trichuris muris* and comorbidities- within a mouse model context. *Parasitol.* 148(14), 1774-1782.

Hayes K.S., B. A. J., Goldrick M., Portsmouth C., Roberts I.S., Grencis R.K. (2010) Exploitation of the intestinal microflora by the parasitic nematode *Trichuris muris*, *Science*, 328, 1391–1394.

Helmbly, H., Takeda, K., Akira, S., Grencis, R. K. (2001) Interleukin (Il)-18 Promotes the Development of Chronic Gastrointestinal Helminth Infection by Downregulating IL-13, *J Exp Med*, 194(3), 355-364.

Hepworth M.R., Grencis, R. K. (2009) Disruption of Th2 immunity results in a gender-specific expansion of IL-13 producing accessory NK cells during helminth infection, *J Immunol*, 183, 3906–3914.

Hepworth, M. R., Hardman, M., J., Grencis, R. K. (2010) The role of sex hormones in the development of Th2 immunity in a gender-biased model of *Trichuris muris* infection, *Eur J Immunol*, 40(2), 406-16.

Herbison, R., Lagrue, C., Poulin, R. (2018) The missing link in parasite manipulation of host behaviour, *Parasites Vectors*, 11(1).

Hernandez-Caballero, I., Garcia-Longoria, L., Gomez-Mestre, I., Marzel, A. (2022) The adaptive host manipulation hypothesis: parasites modify the behaviour, morphology, and physiology of amphibians. *Diversity*, 14(9), 739.

Holbrook, K. L., Badmos, S., Habib, A., Landa, E. N., Quaye, G. E., Pokojovy, M., Su, X., Lee, W. Y. (2023) Investigating the effects of storage conditions on urinary volatilomes for their reliability in disease diagnosis. *Am J Clin Exp Urol* 11(6), 481-499.

Holbrook, K. L., Badmos, S., Habib, A., Landa, E. N., Quaye, G. E., Pokojovy, M., Su, X., Lee, W-Y. (2023) Investigating the effects of storage conditions on urinary volatilomes for their reliability in disease diagnosis. *Am J Clin Exp Urol*. 11(6), 481-499.

Holloway, M. G., Laz, E. V., Waxman, D. J. (2006) Codependence of Growth Hormone-Responsive, Sexually Dimorphic Hepatic Gene Expression on Signal Transducer and Activator of Transcription 5b and Hepatic Nuclear Factor 4 α . *Mol Endocrinol*, 20(3), 647-660.

Holm, J. B., Sorobetea, D., Killerich, P., Ramayo-Caldas, Y., Estellé, J., Ma, T., Madsen, L., Kristiansen, K., Svensson-Frej, M. (2015) Chronic *Trichuris muris* Infection Decreases Diversity of the Intestinal Microbiota and Concomitantly Increases the Abundance of Lactobacilli, *PLOS ONE*, 10(5), e0125495.

Hotez, P. J., Alvarado, M., Basáñez, M. G., Bolliger, I., Bourne, R., Boussinesq, M., Brooker, S. J., Brown, A. S., Buckle, G., Budke, C. M., Carabin, H., Coffeng, L. E., Fèvre, E. M., Fürst, T., Halasa, Y. A., Jasrasaria, R., Johns, N. E., Keiser, J., King, C. H., Lozano, R., Murdoch, M. E., O'Hanlon, S., Pion, S. D. S., Pullan, R. L., Ramaiah, K. D., Roberts, T., Shepard, D. S., Smith, J. L., Stolk, W. A., Undurraga, E. A., Utzinger, J., Wang, M., Murray, C. J. L., Naghavi, M. (2014) The Global Burden of Disease Study 2010: Interpretation and Implications for the Neglected Tropical Diseases, *PLoS Neg. Trop. Dis.*, 8(7), 2865.

Houlden, A., Hayes, K. S., Bancroft, A. J., Worthington, J. J., Wang, P., Grecis, R. K., Roberts, I. S. (2015) Chronic *Trichuris muris* Infection in C57BL/6 Mice

Causes Significant Changes in Host Microbiota and Metabolome: Effects Reversed by Pathogen Clearance, *PLOS ONE*, 10(5), e0125945.

Hubbard, I. C., Thompson, J. S., Else, K. J., Shears, R. K. (2023) Chapter One- Another decade of *Trichuris muris* research: An update and application of key discoveries. *Adv Parasitol.* 121, 1-63.

Humphreys, N. E., Grencis, R. K. (2002) Effects of Ageing on the Immunoregulation of Parasitic Infection, *Infect Immun*, 70(9), 5148-5157.

Humphreys, N. E., Worthington, J. J., Little, M. C., Rice, E. J., Grencis, R. K. (2004) The role of CD8+ cells in the establishment and maintenance of a *Trichuris muris* infection, *Parasite Immunol*, 26(187-196).

Humphreys, N. E., Xu, D., Hepworth, M. R., Liew, F. Y., Grencis, R. K. (2008) IL-33, a Potent Inducer of Adaptive Immunity to Intestinal Nematodes, *J Immunol*, 180(4), 2443-2449.

Hurst, R. J. M., Else, K. J (2013) *Trichuris muris* research revisited: a journey through time, *Parasitology*, 140(11), 1325-1339.

Isseroff, H., Sylvester, P. W., Held, W. A. (1986) Effects of *schistosoma mansoni* on androgen regulated gene expression in the mouse. *Mol Biochem Parasitol*, 18(3), 401-412.

Ito, Y. (1991) The absence of resistance in congenitally athymic nude mice toward infection with the intestinal nematode, *Trichuris muris*: resistance restored by lymphoid cell transfer, *Int J Parasitol.*, 21(1), 65-9.

Jolliffe, I., Cadima, J. (2016) Principal component analysis: a review and recent developments. *Phil. Trans. R. Soc. A*.37420150202.

- Kabelitz, D. (2007) Expression and Function of Toll-like Receptors in T Lymphocytes. *Curr Opin Immunol.* 19(1), 39-45.
- Kaji, H., Hisamura, M., Saito, N., Makato, M. (1978) Evaluation of volatile sulfur compounds in the expired air of patients with liver cirrhosis, *Clin Chim Acta*, 85(3), 279-84.
- Kavaliers, M., Colwell, D. D. (1995) Discrimination by Female Mice between the Odours of Parasitized and Non-parasitized Males. *Proc Royal Soc B.* 261(1360).
- Keely, S, Talley, N. J., Hansbro, P, M. (2012) Pulmonary-intestinal cross-talk in mucosal inflammatory disease, *Mucosal Immunol* 5, 7-18.
- Keerthana, S., Mohammad, S., Harshika, P., Gouri, I., Divyadarshini, V., Selvakumar, M., Ramakrishna, N., Nirmal, M., Chiranjit, G. (2024) Skin emitted volatiles analysis for noninvasive diagnosis: the current advances in sample preparation techniques for biomedical application, *RSC Advances*, 14(17), 12009-12020.
- Khan, W. I., Vallance, B. A., Blennerhassett, P. A., Deng, Y., Verdu, E. F., Matthaei, K. I., Collins, S. M. (2001) Critical Role for Signal Transducer and Activator of Transcription Factor 6 in Mediating Intestinal Muscle Hypercontractility and Worm Expulsion in *Trichinella spiralis* -Infected Mice, *Infect Immun*, 69(2), 838-844.
- Khan, W. I., Richard, M., Akiho, H., Blennerhasset, P. A., Humphreys, N. E., Grecnis, R. K., Van Snick, J., Collins, S. M. (2003) Modulation of Intestinal Muscle Contraction by Interleukin-9 (IL-9) or IL-9 Neutralization: Correlation with Worm Expulsion in Murine Nematode Infections, *Infect Immun*, 71(5), 2430-2438.

Khan, W. I., Motomura, Y., Blennerhasset, P. A., Kanbayashi, H., Varghese, A. K., El-Sharkawy, R. T., Gauldie, J., Collins, S. M. (2005) Disruption of CD40-CD40 ligand pathway inhibits the development of intestinal muscle hypercontractility and protective immunity in nematode infection, *Am J Physiol Gastrointest Liver Physiol*, 288(1), 15-22.

Kim J. J., Khan, W. I. (2013) Goblet cells and mucins: Role in innate defense in enteric infections, *Pathogens*, 2, 55-70.

Kim, S., Prout, M., Ramshaw, H., Lopez, A. F., Legros, G., Min, B. (2010) Cutting Edge: Basophils Are Transiently Recruited into the Draining Lymph Nodes during Helminth Infection via IL-3, but Infection-Induced Th2 Immunity Can Develop without Basophil Lymph Node Recruitent or IL-3, *J Immunol*, 184(3), 1143-1147.

Kimball, B. A., Opienkun, M., Yamazaki, K., Beauchamp, G. K. (2014) Immunization Alters Body Odour. *Physio Behav.* 128, 80-85.

Klementowicz, J. E., Travis, M. A., Grecis, R. K. (2012) *Trichuris muris*: a model of gastrointestinal parasite infection, *Semin Immunopathol*, 34(6), 815-828.

Kondrashova, A., Seiskari, T., Ilonen, J., Knip, M., Hyoty, H. (2013) The Hygiene hypothesis and the sharp gradient in the incidence of autoimmune and allergic diseases between Russian Karelia and Finland, *APMIS*, 121(6), 478-93.

Kontos, E., Samimi, A., Hakze-Van Der Honing, R. W., Priem, J., Avarguès-Weber, A., Haverkamp, A., Dicke, M., Gonzales, J. L., Van Der Poel, W. H. M. (2022) Bees can be trained to identify SARS-CoV-2 infected samples, *Biol Open*, 11(4).

Koo, S., Thomas, H. R., Daniels, S. D., Lynch, R. C., Fortier, S. M., Shea, M. M., Rearden, P., Comolli, J. C., Baden, L. R., Marty, F. M. (2014) A Breath

Fungal Secondary Metabolite Signature to Diagnose Invasive Aspergillosis, *Clin Infect Dis*, 59(12), 1733-1740.

Koyama, K. (2013) Evidence for bacteria-independent hatching of *Trichuris muris* eggs. *Parasitol Res.* 112(4), 1537-42.

Koyama, K. (2002) NK1.1+ cell depletion in vivo fails to prevent protection against infection with the murine nematode parasite *Trichuris muris*. *Parasit Immunol.* 24(11-12), 527-33.

Koyama, K., Ito, Y. (1996) Comparative studies on immune responses to infection in susceptible B10.BR mice infected with different strains of the murine nematode parasite *Trichuris muris*, *Parasite Immunol*, 18(5), 257-63.

Koyama, K., Ito, Y. (2000) Mucosal mast cell responses are not required for protection against infection with the murine nematode parasite *Trichuris muris*, *Parasit Immunol*, 22(1), 21-28.

Koyama, K., Tamauchi, H., Ito, Y. (1995) The role of CD4+ and CD8+ T cells in protective immunity to the murine nematode parasite *Trichuris muris*, *Parasite Immunol*, 17(3), 161-165.

Koyama, K., Tamauchi, H., Tomita, M., Kitajima, T., Ito, Y. (1999) B-cell activation in the mesenteric lymph nodes of resistant BALB/c mice infected with the murine nematode parasite *Trichuris muris*, *Parasitol Res*, 85(3), 194-199.

Kramer, A., Bekeschus, S., Broker, B. M., Schleibinger, H., Razavi, B., Assadian, O. (2013) Maintaining health by balancing microbial exposure and prevention of infection: the hygiene hypothesis versus the hypothesis of early immune challenge, *J Hosp Infect*, 83, 29-34.

Krauss, M. E. Z. (2018) *CD4+ T Cell Metabolism during Trichuris muris Infection*. Manchester, UK: The University of Manchester.

Kubes, P., Jenne, C. (2018) Immune responses in the liver. *Annu Rev Immunol*, 36, 247-277.

Kumar, V. (2014) Innate lymphoid cells: New paradigm in immunology of inflammation, *Immunol. Lett.*, 157, 23–37.

Lan, C-H., H, Y-L., Ho, S-H., Peng, C-Y. (2014) Volatile organic compound identification and characterization by PCA and mapping at a high-technology science park. *Environ Pollut.* 193, 156-164.

Lawyer, P., Killick-Kendrick, M., Rowland, T., Rowton, E., Volf, P. (2017) Laboratory colonization and mass rearing of phlebotomine sandflies (Diptera, Psychodidae). *Parasite*, 24, 42.

Le, L., Khatoon, S., Jimenez, P., Peterson, C., Kernen, R., Zhang, W., Molehin, A. J., Lazarus, S., Sudduth, J., May, J., Karmakar, S., Rojo, J. U., Ahmad, G., Torben, W., Carey, D., Wolf, R. F., Papin, J. F., Siddiqui, A. A. (2020) Chronic whipworm infection exacerbates *Schistosoma mansoni* egg-induced hepatopathology in non-human primates. *Parasit Vectors*, 13(109).

Lee, T., D., Wakelin, D. (1982) The use of host strain variation to assess the significance of mucosal mast cells in the spontaneous cure response of mice to the nematode *Trichuris muris*, *Int Arch Allergy Appl Immunol* 67(4), 302-5.

Lee, T., D., Wakelin, D., Grencis, R. K. (1983) Cellular mechanisms of immunity to the nematode *Trichuris muris*, *Int J Parasitol.*, 13(4), 349-53.

Lefèvre, T., Thomas, F. (2008) Behind the scene, something else is pulling the strings: Emphasizing parasitic manipulation in vector-borne diseases, *Infect Genet Evol*, 8(4), 504-519.

Leung, J. M., Graham A. L., L., K. S. C. (2018) Parasite-microbiota interactions with the vertebrate gut: Synthesis through an ecological lens, *Front. Microbiol.*, 9, 843.

Little, M. C., Bell, L. V., Cliffe, L. J., Else, K. J. (2005) The Characterization of Intraepithelial Lymphocytes, Lamina Propria Leukocytes, and Isolated Lymphoid Follicles in the Large Intestine of Mice Infected with the Intestinal Nematode Parasite *Trichuris muris*, *J immunol*, 175(10), 6713-6722.

Little M. C., Hurst R. J. M., Else K. J. (2014) Dynamic changes in macrophage activation and proliferation during the development and resolution of intestinal inflammation, *J Immunol*, 193, 4684–4695.

Liu, S. F., Lu, H. I., Chi, W. L., Liu, G. H., Kuo, H., C. (2023) Sniffer Dogs Diagnose Lung Cancer by Recognition of Exhaled Gases: Using Breathing Target Samples to Train Dogs Has a Higher Diagnostic Rate Than Using Lung Cancer Tissue Samples or Urine Samples, *Cancers (Basel)*, 15(4), 1234.

Logan, D. W., Marton, T. F., Stowers, L. (2008) Species specificity in major urinary proteins by parallel evolution. *PLoS One*, 3(9), 3280.

Loukas, A., Maizel, R. M., Hotez, P. J. (2022) The yin and yang of human soil-transmitted helminth infections. *Int J Parasitol*, 51(13-14), 1243-1253.

Lucas-Barbosa, D., DeGennaro, M., Mathis, A., Verhulst, N. O. (2022) Skin bacterial volatiles: propelling the future of vector control. *Trends Parasitol*, 38(1), 15-22.

Luzynski, K., Nicolakis, D., Marcnic, M. A., Zala, S. M., Kwak, J., Penn, D. J. (2021) Pheromones that correlate with reproductive success in competitive conditions. *Sci Rep*, 11(21970).

Macdonald, A. S., Maizels, R. M. (2008) Alarming dendritic cells for Th2 induction, *J Exp Med*, 205(1), 13-17.

Mahoney, A., Weetjens, B., Cox, C., Beyene, N., Mgode, G., Jubitana, M., Kuipers, D., Kazwala, R., Mfinanga, G., Durgin, A., Poling, A. (2011) Using giant African pouched rats to detect tuberculosis in human sputum samples: 2010 findings, *Pan Afr Med J*, 9(1).

Mair, I., Else, K. J., Forman, R. (2021) *Trichuris muris* as a tool for holistic discovery research: from translational research to environmental bio-tagging, *Parasitology*, 148(14), 1722-1734.

Mair, I., Fenn, J., Wolfenden, A., Lowe, A. E., Bennett, A., Muir, A., Thompson, J., Dieumerci, O., Logunova, L., Shultz, S., Bradley, J. E., Else, K. J. (2024) The adaptive immune response to *Trichuris* in wild verse laboratory mice: an established model system in context. *PLOS Pathog*, 20(4), e1012119.

Maizels, R. M. (2016) Parasitic helminth infections and the control of human allergic and autoimmune disorders, *Clin Microbiol Infect*. 22(6), 481-486.

Manivannan, B., Rawson, P., Jordan, T. W., Secor, W. E., La Flamme, A. C. (2010) Differential Patterns of Liver Proteins in Experimental Murine Hepatosplenic Schistosomiasis, *Infect Immunol*, 78(2).

Manos, J. (2022) The human microbiome in disease and pathology, *APMIS*, 130(12), 690-705.

Marillier R.G., M. C., Smith E.M., Fick L.C.E., Leeto M., Dewals B., Horsnell W.G.C., Brombacher F. (2008) IL-4/IL-13 independent goblet cell hyperplasia in experimental helminth infections, *BMC Immunol*, 9, 1-9.

Marshall, J. S., Warrington, R., Watson, W., Kim, H. L. (2018) An introduction to immunology and immunopathology, *Allergy Asthma Clin Immunol*, 14(S2).

Martín-Fontecha A., Thomsen L. L., Brett S., Gerard C., Lipp M., Lanzavecchia A., F., S. (2004) Induced recruitment of NK cells to lymph nodes provides IFN- γ for TH 1 priming, *Nat Immunol*, 5(1260-1265).

Maskery, B., Coleman, M. S., Weinberg, M., Zhou, W., Rotz, L., Klosovsky, A.I., Cantey, P. T., Fox, L. M., Cetron, M. S., Stauffer, W. M. (2016) Economic analysis of the impact of overseas and domestic treatment and screening options for intestinal helminth infection among US-bound refugees from Asia. *PLoS Negl Trop Dis*. 10(8).

Massacand, J. C., Stettler, R. C., Meier, R., Humphreys, N. E., Grecis, R. K., Marsland, B. J., Harris, N. L. (2009) Helminth products bypass the need for TSLP in Th2 immune responses by directly modulating dendritic cell function, *Proc Nat Acad Sci*, 106(33), 13968-13973.

Maurer, M., McCulloch, M., Willey, A. M., Hirsch, W., Dewey, D. (2016) Detection of bacteriuria by canine olfaction, *Open Forum Infect Dis*, 3.

Maurya, R., Alti, D., Chandrasekaran, S. (2012) A risk of visceral leishmaniasis in case of helminths co-infection in endemic regions. *J Health Sci Med Res*, 2, 47-50.

Mazzatenta, A., Pokorski, M., Di Giulio, C. (2021) Volatile organic compounds (VOCs) in exhaled breath as a marker of hypoxia in multiple chemical sensitivity. *Physiol Rep*. 9(18), e15034.

Mazzatenta, A., Pokorski, M., Sartucci, F., Domenici, L., Di Giulio, C. (2015) Volatile organic compounds (VOCs) fingerprint of Alzheimers disease, *Neurobiol*, 209, 81-4.

Mbong Ngwese, M., Prince Manouana, G., Nguema Moure, P. A., Ramharter, M., Esen, M., Adégnika, A. A. (2020) Diagnostic Techniques of Soil-Transmitted Helminths: Impact on Control Measures, *Trop. Med. Infect. Dis.*, 5(2), 93.

McBride, J. A., Striker, R. (2017) Imbalance in the game of T cells: what can the CD4/CD8 T-cell ratio tell us about HIV and health? *PLOS Pathog.* 13(11), 1006624.

McCulloch M., J. T., Broffman, M., Hubbard, A., Turner, K., Janecki, T. (2006) Diagnostic accuracy of canine scent detection in early-and late-stage lung and breast cancers., *Integr. Cancer Ther*, 5, 30-39.

McFarlane, M., Millard, A., Hall, H., Savage, R., Constantinidou, C., Arasaradnam, R., Nwokolo, C. (2019) Urinary volatile organic compounds and faecal microbiome profiles in colorectal cancer. *Colorectal Dis*, 21(110), 1259-1269.

McKenzie, G. J., Bancroft, A., Grecis, R. K., McKenzie, A. N. J. (1998) A distinct role for interleukin-13 in Th2-cell-mediated immune responses, *Curr. Biol*, 8, 339-342.

Meireles-Filho, A. C. A., Gustavo, B., Rivas, da S., Gesto, J. S. M., Machado, R. C., Britto, C., de Souza, N. A., Peixoto, A. A. (2006) The biological clock of an hematophagous insect: locomotor activity rhythms, circadian expression and downregulation after blood meal. *FEBS*, 580(1), 2-8.

Meireles-Filho, A. C. A., Kyriacou, C. P. (2013) Circadian rhythms in insect disease vectors, *Mem. Inst. Oswaldo Cruz*, 108(1), 48-58.

Mendes de Oliveira V. N. G., Zuccherato, L. W., Dos Santos T. R., Rabelo E. M. L., Furtado, L. F. V. (2022) Detection of Benzimidazole Resistance-Associated

Single-Nucleotide Polymorphisms in the Beta-Tubulin Gene in *Trichuris trichiura* from Brazilian Populations, *Am J Trop Med Hyg*, 107, 640-8.

Mgode, G. F., Cox, C. L., Mwimanzi, S., Mulder, C. (2018) Pediatric tuberculosis detection using trained African giant pouched rats, *Pediatr Res*, 84, 99-103.

Microbiome Human Project. (2021) Structure, function and diversity of the healthy human microbiome. *Nature*, 487, 207-214.

Millet, P., Opiekun, M., Martin, T., Beauchamp, G. K., Kimball, B. A. (2018) Cytokine contributions to alterations of the volatile metabolome induced by inflammation. *Brain Behav Immun*, 69, 312-320.

Mitchell, S. N., Kakani, E. G., South, A., Howell, P. I., Waterhouse, R. M., Catteruccia, F. (2015) Evolution of sexual traits influencing vectorial capacity in anopheline mosquitoes, *Science*, 347(6225), 985-988.

Moens, M., Smet, A., Naudts, B., Verhoeven, J., Ieven, M., Jorens, P., Geise, H. J., Blockhuys, F. (2006) Fast identification of ten clinically important micro-organisms using an electronic nose, *Lett Appl Microbiol*, 42(2), 121-126.

Mogilnicka, I., Bogucki, P., Ufnal, M. (2020) Microbiota and Malodor- etiology and management. *Int J Mol Sci*, 21(8), 2886.

Molodecky, N. A., Soon, I. S., Rabi, D. M., Ghali, W. A., Ferris, M., Chernoff, G., Benchimol, E. I., Panaccione, R., Ghosh, S., Barkema, H. W., Kaplan, G. G. (2012) Increasing incidence and prevalence of the inflammatory bowel diseases with time, based on systematic review, *Gastroenterology*, 142(1), 46-54.

Moore, J. (2002) *Parasites and the Behaviour of Animals*. New York, NY. : Oxford University Press.

- More, A. S., Rana, D. P. (2017) Review of random forest classification techniques to resolve data imbalance. *ICISM*, 72-78.
- Moser, W., Schindler, C., Keiser, J. (2017) Efficacy of recommended drugs against soil transmitted helminths: systematic review and network meta-analysis, *BMJ* 358.
- Moraes, C. S., Aguiar-Martins, K., Costa, S. G., Bates, P. A., Dillon, R. J., Genta, F. A. (2018) Second Blood Meal by Female *Lutzomyia longipalpis*: Enhancement by Oviposition and Its Effects on Digestion, Longevity, and Leishmania Infection. *BioMed Res Int*, 2018, 1-10.
- Motomura, Y., Khan, W. I., El-Sharkawy, R. T., Verma-Gandu, M., Grecis, R. K., Collins, S. M. (2010) Mechanisms underlying gut dysfunction in a murine model of chronic parasitic infection, *Am J Physiol Gastrointest Liver Physiol*, 299(6), 1354-60.
- Moura, P. C., Raposo, M., Vassilenko, V. (2023) Breath volatile organic compounds (VOCs) as biomarkers for the diagnosis of pathological conditions: A review, *Biomed J*, 46(4), 100623.
- Myhill L. J., Stolzenbach S., Hansen T. V. A., Skovgaard K., Stensvold C. R., Andersen L. O., Nejsum P., Mejer H., Thamsborg S. M., Williams. A. R. (2018) Mucosal barrier and Th2 Immune responses are enhanced by dietary inulin in pigs infected with *Trichuris suis*, *Front. Immunol.*, 9, 2557.
- Nair, M. G., Guild, K. J., Du, Y., Zaph, C., Yancopoulos, G. D., Valenzuela, D. M., Murphy, A., Stevens, S., Karow, M., Artis, D. (2008) Goblet Cell-Derived Resistin-Like Molecule β Augments CD4+ T Cell Production of IFN- γ and Infection-Induced Intestinal Inflammation, *J Immunol*, 181(7), 4709-4715.
- Neill, D. R., McKenzie, A. N. J (2011) Nuocytes and beyond: new insights into helminth expulsion, *Trends Parasitol* 27(5).

Nevatte, T. M., Ward, R. D., Sedda, L., Hamilton, J. G. C. (2017) After infection with *Leishmania infantum*, Golden Hamsters (*Mesocricetus auratus*) become more attractive to female sandflies (*Lutzomyia longipalpis*), *Sci Rep*, 5(6104).

Nguyen, P. L., Vantaux, A., Hien, D. F., Dabiré, K. R., Yameogo, B. K., Gouagna, L.-C., Fontenille, D., Renaud, F., Simard, F., Costantini, C., Thomas, F., Cohuet, A., Lefèvre, T. (2017) No evidence for manipulation of *Anopheles gambiae*, *An. coluzzii* and *An. arabiensis* host preference by *Plasmodium falciparum*, *Sci Rep*, 7(1).

Nigam, Y., Ward, R. D. (1991) The effect of male sandfly pheromone and host factors as attractants for female *Lutzomyia longipalpis* (Diptera: Psychodidae). *Physiol Entomol*, 16(3), 305-312.

Nokes, C., Grantham-Mcgregor, S. M., Sawyer, A. W., Cooper, E. S., Robinson, B. A., Bundy, D. A. P. (1992) Moderate to heavy infections of *Trichuris trichiura* affect cognitive function in Jamaican school children. *Parasitology*, 104(3), 539-547.

Nishijima, S., Stankevic, E., Aasmets, O., Schmidt, T. S. B., Nagata, N., Keller, M. I., Ferretti, P., Juel, H. B., Fullam, A., Robbani, S. M., Schudoma, C., Hansen, J. K., Holm, L. A., Israelsen, M., Schierwagen, R., Torp, N., Telzerrow, A., Hercog, R., Kandels, S., Hazenbrink, D., Arumugam, M., Bendtsen, F., Brons, C., Fonvig, C. E., Holm, J.-C., Neilsen, T., Pedersen, J. S., Thiele, M. S., Trebicka, J., Org, E., Krag, A., Hansen, T., Kuhn, M., Bork, P. (2025) Fecal microbial load is a major determinant of gut microbiome variation and cofounder for disease associations. *Cell*, 188,(1), 22-236.

Nokes, C., Bundy, D. A. P. (1994) Does helminth infection affect mental processing and educational development? *Parasitology Today*, 10(1), 14-18.

- Novella-Rausell, C., Grudniewska, M., Peters, D. J. M., Mahfouz. (2023) A comprehensive mouse kidney atlas enables rare cell population characterization and robust marker discovery. *iScience*, 26(6), 106877.
- O'Connell, E. M., Nutan, T. B. (2016) Molecular Diagnostics for Soil-Transmitted Helminths, *Am J Trop Med Hyg*, 95(3), 508-513.
- Ohnmacht, C., Schwartz, C., Panzer, M., Schiedewitz, I., Naumann, R., Voehringer, D. (2010) Basophils orchestrate chronic allergic dermatitis and protective immunity against helminths, *Immunity*, 33(3), 364-74.
- Olaide, O. Y., Tchuassi, D. P., Yusuf, A. A., Pirk, C. W. W., Masiga, D. K., Saini, R. K., Torto, B. (2019) Zerba skin odor repels the savannah tsetse fly, *Glossina pallidipes* (Diptera: Glossinidae). *Neg Trop Dis*.
<https://journals.plos.org/plosntds/article?id=10.1371/journal.pntd.0007460>
- Oldstone, M. B. A., Ware, B. C., Davidson, A., Prescott, M. C., Beynon, R. J., Hurst, J. L. (2021) Lymphocytic Choriomeningitis Virus Alters the Expression of Male Mouse Scent Proteins, *Viruses*, 13(6), 1180.
- Oliveira, M. R., Neto, M. B. O., Bezerra, T. L., Da Silva, W. S. I., Da Paz, W. S., Dos Santos, I. G., Bezerra-Santos, M., Lima, V. F. S. (2021) Canine leishmaniasis in an endemic region, Northeastern Brazil: a comparative study with four groups of animals, *Parasitol Res*, 120(11), 3915-3923.
- Oliveira-Ferreira, J., Lacerda, M. V., Brasil, P., Ladislau, J. L., Tauil, P. L., Daniel-Ribeiro, C. T. (2010) Malaria in Brazil: an overview, *Malar J J*, 9(1), 115.
- Oudhoff, M. J., Antignano, F., Chenery, A. L., Burrows, K., Redpath, S. A., Braam, M. J., Perona-Wright, G., Zaph, C. (2016) Intestinal Epithelial Cell-Intrinsic Deletion of *Setd7* Identifies Role for Developmental Pathways in Immunity to Helminth Infection, *PLOS Pathogens*, 12(9), e1005876.

Owen, J., Punt, J., Stranford, S. (2013) *Kuby immunology*, New York. W. H. Freeman and Company. 40.

Pearce, E. J., Kane, C. M, Sun, J. "Adaptive Immune Response." *Parasites and Allergy* 90 (2006): 82-90.

Pearce, M. M., Hilt, E. E., Rosenfeld, A. B., Zillox, M. J., Thomas-White, K., Fok, C., Kliethermes, S., Schreckenberger, P., Brubaker, I., Gai, X., Wolfe, A. J> (2014) The female urinary microbiome: a comparison of women with and without urgency urinary incontinence. *mBio*, 5(4).

Pedregosa, F., Varoquaux, G., Gramfort, A., Michel, V., Thirion, B., Grisel, O., Blondel, M., Prettenhofer, P., Weiss, R., Dubourg, V., Vanderplas, J., Passos, A., Cournapeau, D., Brucher, M., Perrot, M., & Duchesnay, E. (2011) Scikit-learn: Machine learning in Python. *Journal of Machine Learning Research*, 12(85), pp. 2825–2830.

Pelchat, M. L., Bykowski, C., Duke, F. F., Reed, D. R. (2011) Excretion and Perception of a Characteristic Odor in Urine after Asparagus Ingestion: a Psychophysical and Genetic Study, *Chem Senses*, 36(1), 9-17.

Penders J, Stobberingh E. E, van den Brandt P. A, Thijs, C. (2007) The role of the intestinal microbiota in the development of atopic disorders, *Allergy*, 62, 1223-1236.

¹Penn, D., Potts, W. K. (1998) Chemical signals and parasite-mediated sexual selection, *Trends Ecol Evol*, 13, 391-396.

²Penn, D., Potts, W. (1998) How do major histocompatibility complex genes influence odor and mating preferences? *Adv Immunol*, 69, 411-435.

Penn, D., Potts, W. (1999) The evolution of mating preferences and major histocompatibility genes. *Am Nat*, 153, 145-164.

Penn, D. J., Zala, S. M., Luzynski, K. C. (2022) Regulation of sexually dimorphic expression of major urinary proteins. *Front Physiol*, 13.

Perez-Carrasco, V., Soriano-Lerma, A., Sriano, M., Gutierrez-Fernandez, J., Garcia-Salcedo, J. A. (2021) Urinary Microbiome: Yin and yan of the Urinary Tract. *Front Cell Infect Microbiol*, 11.

Perrigoue, J. G., Saenz, S. A., Siracusa, M. C., Allenspach, E. J., Taylor, B. C., Giacomini, P. R., Nair, M. G., Yurong, D., Zaph, C., van Rooijen, N., Comeau, M. R., Pearce, E. J., Laufer, T. M., Artis, D. (2009) MHC class II-dependent basophil-CD4⁺ T cell interactions promote T(H)2 cytokine-dependent immunity, *Nat Immunol*, 10(7), 697-705.

Petrucci, G., Hatem, D., Langley, R., Cleary, S., Gentry-Maharaj, A., Pitocco, D., Rizzi, A., Ranalli, P., Zaccardi, F., Habib, A., Rocca, B. (2024) Effect of very long-term storage and multiple freeze and thaw cycles on 11-dehydro-thromboxane-B₂ and 8-iso-prostaglandin F₂ α , levels in human urine samples by validated enzyme immunoassays. *Sci Rep*, 14(5546).

Phillips, R. S., Selby, G. R., Wakelin, D. (1974) The effect of *Plasmodium berghei* and *Trypanosoma brucei* infections on the immune expulsion of the nematode *Trichuris muris* from mice, *Int J Parasitol.*, 4(4), 409-415.

Phillips, N. L. H., Roth, T. L. (2019) Animal Models and Their Contribution to Our Understanding of the Relationship Between Environments, Epigenetic Modifications, and Behavior, *Genes*, 10(1), 47.

Phythian-Adams, A. T., Cook P. C., Lundie R. J., Jones L. H., Smith K. A., Barr T. A., Hochweller K., Anderton S. M., Hämmerling G. J., Maizels, R. M. (2010)

CD11c depletion severely disrupts Th2 induction and development in vivo, *J Exp Med*, 207, 2089–2096.

Pillai, M. R., Mihi, B., Ishiwata, K., Nakamura, K., Sakuragi, N., Finkelstein, D. B., McGargill, M. A., Nakayama, T., Ayabe, T., Coleman, M. L., Bix, M. (2019) Myc-induced nuclear antigen constrains a latent intestinal epithelial cell-intrinsic anthelmintic pathway, *PLOS ONE*, 14(2), e0211244.

Poling, A., Mahoney, A., Beyene, N., Mgode, G., Weetjens, B., Cox, C., Durgin, A. (2015) Using giant african pouched rats to detect human tuberculosis: a review, *Pan Afr Med J*, 21.

Portes, A., Giestal-de-Araujo, Fagundes, A., Pandolfo, P., de Sa Geraldo, A., Lira, M. L. F., Amaral, V. F., Lagrota-Candido, J. (2016) *Leishmania amazonensis* infection induces behavioural alterations and modulates cytokines and neurotrophin production in the murine cerebral cortex. *J Neuroimmunol*. 301, 65-73.

Poulin, R. (1994) The evolution of parasite manipulation of host behaviour: a theoretical analysis, *Parasitology*, 109(18).

Poulin, R. (2000) Manipulation of host behaviour by parasites: a weakening paradigm?, *Proc Royal Soc B*, 267(1445), 787-792.

Poulin, R. (2010) Chapter 5 - Parasite Manipulation of Host Behavior: An Update and Frequently Asked Questions, *Adv Study Behav*, 41, 151-186.

Pullan, R. L., Smith, J. L., Jasrasaria, R., Brooker, S. J. (2014) Global numbers of infection and disease burden of soil transmitted helminth infections in 2010, *Parasit Vectors*, 7(1), 37.

Ramanan D., Bowcutt R., Lee S. C., San Tang M., Kurtz Z. D., Ding Y., Honda K., Gause W. C., Blaser M. J., Bonneau R. A., Lim, Y. A. L., Loke, P., Cadwell,

- K. (2016) Helminth infection promotes colonization resistance via type 2 immunity, *Science*, 352, 608–612.
- Rasquinha, M. T., Sur, M., Lasrado, N., Reddy, J. (2021) IL-10 as a Th2 Cytokine: Differences Between Mice and Humans, *J Immunol*, 207(9), 2205-2215.
- Real, M. V. F., Colvin, M. S., Seehan, M. J., Moeller, A. H. (2024) Major urinary protein (Mup) gene family deletion drives sex-specific alterations in the house-mouse gut microbiota. *Microbiol Spectr*, 12(2), 03566-23.
- Reither, K., Jugheli, L., Glass, T. R., Sasamalo, M., Mhimbira, F. A., Weetjens, B. J., Cox, C., Edwards, T. L., Mulder, C., Beyene, N. W., Mahoney, A. (2015) Evaluation of Giant African Pouched Rats for Detection of Pulmonary Tuberculosis in Patients from a High-Endemic Setting, *PLOS ONE*, 10(10), e0135877.
- Richard, M., Grecis, R. K., Humphreys, N. E., Renauld, J.-C., Van Snick, J. (2000) Anti-IL-9 vaccination prevents worm expulsion and blood eosinophilia in *Trichuris muris*-infected mice, *Proc Nat Acad Sci*, 97(2), 767-772.
- Rivas, G. B. S., Souza, N. A., Peixoto, A. A. (2008) Analysis of the activity patterns of two sympatric sandfly siblings of the *Lutzomyia longipalpis* species complex from Brazil. *Med Vet Entomol*. 22(3), 288-290.
- Roberts, J. M., Clunie, B. J., Leather, S. R., Harrus, E., Pope, T. W. (2023) Scents and sensibility: best practise in insect olfactometer bioassays. *Entomol Exp Appl*, 171(11), 808-820.
- Röck, F., Barsan, N., Weimar, U. (2008) Electronic Nose: Current Status and Future Trends, *Chem Rev*, 108(2).

Rosa, B. A., Snowden, C., Martin, J., Fischer, K., Kupritz, J., Beshah, E., Supali, T., Gankpala, L., Fischer, P. U., Urban, J. F., Mitreva, M. (2021) Whipworm-Associated Intestinal Microbiome Members Consistent Across Both Human and Mouse Hosts, *Front Cell Infect Microbiol*, 11. 10.3389/fcimb.2021.637570

Russell, S. L., Gold, M. J., Hartmann, M, Willing, B. P., Thorson, L., Wlodarska, M., Gill, N., Blanchet, M-R., Mohn, W. W., McNagny, K. M., Finlay, B. B. (2012) Early life antibiotic-driven changes in microbiota enhance susceptibility to allergic asthma, *EMBO rep*, 13, 440-447.

²Saenz, S. A., Noti, M., Artis, D. (2010) Innate immune cell populations function as initiators and effectors in Th2 cytokine responses, *Trends Immunol*, 31(11), 407-13.

¹Saenz, S. A., Siracusa, M. C., Perrigoue, J. G., Spencer, S. P., Urban Jr, J. F., Tocker, J. E., Budelsky, A. L., Kleinschek, M. A., Kastelein, R. A., Kambayashi, T., Bhandoola, A., Artis, D. (2010) IL25 elicits a multipotent progenitor cell population that promotes TH2 cytokine responses, *Nature*, 464(7293), 1362-1366.

Sahputra, R., Ruckerl, D., Couper, K. N., Muller, W., J., Else, K. J. (2019) The essential role played by B cells in supporting protective immunity against *Trichuris muris* infection is by controlling the Th1/Th2 balance in the mesenteric lymph nodes and depends on host genetic background, *Front Immunol*, 10, 2842.

Sakaguchi, S., Y. T., Nomura, T., Ono, M. (2008) Regulatory T cells and immune tolerance, *Cell*, 133, 775-787.

Sawant D. V., Gravano D. M., Vogel P., Giacomini P., Artis D., Vignali, D. A. A. (2014) Regulatory T cells limit induction of protective immunity and promote immune pathology following intestinal helminth infection, *J Immunol*, 192, 2904-2912.

Schachter, J., de Oliveira, D. A., da Silva, C. M., Alencar, A. C. M. d-B., Durate, M., da Silva, M. M. P., Ignacio, A. C. d-P. R., Lopes-Torres, E. J. (2020) Whipworm infection promotes bacterial invasion, intestinal microbiota imbalance, and cellular immunomodulation. *Infect Immunol*, 88(3), 642-19.

Schellinck, H. M., West, A. M., Brown, R. E. (1992) Rats can discriminate between the urine odors of genetically identical mice maintained on different diets, *Physiol Behav*, 51, 1079-1082.

Schmitz, J., O. A., Oldham E., Song Y., Murphy E., McClanahan T.K., Zurawski G., Moshrefi M., Qin J., Li X., Gorman, D. M., Bazan, J. F., Kastelein, R. A. (2005) IL-33, an interleukin-1-like cytokine that signals via the IL-1 receptor-related protein ST2 and induces T helper type 2-associated cytokines, *Immunity*, 23, 479-490.

Schopf, L. R., Hoffmann, K. F., Cheever, A. W., Urban, J. F., Wynn, T. A. (2002) IL-10 Is Critical for Host Resistance and Survival During Gastrointestinal Helminth Infection, *J Immunol*, 168(5), 2383-2392.

Scott, C. L., Bain, C. C., Mowat, A. M. (2017) Isolation and Identification of Intestinal Myeloid Cells. *Methods Mol Biol*, 1559, 223-239.

Sharba S., N. N., Padra M., Persson J.A., Quintana-Hayashi M.P., Gustafsson J.K., Szeponik L., Venkatakrisnan V., Sjöling Å., Nilsson S., Quiding-Jarbrink, M., Johansson, M. E. V., Linden S. K. (2019) Interleukin 4 induces rapid mucin transport, increases mucus thickness and quality and decreases colitis and *Citrobacter rodentium* in contact with epithelial cells, *Virulence*, 10, 97–117.

Shears, R. K., Grencis, R. K. (2022) Whipworm secretions and their roles in host-parasite interactions, *Parasites Vectors*, 15(1).

Shirasu, M., Touhara, K. (2011) The scent of disease: volatile organic compounds of the human body related to disease and disorder, *J Biochem*, 150(3), 257-266.

Singh, P. B., Brown, R. E., Roser, B. (1987) MHC antigens in urine as olfactory recognition cues, *Nature*, 327, 161-164.

Siracusa, M. C., Saenz, S. A., Hill, D. A., Kim, B. S., Headley, M. B., Doering, T. A., Wherry, E. J., Jessup, H. K., Siegel, L. A., Kambayashi, T., Dudek, E. C., Kubo, M., Cianferoni, A., Spergel, J. M., Ziegler, S. F., Comeau, M. R., Artis, D. (2011) TSLP promotes interleukin-3-independent basophil haematopoiesis and type 2 inflammation, *Nature*, 477(7363), 229-233.

Smallegange, R. C., Van Gemert, G.-J., Van De Vegte-Bolmer, M., Gezan, S., Takken, W., Sauerwein, R. W., Logan, J. G. (2013) Malaria Infected Mosquitoes Express Enhanced Attraction to Human Odor, *PLoS ONE*, 8(5), e63602.

Smart, A., De Lacy Costello, B., White, P., Avison, M., Batty, C., Turner, C., Persad, R., Ratcliffe, N. (2019) Sniffing out resistance – Rapid identification of urinary tract infection-causing bacteria and their antibiotic susceptibility using volatile metabolite profiles, *J Pharm Biomed Anal*, 167, 59-65.

Smith, H. L., Monath, T. P., Pazoles, P., Rothman, A. L., Casey, D. M., Terajima, M., Ennis, F. A., Guirakhoo, F., Green, S. (2011) Development of Antigen-Specific Memory CD8+ T Cells Following Live-Attenuated Chimeric West Nile Virus Vaccination. *J infect Dis*, 203(4), 513-522.

Smits, H. H., Everts, B., Hartgers, F. C., Yazdanbakhsh, M. (2012) Chronic helminth infections protect against allergic diseases by active regulatory processes. *Curr Allergy Asthma Rep.* 10(1), 3-12.

Sokol, C. L., Barton, G. M., Farr, A. G., Medzhitov, R. A. (2008) A mechanism for the initiation of allergen-induced T helper type 2 responses, *Nat Immunol*, 9, 310-318.

Sokol, C. L., Chu, N. Q., Yu, S., Nish, S. A., Laufer, T. M., Medzhitov, R. A. (2009) Basophils function as antigen-presenting cells for an allergen-induced T helper type 2 response, *Nat Immunol*, 10(7), 713-20.

Sonoda, H., Kohnoe, S., Yamazato, T., Satoh, Y., Morizono, G., Shikata, K., Morita, M., Watanabe, A., Morita, M., Kakeji, Y., Inoue, F., Maehara, Y. (2011) Colorectal cancer screening with odour material by canine scent detection, *Gut*, 60(6), 814-819.

Sorobetea D., H. J. B., Henningsson H., Kristiansen K., Svensson Frej M. (2017) Acute infection with the intestinal parasite *Trichuris muris* has long term consequences on mucosal mast cell homeostasis and epithelial integrity, *Eur J Immunol*, 47, 257-268.

Sorobetea D., Svensson-Frej M., R., G. (2018) Immunity to gastrointestinal nematode infections, *Mucosal Immunol*, 11(304-315).

Sorwell, K. G., Wesson, D. W., Baum, M. J. (2010) Sexually dimorphic enhancement by estradiol of male urinary odor detection thresholds in mice. *Behav Neurosci*, 122(4), 788-793.

Stanczyk, N. M., Brugman, V. A., Austin, V., Sanchez-Roman Teran, F., Gezan, S. A., Emery, M., Visser, T. M., Dessens, J. T., Stevens, W., Smallegange, R. C., Takken, W., Hurd, H., Caulfield, J., Birkett, M., Pickett, J., Logan, J. G. (2019) Species-specific alterations in Anopheles mosquito olfactory responses caused by *Plasmodium* infection, *Sci Rep*, 9(1).

Stanczyk, N. M., De Moraes, C. M., Mescher, M. C. (2022) Effects of pathogens on mosquito host-seeking and feeding behaviour , in Ignell, R., Lazzari, C. R.,

Lorenzo, M. G. (ed.) *Sensory Ecology of Disease Vectors* Wageningen Academic Publishers 2022, 327-348.

Staniek, M. E., Sedda, L., Gibson, T. D., De Souza, C. F., Costa, E. M., Dillon, R. J., Hamilton, J. G. C. (2019) eNose analysis of volatile chemicals from dogs naturally infected with *Leishmania infantum* in Brazil, *PLOS Neg Trop Dis*, 13(8), e0007599.

Staniek, M. E., Hamilton, J. G. C. (2021) Odour of domestic dogs infected with *Leishmania infantum* is attractive to female but not male sandflies: Evidence for parasite manipulation, *PLOS Pathog*, 17(3), e1009354.

Suckling, D. M., Sagar, R. L. (2011) Honeybees *Apis mellifera* can detect the scent of *Mycobacterium tuberculosis*, *Tuberculosis (Edinb)*, 91(4), 327-8.

Sullivan, B. M., Liang, H.-E., Brando, J. K., Wu, D., Cheng, L. E., McKerrow, J. K., Allen, C. D. C., Locksley, R. M. (2011) Genetic analysis of basophil function in vivo, *Nat Immunol*, 12(6), 527-35.

Stevenson, M. M., Valanparambil, R. M., Tam, M. (2022) Myeloid-derived suppressor cells: expanding the world of helminth modulation of the immune system. *Front Immunol*, 12(13), 874308.

Svensson, M., Russell, K., Mack, M., Else, K. J. (2010) CD4+ T-cell localization to the large intestinal mucosa during *Trichuris muris* infection is mediated by Gα-coupled receptors but is CCR6- and CXCR3-independent, *Immunology*, 129(2), 257-267.

Svensson, M., Bell, L., Little, M. C., Deschoolmeester, M., Locksley, R. M., Else, K. J. (2011) Accumulation of eosinophils in intestine-draining mesenteric lymph nodes occurs after *Trichuris muris* infection, *Parasit Immunol*, 33(1), 1-11.

Tajebe, F., Getahun, M., Adem, E., Hailu, A., Lemma, M., Fikre, H., Raynes, J., Tamiru, A., Mulugeta, Z., Diro, E., Toulza, F., Shkedy, Z., Ayele, T., Modolell, M., Munder, M., Müller, I., Takele, Y., Kropf, P. (2017) Disease severity in patients with visceral leishmaniasis is not altered by co-infection with intestinal parasites. *PLOS Neg Trop Dis*, 11, e0005727.

Takken, W., Knols, B. G. (1999) Odor-mediated behavior of Afrotropical malaria mosquitoes, *Annu Rev Entomol.*, 44, 131-57.

Taylor, M. D., Betts, C. J., Else, K. J. (2000) Peripheral cytokine responses to *Trichuris muris* reflect those occurring locally at the site of infection. *Infect Immun.* 68(4), 1815-1819.

Taylor, B. C., Zaph, C., Troy, A. E., Du, Y., Guild, K. J., Comeau, M. R., Artis, D. (2009) TSLP regulates intestinal immunity and inflammation in mouse models of helminth infection and colitis, *J Exp Med*, 206(3), 655-667.

Taylor, M. T., Broukhanski, J. M., G., Kirpalaney, S., Lutz, H., Powis J. (2018) Using dog scent detection as a point-of-care tool to identify toxigenic *Clostridium difficile* in stool, *Open Forum Infect Dis*, 5, 179.

Thomas, F., Adamo, S., Moore, J. (2005) Parasitic manipulation: where are we and where should we go?, *Behav Proc*, 68(3), 185-199.

Tritten, L., Tam, M., Vargas, M., Jardim, A., Stevenson, M. M., Keiser, J., Geary, T. G. (2017) Excretory/secretory products from the gastrointestinal nematode *Trichuris muris*, *Exp Parasitol* 178, 30-36.

Tyagi, H., Daulton, E., Bannaga, A. S., Arasaradnam, R. P., Covington, J. A. (2021) Non-Invasive Detection and Staging of Colorectal Cancer Using a Portable Electronic Nose, *Sensors*, 21(16), 5440.

Ubeda, C., Vázquez-Carretero, M. D., Luque-Tirado, A., Ríos-Reina, R., Rubio-Sánchez, R., Franco-Macías, E., García-Miranda, P., Calonge, M. L., Peral, M. J. (2022) Fecal Volatile Organic Compounds and Microbiota Associated with the Progression of Cognitive Impairment in Alzheimers Disease, *Int J Mol Sci*, 24(1), 707.

Vallance B.A., G. F., Collins S.M., Snider D.P. (1999) CD4 T Cells and Major Histocompatibility Complex Class II Expression Influence Worm Expulsion and Increased Intestinal Muscle Contraction during *Trichinella spiralis* Infection, *Infect Immun*, 67, 6090–6097.

van de Goor, R., van Hooren, M., Dingemans, A. M., Kremer, B., Kross, K. (2018) Training and Validating a Portable Electronic Nose for Lung Cancer Screening, *J Thorac Oncol*, 13(5), 676-681.

Van de Zande, S., Kaashoek, M., Hesselink, W., Sutton, D., Nell, T. (2009) Comments to 2Comparision of antibody responses after vaccination with two inactivated rabies vaccines *Vet. Microbiol.* 133, 284, 286]. *Vet Microbiol*,138(1-2), 202-3.

van den Bogaart, E., Berkhout, M. M. Z., Nour, A. B. Y. M., Mens, P. F., Talha, A.-B. A., Adams, E. A., Ahmed, H. B. M., Abdelrahman, S. H., Ritmeijer, K., Nour, B. Y. M., Schallig, H. D. F. H. (2013) Concomitant malaria among visceral leishmaniasis in-patients from Gedarif and Sennar States, Sudan: a retrospective case-control study, *BMC Public Health*, 11(13), 332.

Van Den Bogaart, E., Talha, A.-B. A., Straetemans, M., Mens, P. F., Adams, E. R., Grobusch, M. P., Nour, B. Y. M., Schallig, H. D. F. H. (2014) Cytokine profiles amongst Sudanese patients with visceral leishmaniasis and malaria co-infections, *BMC Immunol*, 15(1), 16.

Vantaux, A., de Sales Hien, D. F., Yamego, B., Dabire, K. R., Thomas, F., Coheut, A., Lefevre, T. (2015) Host-seeking behaviors of mosquitoes

experimentally infected with sympatric field isolates of the human malaria parasite *Plasmodium falciparum*: no evidence for host manipulation, *Front Eco. Evol*, 3.

Veldhoen, M, U. C., van Snick, J., Helmbly, H., Westendorf, A., Buer, J., Martin, B., Wilhelm, C., Stockinger, B. (2008) Transforming growth factor-beta reprograms the differentiation of T helper 2 cells and promotes an interleukin 9-producing subset, *Nat Immunol*, 9(12), 1341-6.

Verhulst, N. O., Boulanger, N., Spitzen, J. (2018) Chapter 3- Impact of skin microbiome on attractiveness to arthropod vectors and pathogen transmission. *Skin and Arthropod vectors*. 55-81.

Vickery, W. L., Poulin, R. (2010) The evolution of host manipulation by parasites: a game theory analysis, *Evol Ecol*, 24(4), 773-788.

Viswanath, A., Yarrarapu, N. S., Williams, M. (2023) *Trichuris trichiura* Infection. Treasure Island (FL), StatsPearls [Online]. Available at: <https://www.ncbi.nlm.nih.gov/books/NBK507843/>

Wald O., Weiss I.D., Wald H., Shoham H., Bar-Shavit Y., Beider K., Galun E., Weiss L., Flaishon L., I., S. (2006) IFN- γ acts on T cells to induce NK cell mobilization and accumulation in target organs, *J Immunol*, 176, 4716–4729.

Way, G. W., Lu, H., Wang, X., Zhao, D., Camarena, C., Sarkar, D., Martin, R. K., Zhou, H. (2023) Optimization of high throughout spectral flow cytometry for immune cell profiling in mouse liver. *Liver Res*, 7(3), 263-271.

Webb L. M., Oyesola O. O., Früh S. P., Kamynina E., Still K. M., Patel R. K., Peng S. A., Cubitt R. L., Grimson A., Grenier J. K.(2019) The Notch signaling pathway promotes basophil responses during helminth-induced type 2 inflammation, *J Exp Med*, 216, 1268-1279.

- Wedekind, C., Penn, D. (2000) MHC genes body odours and odour preferences, *Nephrol Dial Transplant*, 15(9), 1269-1271.
- White E. C., Houlden A., Bancroft A. J., Hayes K. S., Goldrick M., Grecis R. K., Roberts, I. S. (2018) Manipulation of host and parasite microbiotas: Survival strategies during chronic nematode infection, *Sci Adv*, 4, eaap7399.
- Weger, B. D., Gobet, C., Yeung, J., Martin, E., Jimenez, S., Bertrisey, B., Foata, F., Bernard, B., Balvay, A., Foussier, A., Charpagne, A., Boizet-Bonhoure, B., Chou, C. J., Naef, F., Gachon, F. (2019) The mouse microbiome is required for sex-specific diurnal rhythms of gene expression and metabolism. *Cell Metabol.* 29(2), 363-383.
- White, E. (2016) *Infection by the gastrointestinal parasite Trichuris muris: Defining the microbiota of the parasite and the host*. PhD thesis, the University of Manchester. Available at:
[https://research.manchester.ac.uk/en/studentTheses/infection-by-the-gastrointestinal-parasite-trichuris-muris-defini/#:~:text=Abstract,\(DGGE\)%20and%20Illumina%20sequencing](https://research.manchester.ac.uk/en/studentTheses/infection-by-the-gastrointestinal-parasite-trichuris-muris-defini/#:~:text=Abstract,(DGGE)%20and%20Illumina%20sequencing).
- White, E. C., Houlden A., Bancroft A. J., Hayes K. S., Goldrick M., Grecis R. K., S., R. I. (2018) Manipulation of host and parasite microbiotas: Survival strategies during chronic nematode infection', *Sci. Adv*, 4, eaap7399.
- World Health Organization (2023) Soil-Transmitted Helminth Infections [Online] Available at: <https://www.who.int/news-room/fact-sheets/detail/soil-transmitted-helminth-infections> [Accessed 13th October 2024].
- Williams, H., Pembroke. A. (1989) Sniffer dogs in the melanoma clinic?, *Lancet*, 333(737).
- Wilson, M. S., Ramalingam T. R., Rivollier A., Shenderov K., Mentink-Kane M. M., Madala S. K., Cheever A. W., Artis D., Kelsall B. L., Wynn, T. A. (2011)

Colitis and Intestinal Inflammation in IL10^{-/-} Mice Results from IL-13R α 2-Mediated Attenuation of IL-13 Activity, *Gastroenterology*, 140, 254-264.

Wu, Z., Zheng, Y., Sheng, J., Han, Y., Yang, Y., Pan, H., Yao, J. (2022) CD3⁺CD4⁻CD8⁻ (double-negative) T cells in inflammation, immune disorders and cancer. *Front Immunol.* 13, 816005.

Wynn, T. A. (2009) Basophils trump dendritic cells as APCs for TH2 responses, *Nat Immunol*, 10, 679-681.

Yan, J., Gangoso, L., Ruiz, S., Soriguer, R., Figuerola, J., Martínez-De La Puente, J. (2021) Understanding host utilization by mosquitoes: determinants, challenges and future directions, *Biol Rev*, 96(4), 1367-1385.

Yin, x-F., Ye, T., Chen, H-L., Junyan, L., Mu, X-F., Li, H., Wang, J., Hu, Y-J., Cao, H., Kang, W-Q. (2024) The microbiome compositional and functional differences between rectal mucosa and feces. *Microbiol Spectr.* 15(8), e03549.

Yousefi, Y., Haq, S., Banskota, S., Kwon, Y. H., Khan, W. I. (2021) *Trichuris muris* Model: Role in Understanding Intestinal Immune Response, Inflammation and Host Defense, *J Pathog*, 10(8), 925.

Yousefi, S, Z.-R. A., Rassi, Y., Vatandoost, H., Yaghoobi-Ershadi, M. R., Aflatoonian, M. R., Akhavan, A. A., Aghaei-Afshar, A., Amin, M., Paksa, A. (2020) Evaluation of Different Attractive Traps for Capturing sandflies (Diptera: Psychodidae) in an Endemic Area of Leishmaniasis, Southeast of Iran. *J Arthropod Borne Dis.*, 14(2), 202-213.

Zaph C., Troy A. E., Taylor B. C., Berman-Booty L. D., Guild K. J., Du Y., Yost E. A., Gruber A. D., May M. J., Greten F. R., Eckmann, L., Karin, M., Artis, D. (2007) Epithelial-cell-intrinsic IKK- β expression regulates intestinal immune homeostasis, *Nature*, 446, 552–556.

Zhu, J., Bean, H. D., Kuo, Y.-M., Hill, J. E. (2010) Fast Detection of Volatile Organic Compounds from Bacterial Cultures by Secondary Electrospray Ionization-Mass Spectrometry, *J Clin Microbiol*, 48(12), 4426-4431.

Zlatkis, A. B. R., Poole, C. F. (1981) The role of organic volatile profiles in clinical diagnosis, *Clin Chem*, 27(6), 789-97.